Zeng *et al. Molecular Cancer* (2025) 24:176
https://doi.org/10.1186/s12943-025-02366-y

Molecular Cancer

REVIEW

Open Access

Enhancing radiotherapy-induced anti-tumor immunity via nanoparticle-mediated STING agonist synergy

Qian Zeng[1], Min Liu[2], Ziqi Wang[1], Rongrong Zhou[1,5*] and Kelong Ai[2,3,4*]

Abstract

Radiotherapy (RT) remains a cornerstone treatment for over 50% of cancer patients, primarily via ionizing radiation-induced DNA damage to exert therapeutic effects. Notably, emerging studies have revealed its additional capacity to activate systemic anti-tumor immune responses through inducing immunogenic cell death (ICD) and activating the cGAS-STING pathway, further expanding its therapeutic potential. However, its efficacy is often limited by immunosuppressive tumor microenvironment (TME). Additionally, while RT can activate the cGAS-STING pathway, this activation remains transient and suboptimal, failing to sustain robust anti-tumor immunity. Therefore, combining RT with STING agonists may benefit traditional therapy by amplifing tumor immunogenicity and counteracting immune evasion. Despite promising results, challenges such as off-target toxicity, poor cell membrane permeability and poor bioavailability, remain obstacles to clinical translation of conventional STING agonists. Nanomedicine offers a promising approach by enabling targeted delivery of STING agonists and amplifying RT-induced DNA damage through nanoscale radiosensitizers. In this review, we provide a detailed discussion of the immune-stimulatory and immune-suppressive effects of RT, as well as the mechanisms and biological effects of selectively activating the cGAS-STING pathway in key TME components. On this basis, we further explore recent advancements in nano-STING agonists-mediated anti-tumor immunity in synergy with RT. This combinatorial approach achieves dual radiosensitization and immunostimulation, ultimately driving immune memory formation and TME reprogramming. Finally, the application prospects and challenges of nano-STING agonists-based immunotherapy are also discussed from the perspective of clinical translation.

Keywords Radiotherapy, Cancer, CGAS–STING signaling, Nanoparticle, Target

*Correspondence:
Rongrong Zhou
zhourr@csu.edu.cn
Kelong Ai
aikelong@csu.edu.cn
[1] Department of Oncology, Xiangya Hospital, Central South University, Changsha 410008, China
[2] Xiangya School of Pharmaceutical Sciences, Central South University, Changsha 410013, China
[3] Hunan Provincial Key Laboratory of Cardiovascular Research, Xiangya School of Pharmaceutical Sciences, Central South University, Changsha 410013, China
[4] Key Laboratory of Aging-Related Bone and Joint Diseases Prevention and Treatment, Ministry of Education, Xiangya Hospital, Central South University, Changsha 410008, China
[5] National Clinical Research Center for Geriatric Disorders, Xiangya Hospital, Central South University, Changsha 410008, China

Introduction

While immunotherapy has demonstrated remarkable clinical success in certain cancer types, its survival benefits remain limited for most solid tumors, with patient response rates typically ranging between 10–30% [1, 2]. The efficacy of anti-tumor immunotherapy hinges on the activation of a comprehensive cancer-immunity cycle, encompassing the release and presentation of cancer antigens, the priming and activation of T cells, the trafficking and infiltration of T cells into tumor tissue, and the subsequent recognition and elimination of cancer cells by T cells [3, 4]. However, therapeutic approaches such as immune checkpoint blockade (ICB), adoptive cell transfer (ACT), cytokine-based immunotherapy, or combination therapies often fail to achieve desired clinical effects due to the immunosuppressive tumor microenvironment (TME) [5]. This dilemma underscores an urgent need to develop novel strategies for systematically reinvigorating the cancer-immunity cycle through comprehensive modulation of immune-tumor interactions.

Reprogramming the TME from "cold" to "hot" represents a critical therapeutic paradigm [6, 7]. Recent studies demonstrate the immunostimulatory properties of radiotherapy (RT) [8]. In general, RT occupies a unique and indispensable position in many cancer treatment regimens with its deep tissue penetration, precise dose distribution guided by gross tumor volume (GTV) delineation, and minimal systemic side effects. Interestingly, RT has been observed to induce "abscopal effects" in various cancer types, including breast cancer [9], melanoma [10], lymphoma [11], and renal cell carcinoma [12] and other metastatic solid tumors [13, 14]. This phenomenon, first described by Mole in 1953 [15], is typically observed in patients with widespread disease where irradiation of one affected site leads to clinical responses in other non-irradiated lesions. "Abscopal effects" are primarily attributed to the activation of systemic immunity following RT. First, RT can induce immunogenic cell death (ICD) of tumor cells [16], that is, tumor-associated antigens (TAAs) and tumor cell surface-exposed damage-associated molecular patterns (DAMPs) can be released after tumor cell ruptures, driving the maturation of antigen-presenting cells (APCs) and the activation of effector T cells. Second, RT-induced DNA damage releases into the cytosol or extracellular space, activating the cGAS-STING pathway in tumor cells and immune cells to stimulate anti-tumor immunity via type I interferons (IFN).

Although RT remains a cornerstone of cancer treatment, its therapeutic efficacy is constrained by intrinsic radiobiological limitations. Dose-dependent toxicity to healthy tissues and immune system, particularly radiation-sensitive $CD8^+$ T cells in lymphoid organs, compromises systemic anti-tumor responses [17]. RT also induces the upregulation of programmed cell death ligand 1 (PD-L1) and stimulates the secretion of immunosuppressive cytokines, such as TGF-β and IL-10, which promote the differentiation of regulatory T cells (T_{reg}) [18]. Additionally, RT enhances the infiltration of myeloid-derived suppressor cells (MDSCs) and tumor-associated macrophages (TAMs) into the tumor stroma, leading to immune tolerance. These immunosuppressive effects constitute a significant bottleneck for RT-induced immunotherapy.

RT can activate the cGAS-STING pathway in tumor or immune cells, this activation is typically transient and insufficient [19], therefore, the development of STING agonists is warranted. Emerging studies have demonstrated that enhancing the activation of the cGAS-STING pathway can potentiate the efficacy of RT while alleviating immunosuppression within the TME [20–23]. Currently, STING agonists are usually used in high-dose intratumoral injections to treat tumors because of poor cell membrane permeability, poor targeting, poor stability, and low bioavailability, where hides inevitable side effects [24].

Nanomedicine offers a promising approach for the combination of RT and STING agonists [25] (Scheme). On one hand, nanoscale radiosensitizers with high atomic number (High-Z) metals, such as gold (Au) and hafnium (Hf), can enhance RT efficacy by depositing radiation energy and generating reactive oxygen species (ROS) to induce DNA damage. Notably, functionalized hafnium oxide (HfO_2) nanoparticles ($NBTXR_3$) demonstrated clinically significant benefits for patients with locally advanced soft tissue sarcoma in a European phase II/III clinical trial (NCT02379845) [26]. On the other hand, nanocarriers can selectively deliver STING agonists to enhance radioimmunotherapy while minimizing off-target toxicity. The combination of RT and STING agonists exhibits dual effects of radiosensitization and immune stimulation, induces long-lasting immune memory, and remodels the TME. Recently, innovative and meticulously designed nanomedicines have recently emerged, aiming to enhance cancer therapy by combining RT with the activation of the cGAS-STING pathway. However, to the best of our knowledge, no comprehensive review has been published in this area, likely due to the interdisciplinary nature of the topic, which makes it challenging to provide a holistic overview of progress in this field. To address this gap, we provided an in-depth review of the latest advancements in the combined treatment of STING agonists and RT. We first outline the mechanisms by which RT induces anti-tumor immunity, with a focus on RT-mediated activation of the cGAS-STING pathway in tumor cells and the associated immunosuppressive effects of RT. We then elaborate on the

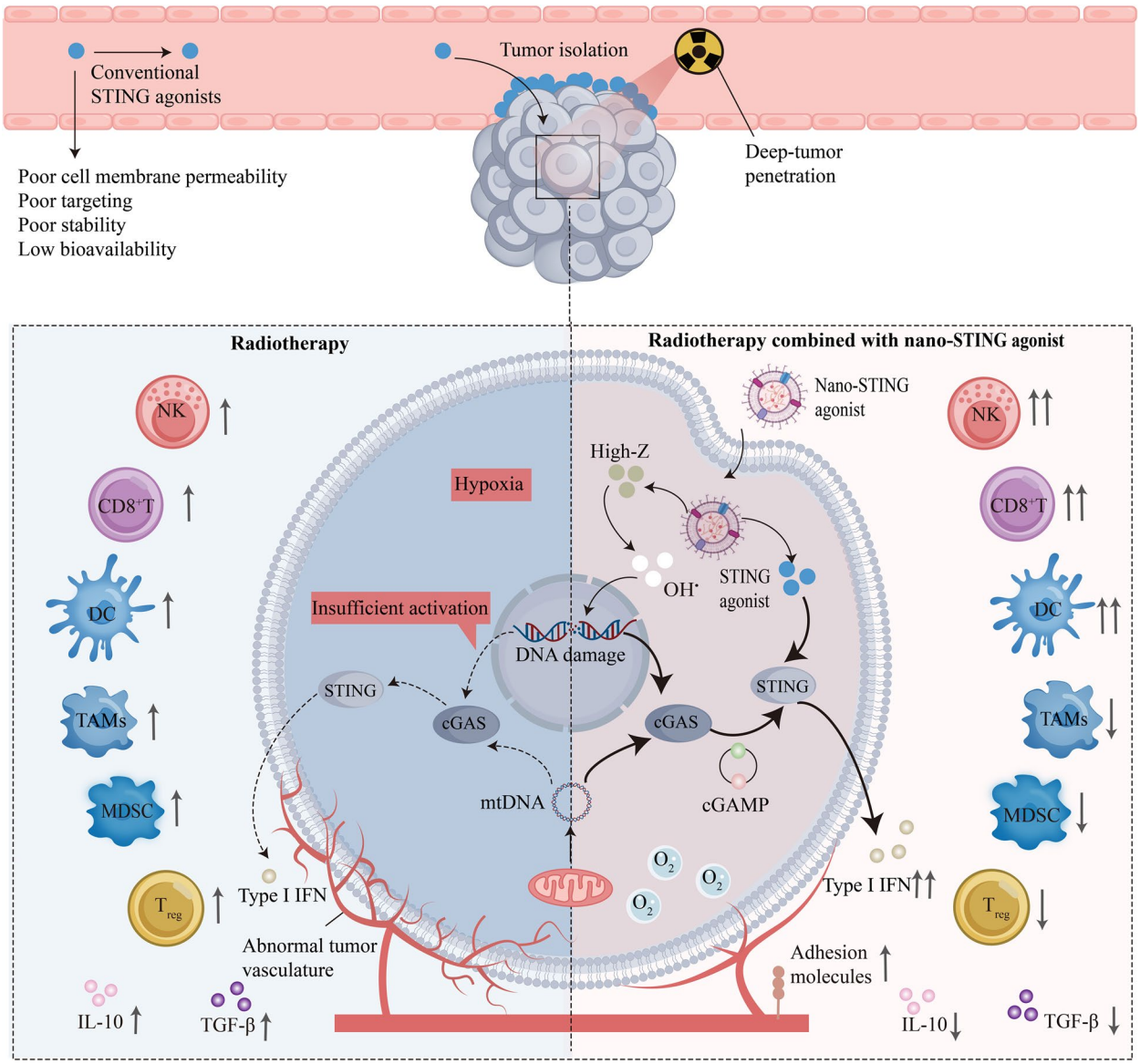

Scheme 1 Scheme. Synergistic effect of nanoparticle-mediated STING agonists and RT. RT offers profound tissue penetration capacity, enabling precise targeting of deep-seated malignancies. The dual immunomodulatory effects of RT-activating anti-tumor responses while simultaneously sculpting an immunosuppressive TME-create a self-limiting therapeutic paradox. Transient cGAS-STING activation fails to sustain immunostimulatory effects against dominant immunosuppressive networks, underscoring the need for combinatorial strategies to amplify and prolong pathway engagement**.** Compared with RT alone, the combination of RT and nano-STING agonists can convert "cold tumors" into "hot tumors". Sufficient type I IFNs not only enhance the function of immune cells such as DCs but also suppress the immunosuppressive cells such as MDSCs [27]. Nanoparticle-mediated delivery of STING agonists surmounts the intrinsic limitations of conventional agonist formulations.

mechanisms and biological effects of cGAS-STING pathway activation in cancer cell and other cells, including vascular ECs, DCs, TAMs, and NK cells. Building on this foundation, we highlight representative studies that integrate RT with cGAS-STING pathway activation, focusing on three key aspects: (1) enhancing tumor and immune cell responses, (2) remodeling the TME, and (3) multimodal therapies combining RT, STING agonists, and other therapeutic strategies. This review aims to explore the synergies, future directions and challenges of RT with STING agonists through advanced nanomaterial-enabled platforms. By synthesizing insights from preclinical breakthroughs and early clinical trials, it establishes a roadmap for the development of next-generation radioimmunotherapy, an approach that leverages the cGAS-STING axis to overcome treatment resistance in solid

tumors. The convergence of nanotechnology with radiation biology enables precise control of STING activation while mitigating systemic toxicity.

RT and cancer immunology

DNA serves as the blueprint of life, safeguarded by a series of DNA damage response pathways to maintain genomic integrity. DNA damage, however, represents a double-edged sword in cancer cells. On one hand, DNA damage increases mutation rates and cancer risk. Mutations in critical DNA repair genes, such as BRCA1 and/or BRCA2, induce genomic instability and promote tumorigenesis [28]. On the other hand, DNA damage induced by chemical agents or radiation can effectively kill cancer cells [28]. Once DNA is released into the cytoplasm or extracellular space, it triggers a strong inflammatory and immune response.

Current cancer treatment modalities include surgery, RT, chemotherapy, immunotherapy, targeted therapy, and novel therapies such as photodynamic therapy (PDT) and sonodynamic therapy (SDT). Compared to surgery and chemotherapy, RT offers significant advantages, including high spatiotemporal selectivity, low invasiveness, and strong therapeutic effects. Unlike external beam PDT (EB-PDT), RT has the ability to penetrate deeply to treat deep-seated tumors, such as brain cancer, lung cancer, breast cancer, intestinal cancer, etc., while also maintaining controllable side effects (Fig. 1A). While intra-tumor light delivery (interstitial PDT, I-PDT) enables treatment of deeply seated tumors or tumors exceeding 10 mm in thickness, this approach necessitates percutaneous or intraoperative implantation of optical fibers into tumor cores, which may lead to procedure-related complications including hemorrhage, infection, and tumor cell seeding along needle tracts. SDT possesses deep penetration capability and favorable safety profiles, making it suitable for treating deep tumors (brain cancer, lung cancer, breast cancer, intestinal cancer, etc.), similar to RT; however, it has a lower efficiency in ROS production and insufficient targeting ability [29–31]. Advancements in hardware and software technologies have enabled the development of conformal RT, which can precisely delineate the tumor target area (GTV, CTV, PTV) on patient images (Fig. 1B), delivering the required radiation dose to the precise location of the tumor, thereby maximizing treatment efficacy while minimizing radiation damage to normal organs [32]. Ionization radiation can directly kill tumor cells by damaging their DNA and proteins, or indirectly kill tumor cells by interacting with water molecules to produce ROS that damage DNA and proteins [33] (Fig. 1C). This process can result in several types of DNA damage, including single-strand breaks (SSBs), double-strand breaks (DSBs), base change, and crosslinks with proteins or other DNA molecules [34, 35]. Under physiological conditions, DNA strand breaks can be repaired by three central DDR kinases: DNA-dependent protein kinase (DNA-PK), ataxia telangiectasia-mutated (ATM), and ataxia telangiectasia and Rad3-related protein (ATR), which prevent cells with DNA damage from progressing to mitosis and avoid DNA exposure in the cytoplasm [36]. However, disruptions in DDR processes are common in cancer, and RT exacerbates DDR dysfunction. This leads to the formation of micronuclei, which can activate the cGAS-STING pathway, promoting the production of type I IFN in cancer cells and triggering subsequent innate immune signaling cascades [37].

Mechanism of activation of the cGAS-STING pathway in tumor by RT

Damaged DNA fragments can accumulate in the cytosol of irradiated cancer cells. cGAS is a cyclic GMP-AMP synthetase that acts as a cytoplasmic DNA sensor to recognize double-stranded DNA (dsDNA). After recognizing dsDNA in cytoplasm, cGAS in cytoplasm undergoes conformational changes to form dimer and has enzyme activity, which can catalyze guanosine triphosphate (GTP) and adenylate triphosphate (ATP) to generate the second messenger 2′, 3′—cyclic GMP -AMP (cGAMP). cGAMP has a high affinity for STING, and binding STING causes its conformational change to form a dimer, thus activating STING. Upon activation, STING translocates from the ER to the Golgi, where it recruits kinases such as TANK-binding kinase 1 (TBK1) and IκB kinase (IKK), which phosphorylate interferon regulatory factor 3 (IRF3) and the nuclear factor-κB (NF-κB) inhibitor IκBa, respectively. IRF3 and NF-κB then translocate to the nucleus to activate transcription of genes encoding type I IFN and inflammatory cytokines (IL-6 and TNF-α) [39]. Type I IFN binds to its heterodimeric receptor IFNAR1/2 mainly through autocrine and paracrine modes. IFNAR1/2 subsequently activates Janus kinase 1 (JAK1) and tyrosine kinase 2 (TYK2), leading to the phosphorylation of signal transducer and activator of transcription 1 (STAT1) and STAT2, thereby initiating the transcription of interferon-stimulated genes (ISGs) [40]. Numerous functionally distinct ISGs have been described, including C-X-C motif chemokine ligand (CXCL) 10, CXCL9, C–C motif chemokine ligand (CCL) 4, CCL5, guanylate-binding proteins (GBPs), interferon-induced with tetratricopeptide repeats 1 (IFIT1), interferon-stimulated response elements (ISREs), major histocompatibility complex (MHC), and tumor necrosis factor-related apoptosis-inducing ligand (TRAIL), etc. [41]. Type I IFN can promote DCs maturation, activate $CD8^+$ T and NK cell, induce Th1 differentiation, promote the repolarization of anti-inflammatory M2 macrophages

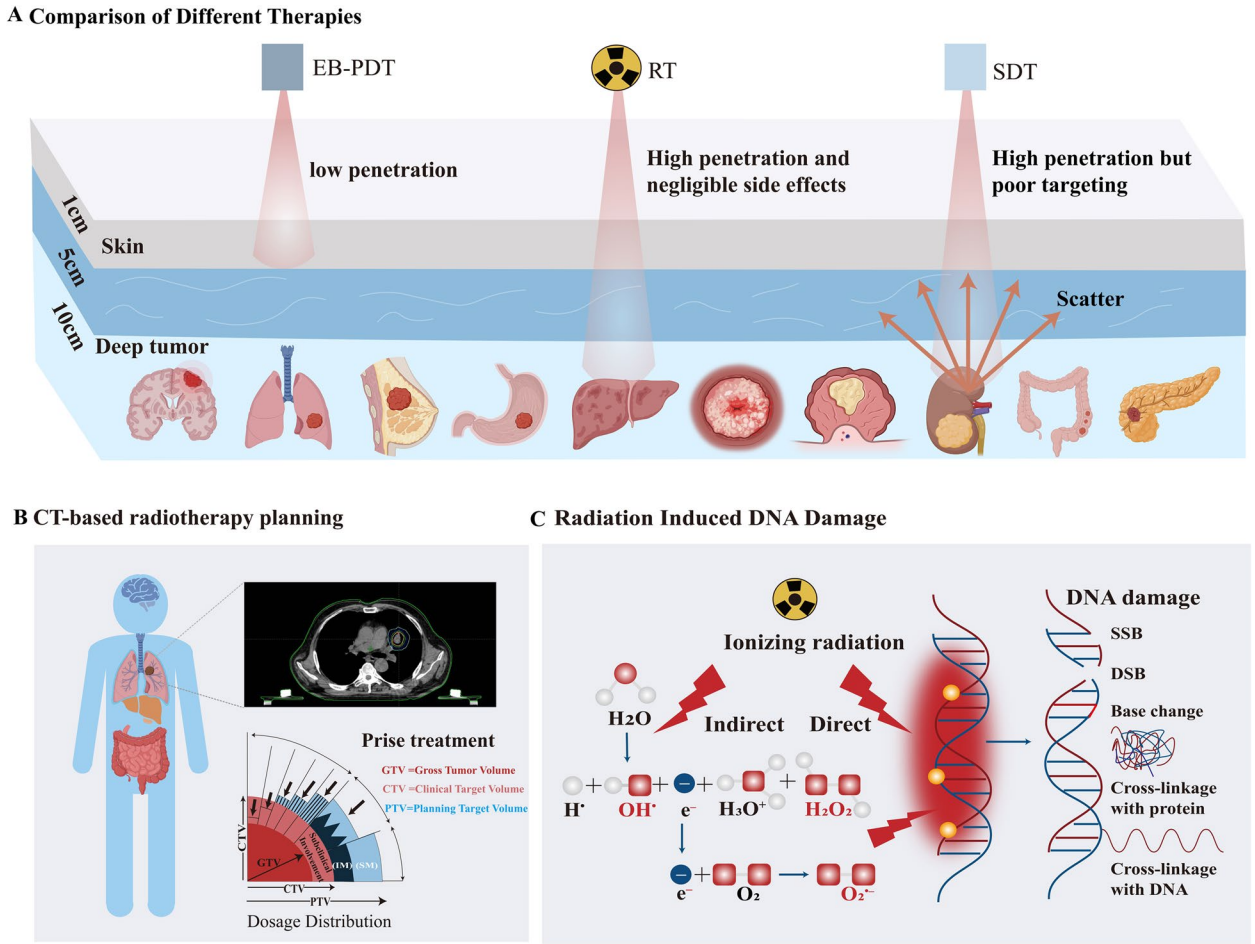

Fig. 1 Mechanisms and clinical advantages of RT. **A** Comparison of tissue penetration in different therapies. EB-PDT is more suitable for superficial tumor treatment due to the poor tissue penetration depth of near-infrared (NIR) light (around 5–10 mm) [38]. SDT has deep penetration capability; however, ultrasound attenuates and scatters as it traverses through tissues. **B** To precisely delineate the target volumes (GTV, CTV, PTV) on patient imaging and deliver the prescribed radiation dose accurately to the tumor while minimizing damage to surrounding tissues, a meticulous approach is required in RT. The gross tumor volume (GTV) encompasses the primary tumor, metastatic lymph nodes, and distant hematogenous metastases. The clinical target volume (CTV) extends beyond the GTV to include potential subclinical malignant lesions. The planning target volume (PTV) further expands the CTV to account for physiological variations caused by respiration, cardiac motion, and the filling or emptying of hollow organs, as well as setup errors from fractionated treatments and mechanical uncertainties of the RT equipment. **C** Schematic diagram of the mechanism of ionizing radiation (IR)

to pro-inflammatory M1 macrophages, and inhibit the activity of MDSCs and T_{reg} cells [27], thus enhancing the effect of RT.

Cytosolic dsDNA that activates the cGAS-STING pathway following RT can be categorized into two types based on its origin: nuclear DNA leakage and mitochondrial DNA (mtDNA). Nuclear DNA leakage is categorized by its components, which mainly include cytosolic micronuclei, cytoplasmic chromatin fragments (CCFs) from senescent cells, retrotransposon [42]. The formation of micronuclei takes a long time, usually peaking at 96 h after RT, and results from chromosome segregation errors after RT [43]. Micronuclear envelopes are prone to rupture due to the lack of a stable nuclear lamina, releasing dsDNA into the cytoplasm [44]. In senescence, chromatin herniations can bud off the main nucleus leading to accumulation of cytoplasmic CCFs. RT can lead to entry of nuclear DNA into the cytoplasm through the derepression of retroelements [45]. mtDNA damage may be more sensitive to disruptions in the DDR process compared to nuclear DNA, as mtDNA is located near the electron transport chain (ETC) and lacks the protective histone shielding present [46]. In stressed cells, the integrity of the mitochondrial membrane is disrupted by the formation of BAK/BAX pores which promote mitochondrial outer membrane permeabilization

(MOMP) and cytochrome c (cyt c) release into the cytoplasm, thus starting the caspase cascade of apoptosis [47].The recognition of leaked mtDNA by cGAS occurs prior to apoptosis, as mtDNA is released into the cytoplasm through BAK/BAX and voltage-dependent anion channel (VDAC) pores [48, 49]. Low-dose segmentation maximizes activation of the cGAS-STING pathway. Radiation doses above 12–18 Gy induce the production of the three prime repair exonuclease 1 (Trex1) in various cancer cells. Trex1 is a DNA exonuclease that degrades DNA accumulated in the cytoplasm during radiation to reduce its immunogenicity [50, 51]. Extracellular cGAMP has anionic and hydrophilic properties and is regulated by ectonucleotide pyrophosphatase phosphodiesterase 1 (ENPP1) [52].

Radiated tumor cells can transmit cGAS-STING signals to adjacent non-tumor cells, such as myeloid cells (monocytes, macrophages, DCs, granulocytes or lymphocytes) via direct cell-to-cell contact or extracellular space [53] (Fig. 2). Direct cell-to-cell contact includes endocytosis and gap junctions [53]. Endocytosis includes phagocytosis and transcytosis. Myeloid cells can directly phagocytose tumor cells or tumor debris to activate the cGAS–STING pathway. Gap junctions are composed of tumor cell connexin CX43 and myeloid cell connexin CX45 [54]. Tumor-derived dsDNA and cGAMP can also trigger this pathway via gap junctions [55]. dsDNA or cGAMP released by tumor cells can also be internalized into the cytoplasm of myeloid cells via tumor cell exosomes [53], allowing cGAS-STING signals to propagate from tumor cells to myeloid cells through the extracellular space. cGAMP can also be released into the extracellular space via protein export such as ABCC1 and translocated to myeloid cells via Volume regulated anion channels (VRACs), SLC19A1 and P2X7R on the cell membrane [56].

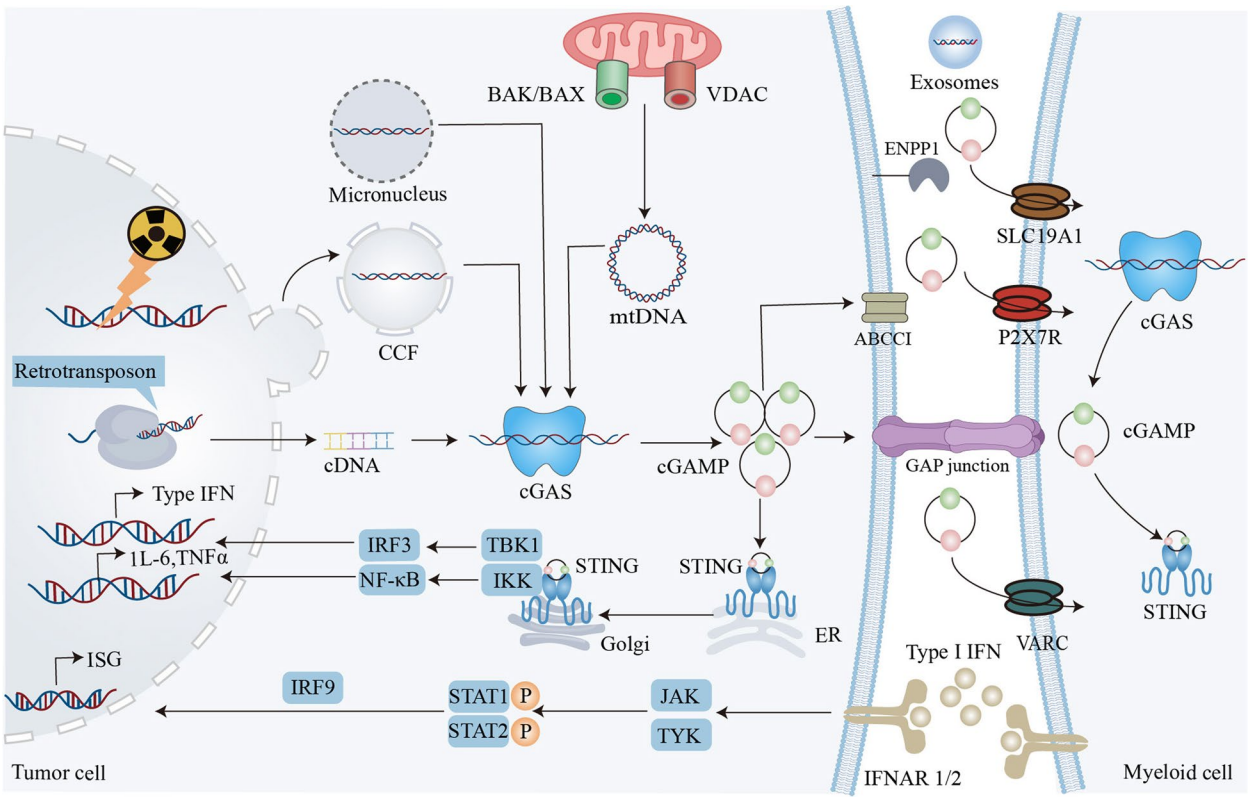

Fig. 2 Molecular mechanism of the cGAS-STING pathway by RT. After tumor cells receive RT, dsDNA derived from micronuclei, CCF, cDNA from retrotransposons, and mitochondrial DNA activates cGAS and drives the synthesis of cGAMP. Upon binding with cGAMP, the activated STING translocates from the ER to the Golgi apparatus, where it recruits TBK1 and IKK, which phosphorylate IRF3 and IκBa, respectively. Phosphorylated IRF3 and NF-κB then translocate to the nucleus to activate transcription of genes encoding type I IFN and inflammatory cytokines (IL-6 and TNF-α). Type I IFN bind to their heterodimeric receptor IFNAR1/2, which activates JAK and TYK, leading to the phosphorylation of STAT1 and STAT2. The STAT1-STAT2 heterodimer binds to IRF9 and translocates to the nucleus, driving the transcription of ISGs. cGAMP released by tumor cells can also be internalized into the cytoplasm of myeloid cells through gap junctions, membrane transporters (LRRC8, P2X7R, SCL19A1), or via the uptake of extracellular vesicles

Immunosuppressive effects of RT

Irradiated tumor cells undergoing ICD release tumor-associated antigens and expose damage-associated molecular patterns (DAMPs) on their surface, driving the maturation of APCs and the activation of effector T cells [16]. Additionally, tumor-derived cGAMP and DNA can be internalized by DCs, leading to the activation of their cGAS-STING pathway, which is a critical factor in promoting DC maturation. The activation of the cGAS-STING-IFN signaling pathway promotes the secretion of chemokines, such as CXCL9, CXCL10, and CXCL16, by both tumor cells and DCs, thereby facilitating T cell infiltration [57]. RT can also enhance the surface expression of MHC class I on tumor cells, thereby promoting the induction of tumor-specific T lymphocyte responses. IFN-β further enhances the expression of NKG2D on NK cells, which interacts with UL16-binding protein (ULBP1-6) and MHC class I chain-related proteins A and B (MICA/B) on tumor cells, enhancing the direct cytotoxicity of NK cells [58, 59]. However, the positive effects of RT on antigen presentation, DC function, $CD8^+$ T cell infiltration, and NK cell activity are counterbalanced by inhibitory signals induced by RT (Fig. 3).

Type I IFN generated by cGAS-STING activation promotes indoleamine 2,3-dioxygenase (IDO) production, inhibits Th1 cell proliferation, promotes Th2 cell proliferation, and induces T_{reg} differentiation, leading to immunosuppressive effects [62]. IDO-1 is an immunosuppressive enzyme expressed in the placenta, tumor cells, and macrophages that repels T cells and activates T_{reg} cell by converting tryptophan (Trp) to kynurenine (Kyn). T_{reg} cells contribute to immunosuppression through cytotoxic T lymphocyte-associated antigen 4 (CTLA-4) signaling, the production of TGF-β and IL-10, and the conversion of ATP to adenosine via CD39 and CD73 [37]. T_{reg} cells express CTLA-4, which has a higher affinity for CD80 and CD86 on DCs compared to CD28 on T cells [63]. This effectively inhibits co-stimulatory signaling, leading to impaired T cell activation. CCL2 secreted by tumor cells can also promote T_{reg} cell infiltration [37].

RT also promotes the expression of tumor cell chemokine CCL2, and CCL5 ligands, thereby recruiting monocyte chemotactic proteins $CCR2^+$ and/or $CCR5^+$ receptor TAMs to infiltrate into the TME [18]. Colony-stimulating factor 1 (CSF-1) is abundant in the hypoxic TME and promotes the proliferation, differentiation, and migration of TAMs by binding to CSF-1R on TAMs [64]. Additionally, tumor-derived exosomes released during RT-induced ICD carry HMGB1, which can enhance M2 polarization by increasing glycolytic metabolism, leading to the upregulation of PD-L1 [65].

MDSCs are primarily categorized into two subsets: monocytic MDSCs (M-MDSCs) and polymorphonuclear MDSCs (PMN-MDSCs) [66]. Irradiated cancer cells attract MDSCs into the TME by releasing CCL2, CCL5, and CSF-1 [67, 68]. MDSCs make tumors radio-resistant [69], inhibit T cell proliferation and NK cell function [70], and can rapidly differentiate into immunosuppressive M2-like TAMs [67]. In addition to this, another characteristic of the immunosuppressive effect of MDSCs is the high expression of PD- L1 [71]. PD-L1 blockade of MDSCs leads to an increase in activated T cells [72, 73]. RT also leads to recruitment of MSCs into the TME [74]. Cytokines (e.g., CCL5) produced by activation of the cGAS-STING pathway in MSCs can promote distant tumor metastasis [75]. Cancer associated fibroblasts (CAF) activation following radiation leads to altered growth factor secretion and release of numerous modulators of the extracellular matrix (ECM) and cytokines [76].

DNA damage signaling is also important for inducing PD-L1 expression. Upregulation of PD-L1 leads to insufficient production of effector T cells, resulting in immune escape and making tumor cells radio-resistant. RT upregulates PD-L1 expression through four main mechanisms: (I) DNA damage signaling pathway [77]; (II) the cGAS-STING pathway [78]; (III) IFN-γ signaling [79]; and (IV) the epidermal growth factor receptor (EGFR) pathway [80]. The response to DNA damage, including DNA double-strand breaks, single-strand breaks, and base damage, activates the ATM/ATR/Chk1 kinase pathway, leading to upregulated PD-L1 expression in cancer cells. Notably, DNA damage signaling following RT upregulates PD-L1 by activating the cGAS-STING pathway to phosphorylate IRF3 to enter the nucleus stimulating PD-L1 transcription [78]. In addition, activated tumor-infiltrating lymphocytes (TILs) release IFN-γ, which acts on tumor cells to mediate STAT1/3-dependent PD-L1 upregulation. Furthermore, post-irradiation EGFR signaling promotes PD-L1 expression through the IL-6/JAK/STAT3 pathway. Anti-PD-L1/PD-1 has a synergistic effect with STING agonists. Anti-PD-L1/PD-1 neutralizes the immunosuppressive effect of STING agonists up-regulating PD-L1, and STING agonists enhances T-cell infiltration in the TME, which strengthens the efficacy of anti-PD-L1. It has been demonstrated that the anti-tumor effect of anti-PD-L1/PD-1 is dependent on the cGAS-STING in tumor-infiltrating DCs [81].

Current progress and barriers of RT combined with STING agonists

While RT can trigger the cGAS-STING pathway in tumor or immune cells, this effect is often transient, necessitating the application of STING agonists in synergies. The combination of RT and STING agonists holds promise

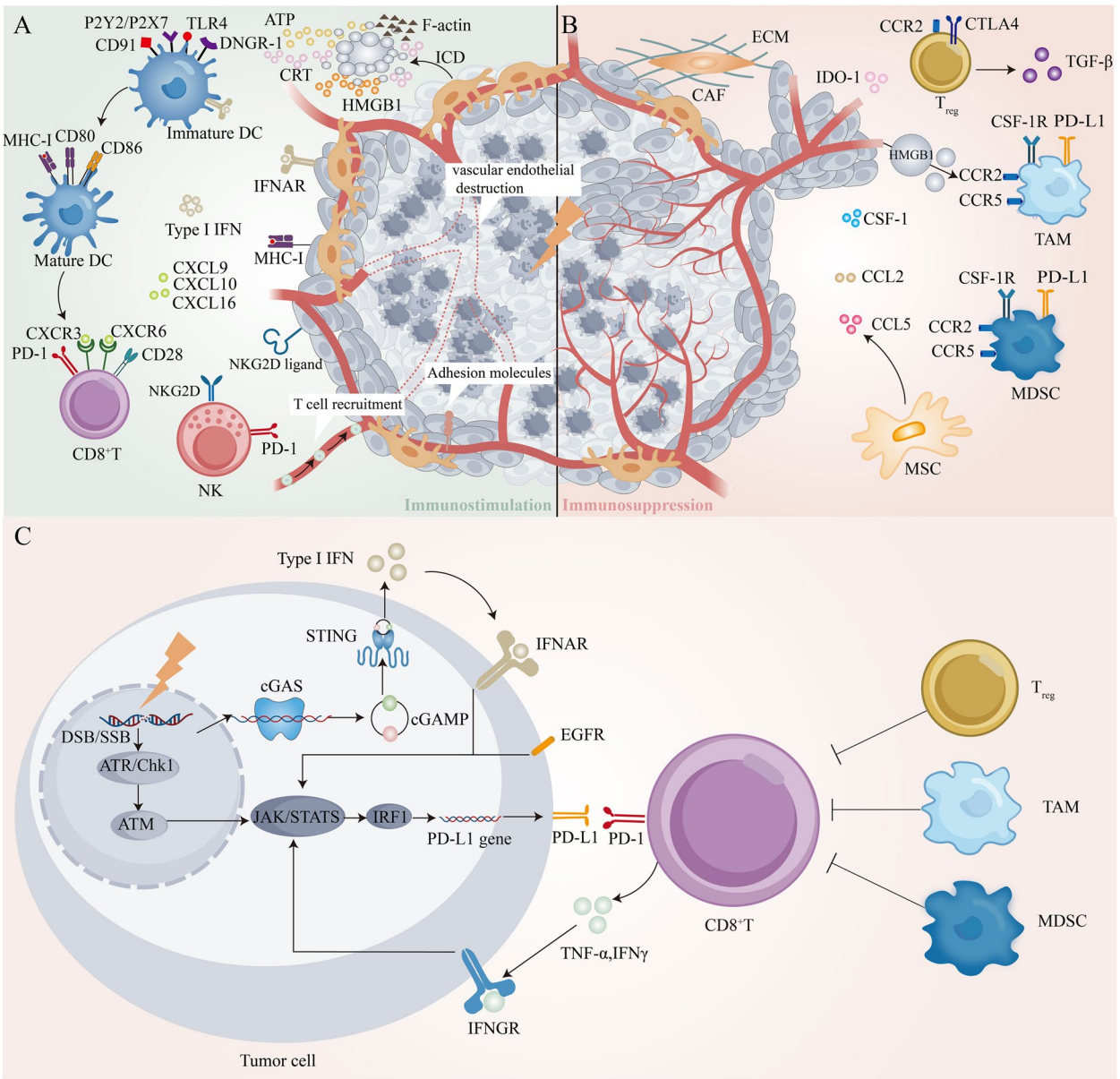

Fig. 3 RT regulates both immunosuppressive and immunostimulatory effects in the TME. **A** DAMP from irradiated cancer cells, such as CRT, ATP, HMGB1, and F-actin, can facilitate DC processing, TAA presentation and consequently activate T cells by binding to the receptors CD91, P2Y2/P2X7, TLR4, and DNGR-1 on DCs, respectively [60]. Activation of the cGAS-STING pathway in tumor cells following RT, or the uptake of tumor-derived DNA and cGAMP by DCs, leads to cGAS-STING activation in DCs, resulting in type I IFN production. Chemokines CXCL9, CXCL10, and CXCL16 from both tumor and DCs facilitate T-cell infiltration. RT induces upregulation of NKG2D, enhancing NK cell-mediated cytotoxic responses. Furthermore, RT modulates the tumor vasculature by upregulating adhesion molecules, thereby further promoting the recruitment of effector T cells [61]. **B** Type I IFN production following cGAS-STING activation promotes the generation of IDO-1, which induces T_{reg} differentiation. Irradiated tumor cells release CCL2, CCL5, and CSF-1, recruiting TAMs, MDSCs, and T_{reg} into the TME. RT also recruits MSCs and induces the activation of CAFs, contributing to an immunosuppressive TME. **C** Several mechanisms underlying the upregulation of PD-L1 on tumor following RT have been reported, including: (1) IFN-γ signaling, (2) EGFR signaling, (3) DNA damage and repair pathways, and (4) cGAS-STING activation. In all pathways, PD-L1 expression is ultimately induced through the STAT/IRF axis

for converting immunologically "cold tumors" into "hot tumors" by amplifying anti-tumor immune responses. However, this approach currently remains in the early stages of clinical exploration, with only a limited number of trials initiated [82]. Clinical translation is hindered by pharmacokinetics and adverse effects linked to excessive

cGAS-STING activation, including cytokine storms [83, 84], autoimmune disorders [85], and radiation-induced tissue damage [86]. Currently, the combination of RT and STING agonists still faces significant challenges, necessitating the development of diverse STING agonists.

Clinical trials of RT combined with STING agonists

Currently, common STING agonists in the clinic are synthetic cyclic dinucleotide (CDN) and its analogs, chemical drugs such as platinum and paclitaxel, metal ions such as manganese/zinc/iron/calcium, small-molecule inhibitors such as PAPR, small-molecule drugs such as SR-717, and small interfering RNAs (siRNAs) [10, 11]. A variety of STING agonists are currently in clinical trials, most of which focus on the anti-tumor effects of combinations of STING agonists with ICIs (Table 1). Currently, clinical trials investigating the combination of STING agonists with RT are scarce, and no clinical efficacy data are available. In this article, we summarize the clinical trials that have been conducted to explore the combination therapy of STING agonists and RT.

TAK-676 (egasodimod sodium), a synthetic CDN analog, is a well-characterized and potent STING agonist [87]. Unlike many other CDN-based drugs that rely on intratumoral delivery, TAK-676 can be administered intravenously. It is currently being evaluated in a Phase I trial for patients with advanced non-small cell lung cancer, triple-negative breast cancer, or squamous cell carcinoma of the head and neck who have progressed on checkpoint inhibitor therapy and have two or more measurable lesions. In the NCT04879849 trial, one lesion will be treated with RT at a total dose of 24 Gy delivered in three fractions, followed by PD-1 inhibitor administration on Day 1 and dose-escalated TAK-676 administration on Days 1, 8, and 15 [82]. While the primary endpoint of the trial is safety, secondary endpoints, including tumor responses at both irradiated and non-irradiated lesions, will provide early insights into the anti-tumor immune responses elicited by this regimen.

The novel STING agonist IMSA101, a cGAMP analog, is administered intratumorally to treat accessible tumors and has demonstrated a favorable safety profile in Phase I clinical trials. IMSA101 has been shown to enhance CAR-T cell function, facilitated by its induction of IL-18 secretion [88]. Currently, Phase II trials are underway to evaluate the combination of IMSA101 with immune checkpoint inhibitors and RT (NCT05846659, NCT05846646, and NCT06601296). These trials are Phase II randomized studies designed to assess the safety and efficacy of combining personalized ultrahypofractionated stereotactic adaptive radiotherapy (PULSAR) and immune checkpoint inhibitors, with or without the addition of the STING agonist IMSA101, in patients with oligoprogressive solid tumors (non-small cell lung cancer or renal cell carcinoma). In these trials, RT will be delivered to one lesion at a total dose of 36 Gy in three fractions, followed by PD-1 inhibitor administration on Day 2. IMSA101 will be administered intratumorally once weekly during the first three weeks of the first cycle (Days 1, 8, and 15), followed by administration on Day 1 of the second and third cycles. The primary endpoint of the trials is the progression-free rate at 12 months, while secondary endpoints include the occurrence of treatment-related adverse events and serious adverse events (SAEs). Currently, the NCT05846659 and NCT05846646 trials have been terminated, while NCT06601296 remains in the non-recruiting phase.

Challenges in clinical translation of RT combined with STING agonists

The clinical translation of STING agonists is hampered by their pharmacological challenge and adverse effects. Pharmacological challenges encompass poor membrane permeability, limited stability, and insufficient targeting specificity [89]. Natural CDNs face significant pharmacological challenges due to their high molecular weight, strong polarity, and poor membrane permeability through negatively charged cell membranes, compounded by inefficient transporter-mediated uptake. Their phosphodiester bonds are highly susceptible to hydrolysis by ENPP1, resulting in metabolic instability. Furthermore, STING agonists must reach the cytosol to activate signaling but risk lysosomal degradation in acidic, enzyme-rich lysosomal environments (e.g., nucleases, lipases, proteases) [90]. A critical pharmacological hurdle lies in achieving tumor-selective delivery: systemic administration of STING agonist-loaded nanoparticles activates STING not only in tumors but also in plasma and major organs (spleen, liver, lungs, kidneys) [91]. However, robust systemic immune activation in non-target tissues, particularly the spleen and liver, may trigger acute inflammation or cytokine storms. Intratumoral administration has been shown to generally be safe, but it may not be easily applicable to all tumor types. It can also have potential side effects, including fever, chills, and pain at the injection site.

Some studies also suggest that high-dose STING agonists can cause T cell apoptosis. Larkin [92] et al. found that failure to resolve ER stress caused by STING agonists is the main cause of T cell death. Although unfolded protein (UPR) relieves ER stress, it is not sufficient to counteract Ca^{2+} imbalance on the ER [92]. UPR increases the folding capacity of the ER to prevent cell death. Cerboni [93] et al. found that that activated STING inhibits T cell proliferation, requiring its relocalization to the Golgi apparatus and causing mitosis errors, and is

Table 1 Clinical trials of STING agonists

Name	Status	Tumor	Company	Route	Description	Number
E7766	Phase 1/1b (terminated)	Advanced Solid Tumors or Lymphomas	Eisai	Intratumoral injection	A safety study	NCT04144140
E7766	Phase 1/1b (withdrawn)	Non-muscle Invasive Bladder Cancer (NMIBC) Including Participants Unresponsive	Eisai	Intravesical injection	A safety study	NCT04109092
MIW 815(ADU-S100)	Phase 1b (terminated)	Advanced/Metastatic Solid Tumors or Lymphomas	Aduro BioTech	Intratumoral injection	A safety and efficacy study with PD-1 checkpoint inhibitor PDR 001	NCT03172936
ADU-S100	Phase 2 (terminated)	Head and Neck Cancer	Chinook Therapeutics	Intratumoral injection	A safety and efficacy study with pembrolizumab	NCT03937141
ADU-S100	Phase 1 (terminated)	Advanced/Metastatic Solid Tumors or Lymphomas	Chinook Therapeutics	Intratumoral injection	A safety and efficacy study with ipilimumab	NCT02675439
CRD 3874-SI	Phase 1a/1b (recruiting)	Solid Tumors	Memorial Sloan Kettering Cancer Center	Intravenous injection	A safety study	NCT06021626
CRD 3874-SI	Phase 1 (recruiting)	Relapsed/refractory Acute Myeloid Leukemia	University of Maryland, Baltimore	Intravenous injection	A safety study	NCT06626633
IMSA 101	Phase 2 (terminated)	Oligoprogressive Solid Tumor Malignancies	ImmuneSensor Therapeutics Inc	Intratumoral injection	A Safety and Efficacy study with **RT** + Pembrolizumab or Nivolumab ±IMSA101	NCT05846659
IMSA 101	Phase 1/2(active, not recruiting)	Advanced Malignancies	ImmuneSensor Therapeutics Inc	Intratumoral injection	A Safety and Efficacy study with Immune Checkpoint Inhibitor	NCT06026254
IMSA 101	Phase 1/2 (completed)	Refractory Malignancies	ImmuneSensor Therapeutics Inc	Intratumoral injection	A safety and efficacy study with/without immune checkpoint inhibitor	NCT04020185
IMSA101	Phase 2 (terminated)	Oligometastatic NSCLC and RCC	ImmuneSensor Therapeutics	Intratumoral injection	A Safety and Efficacy study with **RT** + Pembrolizumab or Nivolumab ±IMSA101	NCT05846646
IMSA101	Phase 2 (not yet recruiting)	Metastatic Kidney Cancer (SPARK)	Niversity of Texas Southwestern Medical Center	Intratumoral injection	A Safety and Efficacy study with **RT** + Nivolumab ±IMSA101	NCT06601296
TAK-500	Phase 2 (recruiting)	Select Locally Advanced or Metastatic Solid Tumors	Takeda	Intravenous injection	A safety and efficacy study with or without Pembrolizumab	NCT05070247
SNX 281	Phase 1 (terminated)	Advanced Solid Tumors and Lymphoma	Stingthera	Intravenous injection	A safety and efficacy study with or without pembrolizumab	NCT04609579
TAK-676	Phase 1 (completed)	Non-small Cell Lung Cancer, Triple-negative Breast Cancer, and Head and Neck Cancer	Takeda	Intravenous injection	A Safety and Efficacy study with **RT** + Pembrolizumab +TAK-676	NCT04879849

Table 1 (continued)

Name	Status	Tumor	Company	Route	Description	Number
TAK-676	Phase 0 (completed)	Head and Neck Squamous Cell Carcinoma	Takeda	Intratumoral injection	A safety study with surgery and Carboplatin and Paclitaxel	NCT06062602
TAK-676	Phase 1/2 (recruiting)	Advanced or Metastatic Solid Tumors	Takeda	Intravenous injection	A safety and efficacy study with or without Pembrolizumab	NCT04420884
GSK 3745417	Phase 1 (active, not recruiting)	Advanced Solid Tumors	GlaxoSmithKline	Intravenous injection	A safety and efficacy study with or without dostarlimab	NCT03843359
GSK 3745417	Phase 1 (terminated)	Relapsed or Refractory Myeloid Malignancies Including AML and HRMDS	GlaxoSmithKline	Intravenous injection	A safety and efficacy study with or without dostarlimab	NCT05424380
CDK-002 (exoSTIN)	Phase 1/2 (completed)	Advanced/Metastatic, Recurrent, Injectable Solid Tumors	Codiak BioSciences	Intratumoral injection	A safety, pharmacodynamics, and pharmacokinetic study	NCT04592484
ONM-501	Phase 1 (recruiting)	Advanced Solid Tumors and Lymphomas	OncoNano Medicine	Intratumoral injection	A safety and efficacy study with or without Cemiplimab	NCT06022029
TXN10128, an inhibitor of ENPP1	Phase 1 (recruiting)	Locally advanced (unresectable) or Metastatic Soild Tumors	Txinno Bioscience	Capsules orally	A safety,pharmacodynamics, and pharmacokinetic study	NCT05978492
KL340399	Phase 1 (recruiting)	Advanced Solid Tumors	Sichuan Kelun Pharmaceutical Research Institute Co.,Ltd	Intratumoral injection	A safety, tolerabilit, Pharmacokinetics and Preliminary Efficacy Study	NCT05387928
KL340399	Phase 1 (recruiting)	Advanced Solid Tumors	Sichuan Kelun Pharmaceutical Research Institute	Intratumoral injection	Safety, tolerability, pharmacokinetic (PK) profile, and anti-tumor efficacy	NCT05549804
SB 11285	Phase 1a/1b (completed)	Advanced Solid Tumors	InvoX Pharma Limited	Intravenous injection	A safety study with/without atezolizumab	NCT04096638
BMS-986301	Phase 1 (completed)	Advanced Solid Cancers	Bristol-Myers Squibb	Intramuscular, Intratumoral, and intravenous injection	A safety and route study with/without nivolumab and ipilimumab	NCT03956680
MK-2118	Phase 1 (terminated)	Lymphoma and advanced solid tumors	Merck Sharp & Dohme LLC	Intratumoral, subcutaneous injection	A safety and maximum tolerable dose study with/without pembrolizumab	NCT03249792
Ulevostinag (MK-1454)	Phase 2 (completed)	Metastatic or Unresectable, Recurrent Head and Neck Squamous Cell Carcinoma (HNSCC)	Merck Sharp & Dohme LLC	Intratumoral injection	A safety study with MK-1454 and pembrolizumab VS pembrolizumab	NCT04220866
MK-1454	Phase 1 (completed)	Advanced/Metastatic Solid Tumors or Lymphomas	Merck Sharp & Dohme LLC	Intratumoral injection	A safety study with/without pembrolizumab	NCT03010176

NF-κB pathway dependent. This antiproliferative activity was independent of TBK1 and IRF3 recruitment and IFN. Wu [94] et al. proposed that STING-mediated IFN-independent T-cell death occurs after IFN-dependent T cell recruitment to the tumor and requires palmitoylation of STING on the Golgi apparatus. Inhibitors targeting STING palmitoylation effectively block STING-mediated T cell death in vitro. STING-mediated T cell death may vary with different types of STING agonists [94]. Different STING agonists have been reported to stimulate different degrees of calcium leakage from the ER when STING leaves the ER. In addition to the presence of some IFN-independent STING activity in BMDM, STING activity in T cells is predominantly IFN-independent, such as Th17 signaling, Th1 pathway, NF-κB, NFAT, UPR, IL-2 pathway and cell death [95]. And excessive IFN has also been reported to promote apoptosis in DCs [96]. Therefore, the development of novel STING agonists should minimize the dosage, not only to avoid toxicity but also to have targeted properties.

RT combined with STING agonist can not only promote the immunostimulatory TME, but also promote the inflammatory TME, to achieve the maximum anti-tumor effect [19, 21, 23, 97, 98]. STING activation promotes the activation of downstream NF-κB and MAPK pathways, which, together with IRF3, drive the transcription of pro-inflammatory cytokine genes [99]. Phosphorylation of IκB kinase (IKK) recruits NF-κB to the nucleus and promotes transcription of genes encoding the pro-inflammatory cytokines IL-6 and TNF-a. How STING activates the MAPK pathway remains to be elucidated. Overactivation of the cGAS-STING pathway in normal tissues leads to an overproduction of type I IFN, which can cause a range of inflammatory diseases, known as "type I interferonopathies", such as autoimmune diseases and chronic inflammatory diseases [85]. Diseases currently associated with overactivation of the cGAS-STING pathway include systemic lupus erythematosus (SLE), aicardi–Goutières syndrome (AGS), silicosis, neurodegenerative diseases, etc. [100]. And hyperactivation of the cGAS-STING pathway in various cells can trigger a cytokine storm, characterized by the uncontrolled release of pro-inflammatory cytokines (IL-1, IL-6, IFN-γ, TNF-a, and IL-18), leading to severe systemic inflammatory responses and potentially resulting in multi-organ failure [83, 84]. Cytokine storms manifest with a range of clinical symptoms, including fever, hepatosplenomegaly, progressive liver failure with coagulopathy, cytopenia, and hyperferritinemia.

Beyond cytokine storm-mediated toxicity, dysregulated activation of the cGAS-STING pathway may potentiate radiation-induced normal tissue complications, including pneumonitis and enteritis [86]. Du et al. demonstrated that RT-induced dsDNA release from hepatocytes activates the cGAS-STING pathway in hepatic non-parenchymal cells (NPCs), triggering type I IFN production that paradoxically exacerbates radiation-associated hepatocellular damage [101]. Zhao et al. revealed that radiation-generated cytosolic dsDNA engages cGAS-STING signaling in pulmonary macrophages, driving their M1 polarization and excessive secretion of IL-6/IL-1β, which amplifies inflammatory cascades and culminates in acute lung injury [102]. As a type of innate immune cell, macrophages play a key role in the development of radiation-induced lung injury (RILI) [103]. In the early stages of RILI, macrophages are activated and polarized into the M1 phenotype, leading to the production of pro-inflammatory cytokines. In the later stages of radiation-induced pulmonary fibrosis, M2 activation promotes aberrant repair. The activation of the cGAS-STING pathway after RT also triggers the senescence-associated secretory phenotype (SASP), which in turn facilitates tissue fibrosis [104]. For example, the senescence of type II alveolar cells [105] and alveolar stem cells [106] contributes to radiation-induced fibrosis (RIF) in the lungs.

Cell type-specific activation of the cGAS-STING pathway

Besides various tumor cells, STING is also expressed in other cells, including all APCs, endothelial cells (ECs), MDSCs, T cells, NK cells and B cells (Fig. 4A). RT activates the cGAS-STING pathway in tumor cells, and while dsDNA and cGAMP can be transmitted to myeloid cells through multiple mechanisms to activate their cGAS-STING pathway, this activation is often transient and insufficient. This limitation arises partly due to radiation dose constraints and partly due to the immunosuppressive TME. To evade immune surveillance and promote tumor progression, invasive tumor cells often exhibit low STING protein expression [107] and may also be unresponsive to type I IFN [108]. Understanding the mechanisms and biological effects of cGAS-STING pathway activation across different cell types [109], and selectively activating cGAS-STING signaling in relevant cells, could facilitate the effective combination of RT and STING agonists.

Tumor vascular ECs

Compared to normal blood vessels, tumor vessels are characterized by slow and irregular blood flow, uneven diameters, irregular branching (vessels are tortuous), many dysfunctional microvessels, high erythrocyte flux, permeability/leakage due to excessively large pores, increased interstitial fluid pressure (IFP), low or lack of pericyte coverage, and the vessels may lack a basement membrane or have an abnormally thick basement

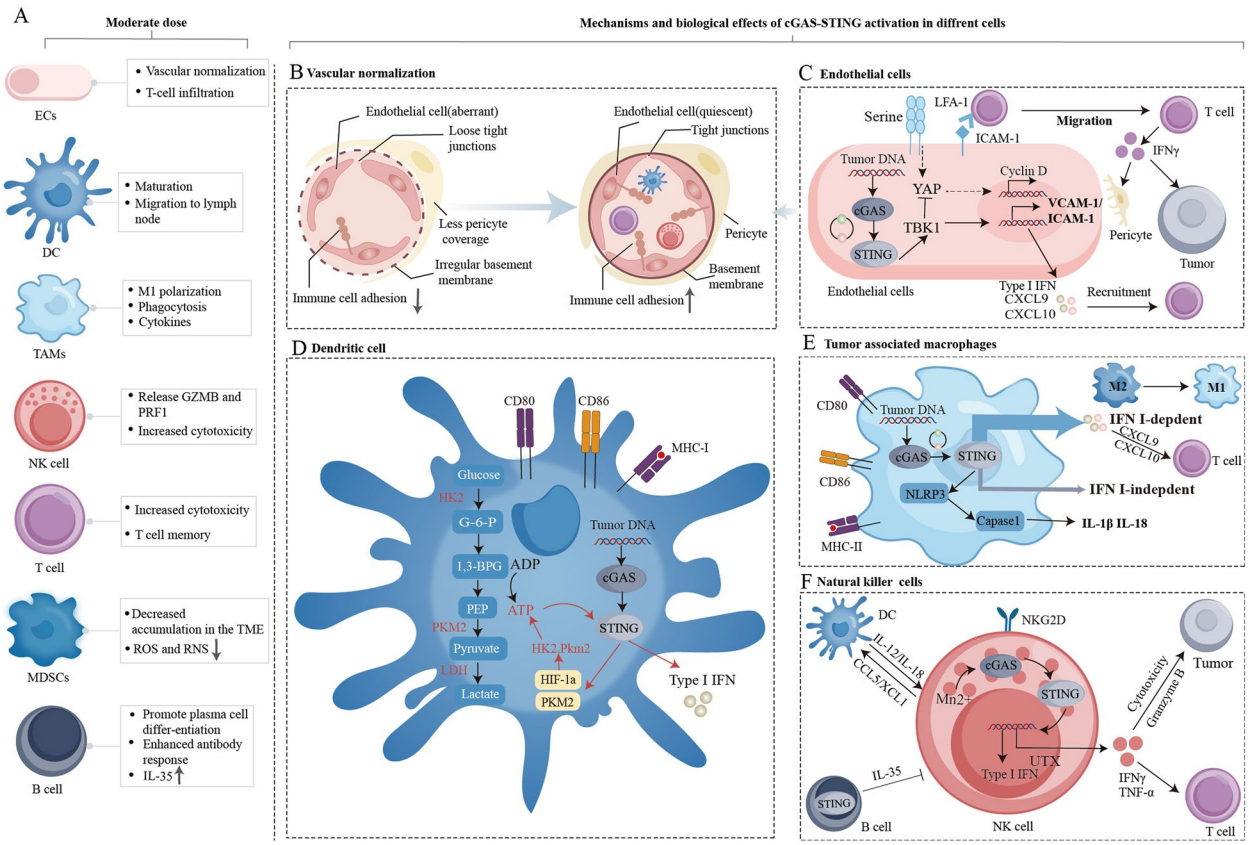

Fig. 4 Mechanisms and biological effects of cGAS-STING activation in different cells. **A** STING activation in different cells can produce different biological effects. Moderate STING agonists can have a stimulatory effect on immune cells. **B** vascular normalization. **C** Activation of the cGAS-STING pathway in tumor vascular ECs promotes vascular normalization and enhances T-cell infiltration. Inhibition of serine metabolism facilitates the activation of the cGAS-STING pathway in tumor vascular ECs. **D** Activation of the cGAS-STING pathway in DCs promotes their maturation and migration to lymph nodes, thereby enhancing the process of antigen cross-presentation. Glycolysis and the cGAS-STING pathway mutually reinforce each other. **E** Activation of the cGAS-STING pathway in TAMs drives polarization from the M2 to the M1 phenotype and enhances antigen presentation. STING activation promotes both type I IFN-dependent pathways, including STING/TBK1/IRF3 and STING/IKK/NF-κB, as well as type I IFN-independent pathways, such as the antigen presentation pathway. **F** Activation of the cGAS-STING pathway in NK cells directly enhances their activation, thereby exhibiting enhanced killing and secreting activity

membrane [110–112]. Collectively, these properties lead to a hypoxic state and accumulation of metabolic waste products that favor the recruitment of macrophages, T_{reg} cells and MDSCs, while inhibiting $CD4^+$ and $CD8^+$ T cells, NK cells, and DCs [110, 113, 114]. Leukocyte infiltration into tumors is a multistep event regulated spatiotemporally by leukocyte rolling, crawling, firm adhesion, arrest, docking structure formation and transendothelial migration on ECs. This process is initiated by inflammatory cytokines such as TNF-a, primarily through activation of the NF-kB pathway. In response to inflammatory cytokines, IkB is ubiquitinated and degraded, leading to nuclear translocation of the NF-kB complex and expression of molecules mediating endothelial-leukocyte interactions [115]. The molecules of endothelial-leukocyte interaction, i.e. adhesion molecules, mainly include intercellular adhesion molecule-1 (ICAM-1), vascular cell adhesion molecule-1 (VCAM-1), E-selectin, P-selectin, platelet endothelial cell adhesion molecule-1 (PECAM-1, CD31) and CD99 [116, 117]. However, VEGF released by tumor cells inhibits TNF-a signaling-induced gene expression by interfering with components of the NF-kB pathway (reduction of p-IKKa/b and inhibition of IkB degradation), including T-cells attracting chemokines CXCL10 and CXCL11 and intercellular adhesion molecules [118]. CXCL10 and CXCL11 act as chemotactic agents for T cells through their interaction with the shared T cell receptor, CXCR3. The dysfunctional tumor vasculature primarily inhibits the homing of $CD8^+$ T cells through the following mechanisms. Tumor-derived angiogenic growth factors such as VEGF and endothelin-1 (ET-1) signal through their respective homologous receptors, VEGFR and ETBR, to inhibit T cell infiltration into tumors by suppressing the expression of adhesion

molecules like ICAM-1 and VCAM-1 [119–121]. Under the influence of tumor-derived factors such as VEGF, ECs can directly inhibit T cell activation by upregulating inhibitory molecules including PD-L1, PD-L2, T cell immunoglobulin mucin-3 (TIM-3), B7-H3 (known as CD276), IDO-1, IL-6, and IL-10 [113]. Tumor ECs can also express FasL and tumor necrosis factor-related apoptosis-inducing ligand (TRAIL), leading to T cell apoptosis [122]. Additionally, the aberrant tumor vasculature is believed to hinder drug delivery and contribute to resistance to RT [113].

Vascular normalization is regarded as an effective vascular-targeted therapeutic strategy [123](Fig. 4B). Unlike anti-angiogenic approaches that prune the tumor vasculature, vascular normalization restores the abnormal tumor vasculature to a more normal state, thereby reinstating structural and functional vascular integrity [124]. During vascular normalization, disorganized and highly proliferative tumor ECs become more quiescent and less active. Normalized endothelium tends to form tighter interendothelial junctions between neighbouring cells, which involve adhesion junction molecules such as tight junctions (e.g., zona occludens (ZO)−1, ZO-2 and Claudin-5) [125]. Pericyte coverage was significantly enhanced, and the basement membrane appeared more normalized, contributing to a strengthened and matured vascular network. Importantly, these structural changes were accompanied by functional improvements in the tumor vasculature, as evidenced by increased vascular perfusion, reduced vascular permeability, and alleviation of hypoxia [124]. In particular, vascular normalization promotes infiltration of T lymphocytes, DCs and NK cells, polarizing TAMs from M2 to M1, while impeding T_{reg} cells and MDSCs [110, 126].

Activation of STING in tumor ECs normalizes the tumor vasculature and enhances endothelial-lymphocyte interactions, thereby promoting intratumoral infiltration of activated $CD8^+$ T cells [127]. ECs represent a crucial target for STING activation within the TME. Compared to other stromal cells, the ECs exhibits the most pronounced STING expression [128]. The level of STING expression in ECs varies across different tumor models. Compared to the MMTV-PyMT breast cancer model, CT26 colon cancer and Lewis lung carcinoma (LLC) models demonstrate stronger endothelial STING expression [129]. High endothelial STING expression is associated with a reduced incidence of lymphovascular infiltration within tumor tissue, increased $CD8^+$ T cell infiltration, and a favorable prognosis in cancers [129].

DCs are generally considered the primary source of type I IFNs during immune responses. However, one study suggests that ECs, rather than DCs, are the main IFN-producing cells in response to STING activation within the TME. One reason for this is that ECs exhibit an enhanced capacity to produce type I IFNs in response to STING activation compared to DCs or macrophages [130]. Another factor contributing to the preferential production of type I IFNs by ECs may be their relative abundance in the TME compared to other immune cells. STING activation in ECs primarily induces IFN-β expression, while IFN-α mRNA is barely detectable [128]. In contrast, DCs or macrophages can produce both IFN-α and IFN-β following STING activation. This discrepancy might be related to the limited capacity of ECs to produce IFN-α upon STING activation, but it could also be due to the requirement of IFN-β-mediated IRF7 upregulation for IFN-α expression [131]. IFN-β can act directly on ECs, presumably in an autocrine or paracrine manner. EC-derived type I IFN initiates an anti-tumor response prior to infiltration of DCs and $CD8^+$ T cells in the TME [128].

Activation of the cGAS-STING pathway in tumor ECs upregulates vascular stabilization genes (Angpt1, Pdgfrb, Mcam, Cdh5, and Col4a) and adhesion molecule genes (Icam1, Icam2, Vcam1, Sele, and Sell), while also promoting the production of type I IFN and inflammatory cytokines [129, 132](Fig. 4C).These transcriptional changes ultimately induce tumor vascular normalization, enhanced pericyte coverage and more intact basement membranes, thereby promoting the intratumoral infiltration of effector $CD8^+$ T cells and alleviating hypoxia in the TME. Vascular normalization and the effects of RT promote the accumulation of immune cells such as M1-like macrophages, $CD8^+$ cytotoxic T-cells and Th1 cells in the tumor tissue, which secrete secreted IFN-γ. IFN-γ stimulates pericyte recruitment by inhibiting EC proliferation and upregulating leucine-encoding genes (for example, CXCL9, CXCL10 and CXCL11) [126]. Moreover, IFN-γ primarily induces the regression of immature tumor ECs lacking pericytes, while those ECs with pericytes can tolerate IFN-γ-mediated vascular damage [133]. The increased pericyte coverage, a hallmark of tumor vascular normalization, coincides with peak $CD8^+$ T cell infiltration into the TME. This demonstrates crosstalk between endothelial STING activation promoting vascular normalization and facilitating T cell migration. Insufficient T cell infiltration and antibody perfusion in solid tumors are major obstacles to the efficacy of ICB therapy. STING agonists targeting the vascular endothelium increase T cell infiltration, potentially enhancing the response to ICB [129, 134]. STING agonists also exhibit effective synergy with VEGF inhibitors, highlighting the potential of integrating anti-angiogenic agents with vascular immunotherapies [135]. In addition to the above mechanisms, activation of the cGAS-STING pathway in tumor ECs also impacts their metabolism.

Activation of the cGAS-STING pathway induces phosphorylation and inactivation of the cell cycle regulatory transcription factor YAP1, impairing the transcription of cyclin D genes and thereby reducing angiogenesis [136]. Inhibition of serine metabolism can lead to YAP degradation, resulting in TBK1 activation and increased production of type I IFN and related cytokines [137]. Serine can be obtained from two sources: extracellular uptake and de novo synthesis from glycolytic intermediates. The flux through the serine biosynthesis pathway (SSP) involves three enzyme-catalyzed reactions that convert 3-phosphoglycerate into serine [138]. Inhibition of the EC glycolytic metabolic process can promote the activation of the cGAS-STING pathway, thereby promoting tumor vessel normalization.

DCs

The TME is a highly stressful, almost hostile environment for APCs, inhibiting the normal function of APCs [139]. Activation of the cGAS-STING pathway in APCs promotes the maturation and cross-presentation of APCs to promote T-cell activation. APCs primarily comprise macrophages and DCs, with DCs being the most potent APCs. Although DCs constitute only 1% of peripheral blood mononuclear cells, they express a diverse array of antigen-presenting molecules on their surface, including MHC-I and MHC-II, as well as co-stimulatory factors (CD80/B7-1, CD86/B7-2, CD40, CD40L, etc.) and adhesion molecules (ICAM-1, ICAM-2, ICAM-3, LFA-1, LFA-3, etc.). The superior cross-presentation capabilities of DCs are primarily attributed to their adept antigen-handling properties. DCs preserve antigens from degradation by lysosomal proteases through the expression of low levels of these enzymes. Furthermore, as most lysosomal proteases are optimally active at acidic pH, maintaining a strongly alkaline environment within the cross-presentation compartment serves to inhibit protease activity, thereby safeguarding antigens from degradation. The alkalinization of phagosomes in DCs is chiefly facilitated by the action of nicotinamide adenine dinucleotide phosphate (NADPH) oxidase-2 (NOX2) [140]. DCs encompass several subsets, as shown in Table 2. Based on their origin and differentiation pathways, DCs can be classified into conventional DCs (cDCs), plasmacytoid DCs (pDCs), monocyte-derived DCs (MoDCs), and Langerhans cells (LCs). cDCs are further subdivided into type 1 conventional DCs (cDC1) and type 2 conventional DCs (cDC2). cDC1 is characterized by the unique expression of the C-type lectin receptor CLEC9 A and the chemokine receptor XCR1. cDC1 is adept at cross-presenting exogenous antigens to $CD8^+$ T cells and is essential for cytotoxic T lymphocyte (CTL) responses [141]. The amount of cDC1 in cancer is positively correlated with patient survival, and can be used to predict the efficacy of anti-PD-1 therapy in melanoma [142, 143]. Therefore, increasing the amount of cDC1 in tumors may be an effective way to improve antitumor response. cDC2 are identified by their high expression of MHC II, CD11c, and SIRPA, and express a range of Toll-like receptors (TLRs). cDC2 is predominantly associated with $CD4^+$ T helper cell responses, presenting MHC class II to $CD4^+$ T helper cells. Although cDC1 is the most potent subgroup for cross-presentation of tumor antigens, the maximal induction of CTL responses involves the interaction of cDC1 and cDC2. MoDCs can be recruited into inflammatory sites by C–C-chemokine factor 2 (CCR2), and these cells typically perform various functions in tissues [144]. LCs are a unique population of mononuclear phagocytes that are restricted to the epidermal skin layer and are mainly associated with tolerance and priming [145]. pDCs also exhibit antigen cross-presentation capabilities, but pDC-derived exosomes transfer antigens to bystander cDC1. Notably, pDC are potent producers of type I and type III IFN and play a major role in antiviral immunity and autoimmune diseases [146]. The innate sensing of nucleic acids remains the major initiating factor for IFN production by pDCs [147]. pDC has been identified as a potential target for novel cancer therapies. Following tumorigenesis, DCs infiltrate solid tumors, where they are referred to as tumor-infiltrating DCs (TIDCs) [148]. Within the TME, all DC subpopulations may be present, albeit with phenotypes and functions that differ from those in healthy tissues. TIDCs are distinguished by high levels of activation markers, such as MHC and CD80/86, as well as markers associated with immune tolerance, including IDO-1 and PD-L1. Tumors frequently induce immunodeficiency in TIDCs, significantly impairing their capacity to produce type I IFN [149]. A characteristic feature of immunologically dysfunctional TIDCs is an increased intracellular lipid content and augmented mitochondrial respiration [27]. Therefore, to facilitate the completion of the cancer-immunity cycle, it is crucial not only to employ cytokines to enhance the infiltration of DCs into tumor tissues but also to effectively promote DC antigen presentation and maturation [27].

Type I IFNs enhance nearly all DCs functions, including promoting monocyte differentiation into DCs, facilitating DCs migration to secondary LNs, upregulating co-stimulatory activity of DCs, and augmenting their ability to cross-present antigens to T cells [96]. Type I IFNs treatment enhances antigen presentation through the following mechanisms: type I IFNs reduces the rate of acidification of intracellular lysosomes, thereby augmenting antigen retention in DCs. Additionally, type I IFNs stimulates the transcription and translation of the

Table 2 Dendritic cell subsets

DC subsets	Key transcription factors	Maker	Functions
cDC1 	BATF3, IRF8	Human: XCR1, CLEC9 A, CD141, CD11c, HLA-DR, CD141 Mouse: XCR1, CLEC9 A, SIRPa, MHCII, CD8a (resident), CD103(migratory), CD11c, CD24, FLT3, CD45RB	$CD8^+$ T cell cross-presentation, CTL initiation, IL-12, IL-6 secretion
cDC2 	IRF2, IRF4, RelB, RBP-J	Human: CD11b, CD11c, CD1c, CD172a, CD5, HLA-DR, FCER1 A Mouse: CD11c, CD11b, FLT3, CD45RB, MHCII, CD172a, Various subset-specific Markers (CLEC9 A, ESAM)	Antigen-presenting $CD4^+$ T cells, helper T cell initiation, IL-6, TNF-α, IL-23 secretion
pDC 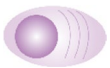	E2-2	Human: HLA-DR, CD11c, CD123, CD303 (BDCA2), CD304, CCR2, CXCR3 Mouse: CD11c(medium), MHCI1(low), B220, CD317, SIGLECH, CD172a, CCR2, CCR9, CXCR3	Type I IFNs
moDC 	KLF4	Human: CD11c, HLA-DR, CD11b, CD1a, CD1c, CD14, CD64, CD206, CD172a, CCR2 Mouse: CD11c, CD11b, MHCII, CD64, CD206, CD14, CCR2	Inflammation, antigen presentation, and TNF-α, IL-12, IL-23 secretion
LCs 	-	Huma: CD11c, HLA-DR, CD207, CD11b, CD24, CD1c, CD1a, EpCAM Mouse: CD11c, MHCII, CD207, CD11b, CD24, EpCAM	Tolerance and priming

immunoproteasome subunits β1i (LMP2), β2i (MECL-1), and β5i (LMP7), consequently enhancing peptide binding and presentation on MHC class I molecules [150, 151]. However, it should be noted that some studies have suggested that type I IFN is a double-edged sword for DCs and can also inhibit DCs differentiation [152]. Excessive type I IFN disrupts DC homeostasis, affecting their development, generation, migration, functional regulation, and self-renewal. Elevated levels of type I IFN also inhibit the production of IL12p70, a heterodimer composed of p40 and p35 subunits, predominantly synthesized by DCs and macrophages, which is crucial for enhancing the activity of cytotoxic T cells and NK cells [153]. Moreover, type I IFN induces the upregulation of PD-L1 and IDO-1 in DCs, contributing to the suppression of T cell responses to tumors. Additionally, type I IFN promotes apoptosis in DCs through the production of inflammatory factors, induction of the Fas/FasL signaling pathway, and mitochondrial stress.

The cGAS-STING pathway in DCs is 100% more sensitive compared to other APCs [154]. Different DC subpopulations exhibit varying levels of STING expression, with the hierarchy in mice being pDC > cDC2 > cDC1 and in humans cDC2 > pDC > cDC1 [155]. One study further found that cGAS and STING expression is comparable in two subpopulations of human pDC, $CD2^{high}$and

$CD2^{low}$ [147].These subpopulations may engage distinct STING signaling pathways. In murine studies, both the cDC1 and cDC2 populations demonstrated similar signaling events within the STING pathway, including the simultaneous activation of NF-κB, TBK1, IRF3, and STING itself. Although pDCs displayed the highest total levels of STING proteins, they exhibited only modest phosphorylation of STING and activation of IRF3, with minimal activation of NF-κB. Pratik et al. did not observe cGAS-STING-stimulated NF-κB nuclear translocation and NF-κB-dependent cytokine production (TNF-α) in human pDC study [147]. Not only that, STING activation is followed by differential cell death response. Mouse pDC were more sensitive to cell death after STING activation than cDC1 and cDC2 [155]. Intrinsic apoptosis is the main mechanism of STING-dependent death of cDCs. STING activation dependently resulted in rapid death of mouse pDC that were partially dependent on intrinsic apoptosis, but this was not observed in human pDC. pDC of both species produced IFN-α, whilst all DC subsets produce IFN-λ2 and IFN-λ3 proteins upon STING activation. IFN-λ1 was the most highly expressed IFN from all human DC subsets, an isoform not present in the mouse genome. The IFN-λ family of genes differs between human and mouse in that the mouse genome encodes only 2 highly homologous genes, IFN-λ2 and IFN-λ3, whilst the human genome universally encodes 3 genes, IFN-λ1, -λ2 and -λ3. These data strongly suggest differential regulation of the STING signaling pathway between cDC and pDC. Selectable activation of the cGAS-STING pathway in DCs subtypes is essential for anti-tumor immunity and reduction of toxic side effects.

Activation of cGAS-STING pathway in immature DCs stimulates the production of type I IFN and pro-inflammatory factors, thus facilitating DC maturation (Fig. 4D). In DCs, cGAS-STING activation enhances antigen uptake, facilitates lysosomal escape of antigens, and upregulates MHC-I, CD40, CD80, and CD86, thereby improving antigen presentation. Additionally, the expression of CCR7 and MIP-3β in DCs is increased, promoting DC migration towards LNs [156]. Upregulation of CCR7 and MIP-3β expression is also characteristic of DC maturation [156]. Type I IFN can induce DCs to express a range of ISGs, such as CXCL10, CXCL9, and CCL5, thereby further promoting T cell activation and proliferation [27, 157]. Notably, distinct DC subsets exhibit differential sensitivity to type I IFN, which may drive divergent functional outcomes in immune regulation. DC intrinsic STING signaling regulation remains unclear. A study has shown that ATP, produced through glycolysis, enhances the phosphorylation of STING in DCs, thereby activating the STING pathway [158] (Fig. 4D). This finding underscores the indispensable role of glycolysis-derived ATP in cytosolic DNA sensing. Intrinsic STING activation in DCs accelerates HIF-1α-mediated glycolysis, which in turn drives STING signaling to enhance DC-mediated anti-tumor immune responses, establishing a positive feedback [158]. The elevated protein levels of HIF-1α induce the upregulation of glycolytic enzymes, such as hexokinase 2 (HK2) and pyruvate kinase M2 (PKM2), thereby enhancing glycolysis. The glycolytic pathway is essential for STING-dependent anti-tumor activity in DCs, thus defining a key metabolic mechanism for DC-intrinsic STING signaling regulation. Additionally, another study propose that oxidative stress ROS triggers the accumulation of SENP3 in DC, enabling SENP3 to promote SENP3-IFI204 interactions and facilitating IFI204 de-SUMOylation, which drives cytosolic DNA-induced STING phosphorylation [159]. Disruption of SENP3 in DCs specifically inhibits STING-dependent cytoplasmic DNA sensing and attenuates anti-tumor T cell responses. Furthermore, ROS-mediated oxidative stress, a hallmark of the TME, activates immunosuppressive mechanisms and induces DNA oxidation, thereby enhancing DC immune recognition.

TAMs

Macrophages are the predominant immune cells in the TME, comprising up to 50% of hematopoietic cells in various cancers [160]. These cells are generally categorized into two phenotypic groups: pro-inflammatory M1 macrophages and anti-inflammatory M2 macrophages. TAMs are an important type of tumor infiltrating immune cells that primarily play an immunosuppressive role. M1 and M2 macrophages represent two extremes on a functional continuum of fully polarized anti-tumor TAMs and immunosuppressive TAMs, respectively [161]. In TAMs, STRN4 mediates PP2A binding to Hippo kinase MST1/2 for its dephosphorylation, stabilizing yes-associated protein/transcriptional coactivator with PDZ-binding motif (YAP/TAZ) to antagonize STING activation [162]. Within tumors, TAMs are the principal host cells involved in the cGAS-STING signaling pathway [163]. Tumor-derived cGAMP or dsDNA can activate the cGAS/STING/TBK1/IRF3 or STING's downstream NF-κB pathway of TAMs, promoting the production of type I IFN and pro-inflammatory factors such as TNF-α and IL-10 [163](Fig. 4E). This process facilitates the polarization of M2 to M1, enhances antigen presentation, and subsequently induces the differentiation of $CD4^+$ and $CD8^+$ T cells to generate a robust anti-tumor response. Several chemokines induced by type I IFN signaling of TAM, such as CXCL9, CXCL10, and CCL5, play a critical role in promoting the trafficking and infiltration of cytotoxic T lymphocytes (CTLs) [95]. Moreover, STING activation can activate the inflammasome (NLRP3),

facilitating the secretion of interleukin-18 (IL-18) and interleukin-1β (IL-1β) by macrophages. This process optimizes the anti-tumor activity of NK cells by promoting the expression of 4-1BBL on macrophages and 4-1BB on NK cells [164].The polarization of macrophages within the TME appears highly complex; besides the aforementioned mechanisms, IFN-γ-induced activation of STAT1 also promotes the polarization of macrophages towards the M1 phenotype [165, 166]. The key transcription factors STAT5, and IRF5 have also been shown to regulate M1 gene expression [167]. Tumor-derived microparticles (T-MPs) containing nuclear and mitochondrial DNA fragments can stimulate the cGAS/STING/TBK1/STAT6 signaling pathway in macrophages, resulting in macrophage polarization towards the M2 phenotype [168]. The key transcription factors STAT3, IRF4, JMJD3, PPARδ, and PPARγ are also implicated in driving macrophages towards M2 polarization [165–167].

STING activation is also followed by activation of several other biological activities in macrophages that are not dependent on type I IFN, such as antigen presentation, HMGB1 signaling, and P38 MAPK signaling [95]. Macrophages are recognized as professional APCs (Fig. 4E); In macrophages, STING activation induces more type I IFN-dependent than type I IFN-independent responses, both of which contribute to anti-tumor immunity. however, unlike DCs, macrophages are non-motile and typically contain higher levels of lysosomal proteases, leading to rapid antigen degradation and consequently limiting antigen cross-presentation [169]. Activation of the cGAS-STING pathway in macrophages delays antigen degradation and enhances the expression of CD80, CD86, and MHC-II molecules, thereby facilitating antigen cross-presentation to T cells (Fig. 4E). Wu et al. and Yang et al. revealed STING induced upregulation of the antigen cross-presentation pathway in macrophages is type I IFNs independent [20, 95]. ZnCDA is a nano-mediated STING agonist that targets the activation of the cGAS-STING pathway in macrophage, and its anti-tumor effect was ineffective after blocking the mouse IFN-γ receptor Ifng, while it remained effective after knocking down mouse type I IFN receptor Ifnar1 or IRF3, and anti-TNF-α, anti-IL-6R blockade [20]. This suggests that the anti-tumor effect of ZnCDA was also dependent on IFN-γ rather than on type I IFN. IFN-γ and type I IFNs show significant overlap in their immune functions, but IFN-γ has a greater immunomodulatory potential because it not only promotes the overall optimization of the immune response, but it also strives to limit the inflammatory response that causes collateral damage to the tissues and organisms [170]. The p38 mitogen-activated protein kinase (MAPK) pathway in macrophages plays a crucial role in the polarization of these cells and enhances their capability for antigen presentation, among other key functions [171]. HMGB1, a critical nuclear factor, functions beyond its traditional role when released extracellularly as a DAMP. In the extracellular space, HMGB1 is implicated in various physiological and pathological processes in macrophages. It mediates pro-inflammatory responses, augments antigen presentation, regulates cell migration, and influences immune tolerance.

CD47 is a transmembrane protein that is highly expressed in tumor-initiating cells. Elevated expression of CD47 inhibits the phagocytic activity of macrophages by engaging its receptor, signal regulatory protein α (SIRPα), which is expressed on macrophages, thereby allowing tumor cells to evade immune surveillance [172]. Studies have shown that treatment with anti-CD47 antibodies can enhance phagocytosis. Due to increased phagocytosis and the limited capacity of macrophages to clear engulfed material, there is an abnormal accumulation of tumor cell-derived DNA in the macrophage cytoplasm. Excessive DNA derived from tumor cells can significantly activate the cGAS-STING signaling pathway in macrophages, thereby enhancing antigen presentation and promoting the activation and differentiation of $CD8^+$ T cells, which in turn exerts anti-tumor effects. During tumor progression, the rapid processing of dying tumor cells by TAM prevents the immune system from alarming, effectively eliminating the source of extracellular cGAMP. The specific expression of MerTK in TAM, which binds to the MerTK ligands (Gas 6 and Pros 1) of apoptotic cells, may mediate phagocytosis of dying tumor cells by macrophages, thereby inhibiting immune in response to tumor cell death Activation. Thus, anti-MerTK antibody promotes the avoidance of phagocytosis of dying tumor cells by TAM and the release of dying tumor DNA, thereby activating the cGAS-STING pathway of TAM [173].

There are fewer APCs in the TME, so it is particularly important to design nanoparticles targeting APCs. Macrophages and DCs share some common receptors, and nano-mediated STING agonists can target both macrophages and DCs to activate anti-tumor immunity. For example, since mannose receptor and phosphatidylserine (PS) receptor is expressed in macrophage and DCs, it is possible to modify mannose or PS on the surface of nanomaterials to target APCs [174]. The STING agonist MnO_2@OVA [98] can target both macrophages and DCs via mannose modification, thereby activating the cGAS-STING pathway in both cells.

NK cell and other immune cells

Based on the expression of CD56 and CD16, NK cells can be divided into two main subsets: $CD56^{bright}$ $CD16^{-}$ NK cells and $CD56^{dim}$ $CD16^{+}$ NK cells. $CD56^{bright}$ $CD16^{-}$ NK cells secrete large amounts of cytokines, such as IFN-γ and TNF-α, as well as chemokines like CCL5 and XCL1, which attract cDC1 to the TME [175] (Fig. 4F). $CD56^{dim}$ $CD16^{+}$ NK, which constitute a significant proportion of NK cells in the spleen and peripheral blood, are highly cytotoxic [176]. In the early stages of killing, they directly lyse cancer cells through the release of perforin and granzymes, while in later stages, they induce apoptosis via FasL or TRAIL expression, independent of prior antigen priming [177]. Upon activation by cytokines including IL-15, IL-12, IL-18, and IL-2, NK cells can directly lyse target cells. NK cells express HLA-specific activating receptors, such as NKG2C and NKG2E, as well as the non-HLA-specific activating receptor NKG2D [178]. As cytotoxic lymphocytes, NK cells serve as an important complement to T cell-based immunotherapies, particularly in cancers lacking T cell-specific antigens or MHC molecules [179].

Type I IFN is critical in controlling NK cell anti-tumor responses, including limiting metastasis formation in breast cancer models [180]. In addition, Type I IFN has been shown to play an important role in NK cell development, homeostasis, and the formation of memory responses [181]. In NK cells, Type I IFN stimulation activates mainly STAT1 and, to a lesser extent, STAT3 signaling for transduction [182]. STAT1 and STAT3 are major regulators of cytotoxicity and IFN production in NK cells [181]. IFN-γ plays a crucial role in the cytotoxicity of NK cells and, in addition, IFN-γ has been shown to contribute to the activation of $CD8^{+}$ T cells. STING signaling may play an important role in regulating NK cell function. However, the exact mechanism by which endogenous cGAS-STING signaling in NK cells and its downstream key genes regulate NK cell activity is unknown. NK cell proliferation is not affected by cGAS or STING, but NK cell activation is affected by the cGAS-STING pathway [183]. A study suggests that Mn^{2+} modulates ubiquitously transcribed tetratricopeptide repeat on chromosome X(UTX) expression through activation of cGAS-STING signaling to enhance NK cell responsiveness [183](Fig. 4F). Inhibition of UTX leads to eradication of STING agonist-induced NK cell activation in mice. UTX is a key molecular mediator involved in the effector response of NK cells. Mn^{2+} enhances CD107a expression and stimulates the production of IFN-γ, granzyme B, and perforin in mouse and human NK cells in vitro, leading to a significant increase in cytotoxicity against tumor cells. Another study suggests that STING functions as an intrinsic factor responsible for maintaining the reservoir of $TCF\text{-}1^{+}$ NK cells within the TME [184].

STING activation in T cells promotes T cell recruitment to tumors, but over-activation also leads to T cell death [95], as will be carefully described in the following sections. cGAMP-mediated STING activation in MDSC inhibits ROS and RNS production and suppresses immunosuppressive TME [162]. While STING agonists exert anti-tumor effects through IL-35 production by B cells, this activation paradoxically impairs NK cell effector functions [185]. It has been suggested that STING negatively regulates BCR signaling in normal and malignant B cells [186].

Nano-STING agonists-mediated anti-tumor immunity for enhanced RT

Nanomedicine provides a controlled platform to potentiate the synergy between STING agonists and RT while mitigating systemic toxicity (Table 3). Currently, most nano-STING agonists are primarily administered via intravenous or intratumoral routes to precisely target either tumor cells or immune cells within the TME. Nanocarriers for delivering STING agonists include liposomes [20, 187], cationic polymers [188], inorganic nanoparticles [43, 98, 189, 190], polymeric micelles [191], vesicles [192], exosomes [193], and bionanoparticles [109]. The application of these nanomedicines can improve the membrane permeability and stability of STING agonists, facilitate lysosomal escape, and enable targeted and controlled release of STING agonists. Furthermore, these nanomedicines possess multifunctionality; they can serve as radiosensitizers to enhance the efficacy of RT and can be combined with other treatments such as surgery, chemotherapy, and PTT to work synergistically. For example, Yang [20] et al. constructed PEGylated neutral liposomes, ZnCDA, comprising a non-toxic zinc phosphate hydrophilic core loading STING agonist CDA and a lipid bilayer composed of PEG-conjugated phospholipids (ZnP). This platform enables the delivery of the STING agonist across cell membranes into target cells. The delivery of cGAMP using liposomal NP-cGAMP enables it to evade enzymatic hydrolysis, and ultimately achieve controlled cytosolic release via lysosomal escape [23]. PEGylation and neutral charge of CPs-CDN facilitate evasion of phagocytosis, not only ensuring high and stable loading of ADU-S100 but also enhancing its cytosolic release in DCs [19]. Moreover, nanomedicines can achieve endosomal/lysosomal escape and facilitate the cytosolic release of STING agonists through several mechanisms, including the"proton sponge"effect mediated by cationic polymers or liposomes, fusion with the endosomal membrane, particle swelling, and endosomal membrane destabilization/

Table 3 Recent studies on nano-delivery of STING agonist for tumor radioimmunotherapy

Nano formulations	STING agonist	Target cells	Tumor model	Radiotherapy dose	Route	Size
ZnCDA [20]	CDA	TAMs, EC	Panc02, GL261		Intravenous injection	111.8 ± 0.9 nm
NP-cGAMP [23]	cGAMP	APCs	B16 F10-OVA, 4T1	8GY *3	Inhalation	118.8 nm
PC7A [22]	PC7A	APCs	B16-OVA, TC-1, MC38	20GY *1	Subcutaneous injection	20–30 nm
Alg-Mn [21]	Mn^{2+}	BMDCs, Raw264.7	B16 F10-OVA, CT26	8GY/5GY*1	Intratumoral injection	-
TMA-NPs [207]	c-di-AMP	4 T1	4 T1	2GY*3	Intratumoral injection	25.7 nm
CPs-CDN [19]	ADU-S100	B16 F10, BMDCs	B16 F10	3GY/5GY*3	Intratumoral injection	47 nm
cGAMP/MOL [97]	cGAMP	BMDCs, Raw264.7, BMMs	MC38, CT26	2GY*6	Intratumoral injection	-
Man-MnO_2@OVA [98]	Mn^{2+}	TAMs, DCs	B16 F10-OVA	4GY*1	Intratumoral injection	7.9 ± 2.3 nm
PLGA/STING@EPBM [208]	cGAMP	BMDC	B16-OVA/TC1	7.5 GY*2/ 20GY *1	Subcutaneous injection	157.5 ± 1.9 nm
aPDL1@MnO_2 [209]	Mn^{2+}	CT26, BMDC	CT26	2GY*3	Intravenous injection	100 nm
DSPM [188]	Mn^{2+}	DCs, 4T1	4 T1	2GY*3	Intravenous injection	38 nm
ADU-AAV-PD1@Gel [201]	ADU-S100	Luci + GL261	Luci + GL261	-	Intratumoral injection	-
BLNP/diABZI [187]	diABZI	TAMCs	CT-2 A, PVPF8	3GY*3	Intracranial injection	93 nm
($MnCO_3$@Te) [210]	Mn^{2+}	BMDC, 4T1	4 T1	2GY*2	Intratumoral injection	220 nm
TZM [211]	TZM	K7M2	K7M2	6GY*3	Intravenous injection	260.3–360.4 nm
HNP NPs [212]	Hf^{4+}	CT26	CT26	2GY*3	Intravenous injection	39 nm
$Bi_2 - xMnxO_3$ [189]	Mn^{2+}	4 T1	4 T1	8GY*1	Intravenous injection	120 nm
HfMnH [213]	Mn^{2+}	BMDC	CT26	5GY*1	Intravenous injection	265 nm
Met@HMnER [192]	Mn^{2+}	NK	MCF-7	2GY*4	Intravenous injection	-
XCL1@CaMnP [214]	Mn^{2+}	DCs	CT26	-	Intratumoral injection	-
Tpp-Met@MnO_2@Alb [215]	Mn^{2+}	MB49, DCs	MB49, 4T1	3GY*4	Intravenous injection	23.1 ± 3.1 nm
PLGA-PEG/DMXAA [191]	DMXAA	4 T1, HUVEC	4 T1	-	Intravenous injection	80 nm
PVCL-MnO_2-CpG NGs [216]	Mn^{2+}	B16 F10	Mouse glioblastoma cell lines (C6)	2GY*3	Intravenous injection	106.2 ± 6.4 nm
T-HONs@VE-822 [217]	VE-822 , HfO_2	4 T1	4 T1	3GY*4	Intratumoral injection	-

disruption [194, 195]. For example, after NP-cGAMP is phagocytosed by the cell, the calcium phosphate (CaP) component dissolves rapidly within lysosomes, releasing calcium ions (Ca^{2+}) and phosphate ions (PO_4^{3-}). This process triggers the proton sponge effect, facilitating the release of encapsulated cGAMP into the cytosol. And NPs with a particle size smaller than 500 nm can accumulate in tumor cells via the enhanced permeability and retention (EPR) effect [196]. However, the efficacy of EPR-based nanoparticle tumor targeting exhibits significant interindividual variability. To address this, targeting ligands can be incorporated into nanoparticles to recognize molecules overexpressed on the surface of tumor cells or immune cells (such as cell receptors, membrane transporters, and surface antigens), thereby reducing off-target toxicity [197, 198]. James J. Moon et al. have engineered a novel lipid-based nanoparticle, termed CDA-manganese particles (CMPs), that selectively localizes within tumor-resident innate immune cells—including DCs, macrophages, and MDSCs—to drive robust immune activation and reprogram immunologically "cold" tumors into "hot" phenotypes [199]. Additionally, controlled release strategies are essential, especially considering the timing of DNA damage accumulation following RT. It has been reported in the literature that no DNA damage was seen to accumulate in the cytoplasm

within 6 h after RT, but significant DNA damage was seen to accumulate in the cytoplasm 24–72 h after RT, which was attributed to the fact that the accumulated DNA damage needed to undergo a long period of mitosis in order to form micronuclei and enter the cytoplasm to be recognized by cGAS [200]. The 24–72-h post-RT window serves as a key temporal framework for developing nanocarrier-based controlled release strategies of STING agonists. For example, Wang et al. demonstrated that intratumoral injection of $MnCl_2$ 24 h after RT significantly enhanced the anti-tumor effect of RT [21]. Nanomedicines also enable pH-responsive release of STING agonists through the incorporation of acid-labile bonds, such as amide, ester, imide, oxime, acetal, hydrazone, or keto groups. For instance, the polymer DSPM [188] exhibits pH-responsive properties, where the imine linkers in poly (ethylene glycol)-polyphenol undergo cleavage under acidic conditions, thereby releasing DSNPs and Mn^{2+}. Therapeutic hydrogels (ADU-AAV-PD1@Gel) can respond to elevated ROS in the TME following RT, enabling sustained release of soluble PD-1 (sPD-1) and the STING agonist ADU-S100 [201]. Beyond improving STING agonist delivery, nanomedicines can also enhance radiosensitization. The cytotoxic efficacy of RT against cancer cells generally depends on the radiation energy. High-Z metals (e.g., gold [202], bismuth [203], gadolinium [204], silver [205], and hafnium [43]) interact with x-rays through the photoelectric effect and the compton effect, releasing Auger electrons, Compton electrons, and Photoelectrons, which subsequently interact with water molecules to produce cytotoxic ROS to induce unrepairable DNA damage [206]. Building on the aforementioned advantages of nanomedicines, the nanodelivery system can synergize with RT and STING agonists to not only enhance anti-tumor responses in both tumor and immune cells, but also reprogram the immunosuppressive TME (Fig. 5).

Enhancing tumor and immune cell responses

ICD is a distinct form of regulated cell death (RCD) that can trigger an adaptive immune response against dying cells through DAMPs. Calreticulin (CRT), high-mobility group box protein 1 (HMGB1), and heat shock protein 70 (HSP70) are typical DAMPs of ICD. However, most tumor cells exhibit low immunogenicity to avoid self-induced inflammation [218]. Currently, some

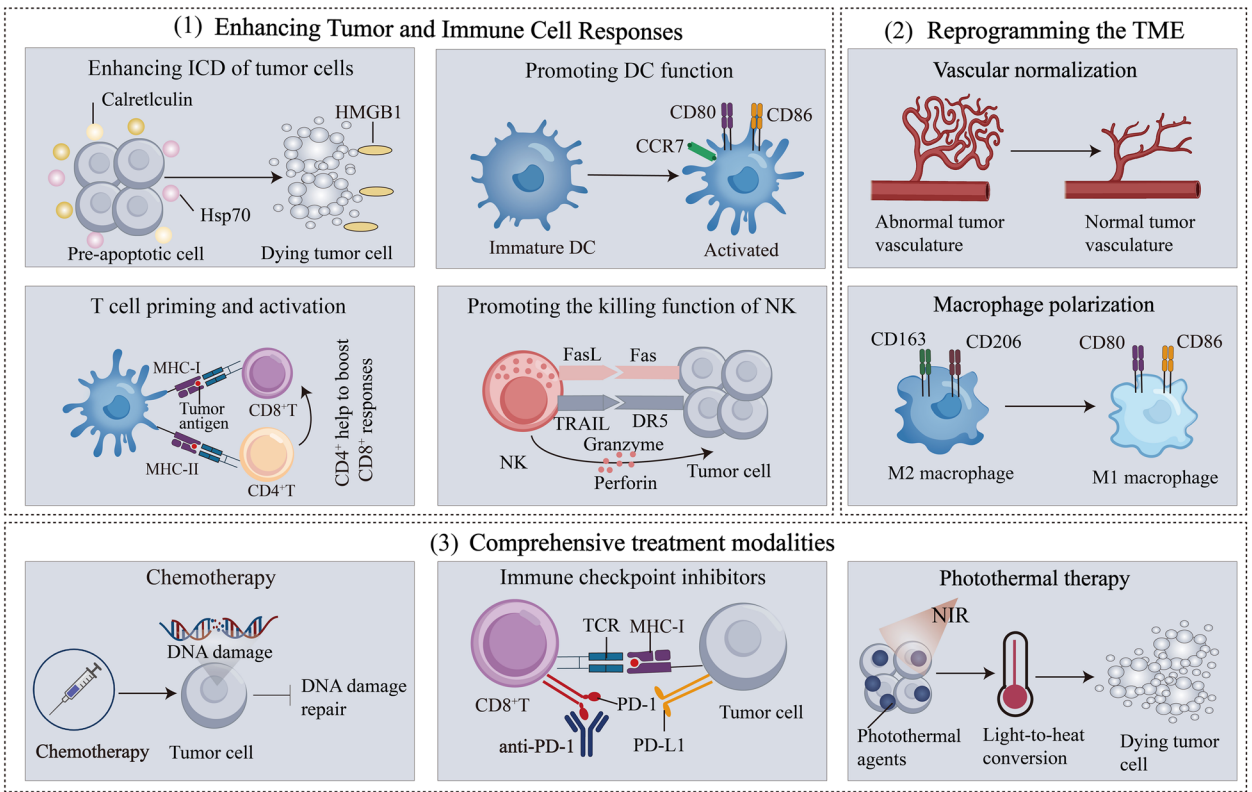

Fig. 5 Nano-STING agonists-mediated anti-tumor immunity for enhanced RT. (1) The combination of RT and STING agonists enhance tumor and immune cell responses, including enhancing ICD, antigen presentation, T cell priming and activation, promoting the killing function of NK. (2) The combination of RT and STING agonists can reprogram the TME, promoting vascular normalization and reducing immunosuppressive cells. (3) Combination of RT, nano-STING agonists, and other therapies (chemotherapy, ICIs, and PTT) to activate anti-tumor immunity

studies suggest that ICD can induce immune responses by activating the cGAS-STING pathway in certain cancer cells. For instance, in neuroblastoma (NB), intratumoral administration of STING-NP enhanced STING activation, transforming a tumor with low immunogenicity into one with a tumor-killing and T cell-inflamed TME [219]. However, adaptive immune responses driven by ICD can only occur in the presence of antigenicity, adjuvanticity, and a permissive microenvironment [220, 221]. RT also leads to the infiltration of immunosuppressive cells, such as TAMs and T_{reg} cells, into the TME, exacerbating radioresistance. To address these challenges, nanoparticles can not only act as radiosensitizers to enhance DNA damage, but also carry STING agonists to activate the cGAS-STING pathway, improving immune-suppressive TME and overcoming RT resistance. For example, in BALB/c mice bearing CT26 tumors, two-dimensional risedronate-manganese nanobelts (RMn-NBs) combined with RT were shown to promote ICD, with significant increases in ICD markers such as CRT, HMGB1, ATP, and IFN-β [222] (Fig. 6A). The maturation of DCs, a critical downstream feature of robust ICD induction, effectively initiated systemic anti-tumor immune responses. Compared to other treatment groups, the proportion of mature DCs was significantly higher in the RMn-NBs + RT group, further enhancing the immunogenicity of tumor cells. Zhang [223] et al. developed an autologous cell-derived exosome-engineered nanoplatform loaded with STING agonist (MnExo@cGAMP) to promote RT-induced immunotherapy of melanoma through cascade activation of the cGAS-STING pathway. Immunohistochemical analysis of tumor tissues after treatment revealed that MnExo@cGAMP + RT significantly promoted the release of CRT, HMGB1, and HSP70 compared to the blank control group. These findings demonstrate that the combination of MnExo@cGAMP and RT enhances the immunogenicity of melanoma.

After capturing tumor antigens, DCs migrate to the draining LNs, where they process and cross-present antigens to activate naïve T cells and upregulate costimulatory molecules on their surface in a process known as DC maturation. However, DC maturation is often suppressed by the TME, directly impairing antigen cross-presentation. Strategies that selectively activate the cGAS-STING pathway in DCs can help overcome this obstacle. Delivery of nano-STING agonists can target peripheral DCs or DCs within LNs. Targeting of peripheral DCs can be achieved passively by non-specific endocytosis, phagocytosis and microcellular drinking, or actively by specifically targeting surface receptors on DCs [224], such as receptors for C-type lectin receptors (CLRs), mannose receptors (MR), DEC-205, DC-SIGN, Dectin-1, and Siglec-H. A significant proportion of resident DCs in LNs are phenotypically immature and are capable of internalizing antigens and particles. In addition, LNs contain large numbers of DCs, T cells, and a high number of tumor antigens, and the site of antigen cross-presentation occurs in the LNs. Therefore, it is also important to develop nano-STING agonists targeting DCs in LNs. Drug LN accumulation can be achieved by LN injection, intravenous injection, and interstitial administration. The size of the nanoparticles also affects their transportation and their location in the LNs. NPs with diameters of 20–50 nm can achieve efficient accumulation in the LNs, whereas large nanoparticles are easily captured by the reticuloendothelial system [225]. When combined with RT, DC-targeting STING agonists can amplify systemic immune responses and enhance the suppression of primary tumor growth and distant metastatic progression. Targeting peripheral DCs: For instance, Guo et al. [208] designed an engineered peptide CBP-12-expressing bionanocarcinoma cell membrane (EPBM)-encapsulated nanovaccine delivery system (PLGA/STING@EPBM), tailored for precisely targeted delivery of tumor antigens and STING agonists to $Clec9a^+$ DCs via CBP-12-targeted receptor Clec9a (Fig. 6B). Clec9a, a c-type lectin receptor on DCs responsible for capturing antigen and initiating subsequent cross-presentation, is expressed on human $BDCA3^+$(CD141) DCs and mouse $CD8\alpha^+$ DCs [226]. The uptake of PLGA/STING@EPBM by $Clec9a^+$ DCs up-regulated the expression of IFN-β, IL-6, IL-21, and CXCL10, with IL-21 playing a pivotal role in mediating antigen-specific cytotoxic T-lymphocyte (CTL) responses. When combined with RT, the PLGA/STING@EPBM demonstrated efficacy in inhibiting tumor growth and extending survival in TC1 and B16-OVA tumor models. Liu [23] et al. prepared an inhalable negatively charged liposome NP-cGAMP, based on RT combined with STING agonists for the treatment of lung metastases. Both layers of liposome membranes consisted of anionic phosphatidylserine (PS), where the exposed outer PS acted as an"eat-me"signal to DCs, while the inner PS interacted with the excess cationic Ca^{2+} in CaP and bound to the core cGAMP complex. NP-cGAMP can be recognized and phagocytosed by PS receptors of APCs, activating the cGAS-STING pathway of DCs. This activation leads to the promotion of antigen cross-presentation by DCs, upregulation inflammatory cytokines (TNF-a, IL-1b, IL-6, IL-12b, and CXCL9, CXCL10) and the activation of tumor antigen-specific $CD8^+$ T cells. The three types of APCs in the lungs mainly consisted of alveolar macrophages (AMs; $CD11c^+F4/80^+$), interstitial macrophages (IMs; $CD11c^-F4/80^+$), and BMDCs ($CD11c^+F4/80^-$), with AMs uptaking the most NP cGAMP at 41.7 ± 7.0%. In mouse models of melanoma lung metastasis and breast cancer lung metastasis,

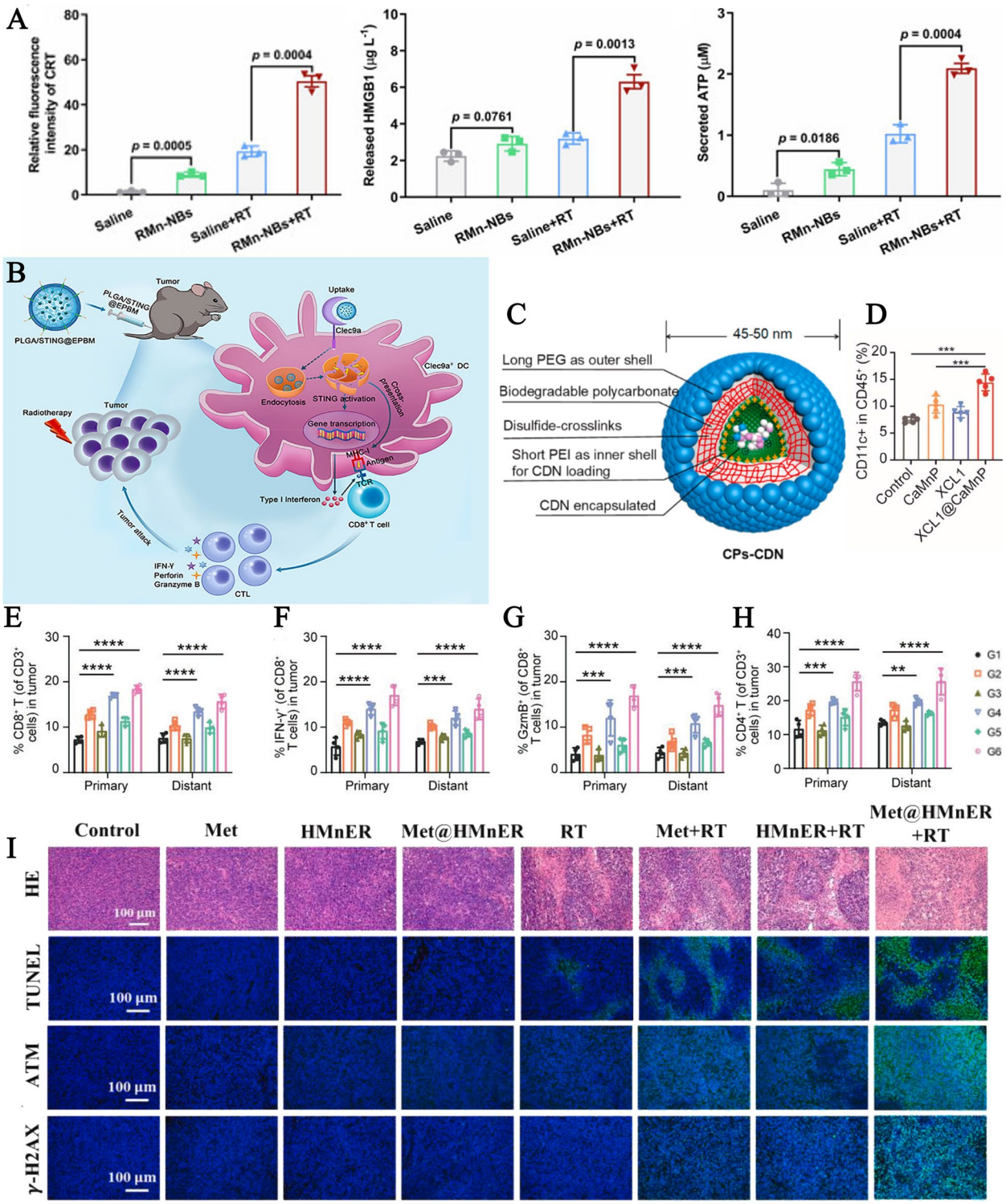

Fig. 6 Enhancing tumor and immune cell responses. A Relative fluorescence intensity of CRT after various treatments. Detection of cytosolic HMGB1 using an ELISA kit. Measurement of extracellular ATP using a luciferase-based ATP assay kit ($n = 3$ cell samples). **B** PLGA/STING@EPBM enhances anti-tumor immunity by targeting Clec9a + DCs. **C** Schematic diagram of CDN-mediated cytoplasmic release in cells and their sizes. **D** Semi-quantitative analysis of tumor-infiltrating DC populations in mice with different treatments. **E** Quantification of CD8 + T cells gated on CD3 + T cells in tumor tissues n after treatments. G1: PBS (–), G2: PBS (+), G3: DSP (–), G4: DSP (+), G5: DSPM (–), G6: DSPM (+), (+): with X-ray irradiation, (–): without X-ray irradiation. (**F**-**G**) Quantification of IFN-γ + (**F**) and GzmB + (**G**) cells gated on CD8 + T cells. (**H**) Quantification of CD4 + T cells gated on CD3 + T cells. (**I**) Anti-tumor effects of different treatment groups. Reproduced with permission from ref treatment [19, 188, 192, 208, 214, 222]

NP-cGAMP combined with RT inhibited not only irradiated but also unirradiated lung metastases. Targeting DCs in LNs: The mannose modification of Man-MnO_2@OVA [98] and its small size (7.9 ± 2.3 nm) enhances lymphatic drainage and targets DCs with high mannose receptor expression. The fluorescence intensities of actin and tubulin are remarkably enhanced upon incubation with Man-MnO_2@OVA, revealing that the migrating ability of BMDCs is improved. The combination of Man-MnO_2@OVA27 with RT resulted in synergistic activation of the cGAS-STING pathway, promoting DC maturation, antigen cross-presentation, and activation of IFN-γ^+ and $CD107^+$ $CD8^+$ T cells. An OVA peptide-containing nanovaccine, PC7A NP [22] with a diameter of 20–30 nm, targeted to lymphoid organs and administered by subcutaneous injection, can load and deliver pre-existing TAAs and tumor neoantigens to LNs and activate DCs in LNs. In addition, PC7A also binds STING to activate the cGAS-STING pathway in DCs and disrupts endosomal membranes to delay STING degradation [227]. In the B16-OVA melanoma tumor model and TC-1 tumors C57BL/6 mice model, subcutaneous administration of PC7A nanoparticles post-RT increased systemic T-cell responses, leaving 40–50% of treated mice tumor-free after 60 days. Zheng [19] et al. created CPs-CDN, which is loaded with the STING agonist ADU-S100 for the treatment of melanoma. PEGylated and neutrally potentiated promoted escape phagocytosis and cytoplasmic release of ADU-S100 in DCs, which in combination with fractionated low-dose irradiation (3GY*3 or 5GY*3) stimulated the maturation of DCs through activation of the cGAS-STING pathway. The efficient delivery of CP-CDN to tumor-draining lymph nodes (TDLN) may be attributed to its small size (47 nm), which makes it easy to enter the lymphatic vessels from the interstitial space (Fig. 6C). Targeting specific DC subpopulations: There is significant downregulation of XCL1 and XCR1 in tumor tissues compared to adjacent normal tissues, suggesting that dysregulation of the XCR1-XCL1 axis within the TME may impair cDC1-mediated immunosurveillance and hinder anti-tumor immune responses. Intratumoral injection of XCL1@CaMnP gel [214] recruited cDC1 into tumors by prolonging the specific interaction between the retained XCL1 ligand and the XCR1 receptor on cDC1(Fig. 6D). Recruitment of cDC1 was evidenced by a significant up-regulation of XCR1 expression among tumor-infiltrating DCs. An increase in migratory DCs ($CD103^+$DCs) was also observed. Concurrently, RT augmented the availability of tumor antigens to the recruited cDC1 s and synergistically activated the cGAS-STING pathway in cDC1 s with XCL1@CaMnP, which facilitated the capture and cross-presentation of tumor antigens by cDC1 s and in turn stimulated the proliferation of IFN-γ^+CD8^+T cells. Furthermore, IFN-β secreted by cDC1 triggers the transformation of TAMs to M1 phenotype, enhancing their tumoricidal activity.

T cells are commonly regarded as key players in antitumor immunity. However, their effector functions are not autonomous. The initiation and activation of T cells require three signals: tumor antigens presented on MHC (signal 1), costimulatory molecules (signal 2), and certain pro-inflammatory cytokines (signal 3) [228]. All these signals can be enhanced through activation of the cGAS-STING pathway. Additionally, the endogenous STING pathway in T cells is critical for anti-tumor immunity. On one hand, STING activation has been shown to promote the differentiation of naïve $CD4^+$ T cells into Th1 and Th9 cells and enhance the production of effector cytokines such as IFN-γ and IL-9, thereby augmenting $CD4^+$ T cell effector functions [229]. On the other hand, the cGAS-STING signaling pathway in $CD8^+$ T cells regulate the expression of the transcription factor TCF1, promoting the expansion and maintenance of the stemness of $CD8^+$ T cells [230]. Yan [188] et al. coordinated an amphiphilic polymer, polyethylene glycol-polyphenol, with a lanthanide-doped radiosensitizer (NaGdF4: Nd@NaLuF4) and Mn^{2+} to form NaGdF4: Nd@NaLuF4@PEG-polyphenol/Mn (DSPM) for radioimmunotherapy. RT combined with the STING agonist DSPM significantly activated adaptive immunity, transforming an immunologically "cold" TME with low T cell infiltration into a "hot" TME with high T cell infiltration. In a 4 T1 tumor mouse model, the combination of RT and DSPM resulted in the highest intratumoral $CD8^+$ T lymphocyte levels (18.3% ± 0.8% in primary tumors and 15.6% ± 1.6% in distant tumors) (Fig. 6E). Furthermore, IFN-γ^+ $CD8^+$ and $GzmB^+$ $CD8^+$ T cells also showed the highest percentages (Fig. 6F-G). The proportion of $CD4^+$ T cells ($CD3^+CD4^+$ helper T cells) in the DSPM (+) group was approximately 2.2-fold and 1.9-fold higher in primary and distant tumors, respectively, compared to the PBS (-) group (Fig. 6H). A ROS-degradable therapeutic hydrogel (ADU-AAV-PD1@Gel) combined with RT significantly increased the proportion of memory $CD8^+$ and $CD4^+$ T cells in the brain tissue of mice [201]. In a glioblastoma (GBM) resection model, mice treated with ADU-AAV-PD1@Gel + RT and surviving for 30 days (complete response mice, CR mice) were rechallenged with $Luci^+$GL261 tumors in the contralateral hemisphere alongside untreated control mice. Long-term survivors from the ADU-AAV-PD1@Gel + RT group remained tumor-free without further treatment, while untreated control mice succumbed to tumor burden. These findings demonstrate that ADU-AAV-PD1@Gel + RT treatment significantly promotes the formation of memory T cell phenotypes, establishing durable immune memory against recurrent brain tumors.

In addition to activating endogenous T cells, the nano-STING agonist B-LNP/diABZI can enhance the migration of CAR-T cells from the circulation to GBM tumors [187]. Excitingly, one dose of B-LNP/diABZI injection induced an over fourfold increase in CAR-T cell infiltration to brain tumors, which led to a reduction of tumor burden by 75%.

In recent decades, cancer therapy has shifted toward the use of ICIs, adoptive immune cell transfer (ACT), and other tumor immunotherapies as primary treatment options. These strategies primarily rely on the endogenous cytotoxicity of $CD8^+$ T cells to destroy cancer cells, which often leads to the development of resistance. NK cells, a subset of lymphocytes within the innate immune system, are considered the innate counterparts of $CD8^+$ cytotoxic T cells [177]. As "first responders", NK cells have the ability to rapidly recognize and eliminate infected, transformed, allogeneic, or stressed cells [231]. RT can upregulate receptors that activate NK cells (e.g., NKG2D, NKG2 C, NKp30, NKp40), thereby enhancing the cytotoxicity of NK cells against cancer cells [232]. However, RT can also upregulate PD-1 on NK cells through the NF-κB pathway, enabling tumor cells to evade the immune system. The activation of NK cells by RT alone is often insufficient, necessitating exogenous stimulation to fully activate NK cells. Several studies suggest that Mn^{2+} can intrinsically activate NK cells through the cGAS-STING pathway, leading to increased secretion of NK cell effector molecules, including CD107a, IFN-γ, granzyme B, and perforin [183]. Manganese (Mn^{2+}) directly activates cGAS by enhancing its sensitivity to double-stranded DNA (dsDNA) and increasing the affinity of STING for cGAMP. However, intravenously injected free Mn^{2+} is rapidly cleared without tumor accumulation and can cause acute toxicity. Nanoplatforms can integrate Mn^{2+}-mediated NK cell activation with RT to reconstruct an immune-stimulatory TME that prevents metastasis and recurrence. A novel nano STING agonist, Met@HMnER [192], composed of Met-loaded hollow manganese dioxide (MnO_2) encapsulated by extracellular vesicles, can activate the cGAS-STING pathway in NK cells. This configuration triggers a prolonged activation of NK cell-mediated innate immunity. After co-incubation of HMnER with NK cells, released Mn^{2+} can cause NK cells to secrete more IFN-γ by activating the cGAS-STING pathway in NK cells. The increased secretion of IFN-γ is indicative of enhanced NK cell activation. Notably, the synergistic application of RT and Met@HMnER not only eradicates primary tumors but also significantly curtails tumor recurrence and metastasis (Fig. 6I). This effect is mediated through the Mn^{2+}-enhanced NK cell immune response, thereby consolidating the therapeutic outcomes.

Reprogramming the TME

Cancer is not a solo performance, but rather an ensemble production [233]. The TME plays a critical role in regulating tumor growth, invasion, and metastasis [234]. The TME is typically characterized by mild acidity, elevated hydrogen peroxide (H_2O_2) levels, hypoxia, aberrant vasculature, and infiltration of immunosuppressive cells [235]. Notably, the TME exerts a decisive influence on the efficacy of radioimmunotherapy [235]. Nanomedicine not only responds to TME-specific features such as high ROS and acidity to enable precise release of STING agonists but also selectively targets the TME to potentiate radioimmunotherapy [236]. The following sections will elaborate on three key mechanisms by which nano-STING agonists modulate the TME: ameliorating hypoxia, normalizing aberrant tumor vasculature, and reducing immunosuppressive cell.

Hypoxia is prevalent in many tumor tissues due to the high oxygen consumption of cancer cells, which is further exacerbated by insufficient oxygen delivery through dysfunctional microvasculature. Hypoxia significantly limits the efficacy of RT by inducing radio-resistance and promoting tumor metastasis [237]. RT directly or indirectly induces DNA damage by generating DNA free radicals (DNA·). These DNA free radicals are typically stabilized by O_2, leading to substantial DNA damage [238]. However, under hypoxic conditions, DNA damage is reduced. General strategies to address hypoxia in the TME include enhancing oxygen delivery and reducing oxygen consumption. For example, nanoparticle-based solutions, such as Hb@Hf-Ce6 developed by Sang et al., encapsulate hemoglobin to improve oxygen levels [239]. Additionally, mitochondrial respiration inhibitors like atovaquone-loaded human serum albumin nanoparticles (HSA-ato NPs) [240] and targeted formulations of metformin (Tpp-Met@MnO_2@Alb) help reduce oxygen consumption by cancer cells [215]. Another strategy to overcome the hypoxic TME relies on converting the high levels of H_2O_2 in the TME into O_2 by delivering natural enzymes such as catalase or using nanomaterials with high catalase-like catalytic activity [241]. Cao [213] et al. developed a nano-radiosensitizer (HfMnH) that catalyzes the decomposition of H_2O_2 into O_2 and H_2O via manganese dioxide (MnO_2) (Fig. 7A), augmenting the immune response through activation of the cGAS-STING pathway. MnO_2 also has glutathione peroxidase-like activity, promoting the oxidation of GSH thiol groups (-SH) into oxidized glutathione disulfide (GSSG) through the reaction: $MnO_2 + 2GSH \rightarrow Mn^{2+} + GSSG + 2H_2O$. GSH, a critical intracellular antioxidant, is overexpressed in tumors and is one of the main barriers to improving RT efficacy. Zhang [222] et al. further employed two-dimensional

manganese risedronate nanobelts (RMn-NBs) to target the HIF-1α/VEGF axis, boosting radioimmunotherapy.

Blood vessels are considered one of the most critical factors in tumor development, as they supply oxygen and other essential nutrients required for cell survival and proliferation. Targeting the tumor vasculature has been recognized as an effective strategy to disrupt solid tumors. The effects of RT on tumor vasculature are dose- and site-dependent [17, 243]. Low-dose radiation (3 Gy) primarily disrupts immature blood vessels, while high-dose radiation (10 Gy) induces endothelial cell apoptosis and reduces blood flow [244, 245]. Although high doses (20 Gy) have been reported to permanently reduce blood flow, such doses often cause severe side effects in healthy tissues. However, RT fails to exert therapeutic effects on distal sites or on newly formed radiation-resistant vasculature [246]. Given the narrow therapeutic window for vascular normalization during anti-angiogenic therapy, the combination of RT with vascular normalization presents a promising treatment strategy. Activation of the cGAS-STING pathway in tumor ECs can promote vascular normalization. Go [242] et al. developed two types of liposomes with STING agonists, PoSTING and NeSTING, where PoSTING allows for selective delivery and superior uptake in $CD31^+$ tumor ECs while enhancing the expression of genes related to vascular normalization (Angpt1 and Pdgrfb) and endothelial cell-lymphocyte interactions (ICAM-1 and ICAM-2) (Fig. 7B). PoSTING delays LLC primary tumor progression, boosts T cell immunity, and effectively controls metastasis. In a study by Yang [135], cGAMP treatment resulted in a 6.4-fold increase in intratumoral $CD8^+$ T cells, a 40% reduction in $CD31^+$ vascular density, a 1.7-fold increase in $NG2^+$ pericyte coverage, and a 1.5-fold increase in $COL4^+$ basement membrane coverage (Fig. 7C). Additionally, intratumoral hypoxia was alleviated by 46% in cGAMP-treated tumors compared to controls. However, studies have reported that this STING-induced activation of tumor ECs can be negatively regulated by VEGF/VEGFR2 signaling through ubiquitin-mediated degradation of IFNAR [247], suggesting that STING agonists may be insufficient to activate type I IFN signaling in VEGF-rich cancers. Moreover, while repeated injections of STING agonists induce strong innate and adaptive immune responses, they inevitably upregulate immune checkpoint molecules, creating a negative feedback loop that may confer adaptive resistance to STING agonist-induced immune responses [248]. In one study, when LLC tumors were treated with a triple immunotherapy regimen consisting of a STING agonist, anti-VEGFR2 antibodies, and either anti-PD-1 or anti-CTLA-4 antibodies, more than half of the tumor-bearing mice exhibited complete tumor regression [135](Fig. 7D). Furthermore, vascular normalization can also enhance NPs accumulation. STAN-induced vascular normalization increases tumor accumulation and cellular uptake of NPs, creating opportunities to improve the delivery of NP-based therapeutics [134].

In cold tumors, such as pancreatic cancer, triple-negative breast cancer (TNBC), and gliomas, the TME is infiltrated by a large number of immunosuppressive cells, including MDSCs, TAMs, and T_{reg} cells. Innovative approaches using nanoparticles containing STING agonists can reduce immunosuppressive cells in the TME. Yang [20] constructed a PEGylated neutral liposome, ZnCDA, which synergizes RT with the STING agonist cyclic di-AMP (CDA) to modulate the TME. ZnCDA promoted TAMs polarization towards M1 and antigen cross-presentation by preferentially targeting and activating the cGAS-STING pathway in $CD45^+CD11b^+F4/80^+$TAMs (Fig. 7E). When the cGAS-STING pathway of TAMs is activated, down-regulated lysosomal enzyme-related genes in TAMs preferentially blocked antigen degradation, thereby regulating antigen cross-presentation in TAMs and further promoting anti-tumor T-cell responses (Fig. 7F-G). Additionally, ZnCDA promotes sustained production of differentiated effector cells from pre-infiltrated stem-like $TCF1^+PD\text{-}1^+CD8^+$T cells in TMEs, enhancing tumor immunity restoration. In immunologically'cold'pancreatic and glioma tumor models, the combination of ZnCDA with RT resulted in a marked amplification of the anti-tumor effects. Glioblastoma is an immunologically"cold"or"silent"tumor, characterized by a lack of sufficient infiltrating effector

(See figure on next page.)

Fig. 7 Remodeling the TME. **A** Photographs of HfMn-PAH at different concentrations reacting with H_2O_2 (top). Ultraviolet–visible (UV–Vis) spectra of H_2O_2 after reacting with different concentrations of HfMn-PAH. **B** Comparative analysis of gene expression related to vascular stabilization and endothelial-lymphocyte interactions. **C** Representative images of CD8 + T cells, CD31 + vasculature, NG2 + pericyte coverage, COL4 + basement membrane (BM) coverage, and hypoxic regions within the tumor. **D** Effects of STING agonist monotherapy, STING agonist combined with anti-VEGFR2 antibody, and the triple combination of STING agonist, anti-VEGFR2 antibody, and immune checkpoint blockade on the TME. **E** Working model of ZnCDA in the TME. (**F**-**G**) Mountain plots of the antigen processing and presentation (**F**) and M1 polarization (**G**) pathways. (**H**) Mechanism of B-LNP/diABZI and RT enhanced immunotherapy. (**I**-**J**) diABZI-treated TAMCs demonstrated a pro-inflammatory phenotype as determined by the expression of a panel of pro-inflammatory cytokines measured by qPCR 6 h post-treatment (**I**) and altered expression of ARG1, CD206, and CD86 measured by flow cytometry 24 h post-treatment (**J**). Reproduced with permission from ref [20, 135, 187, 213, 242]

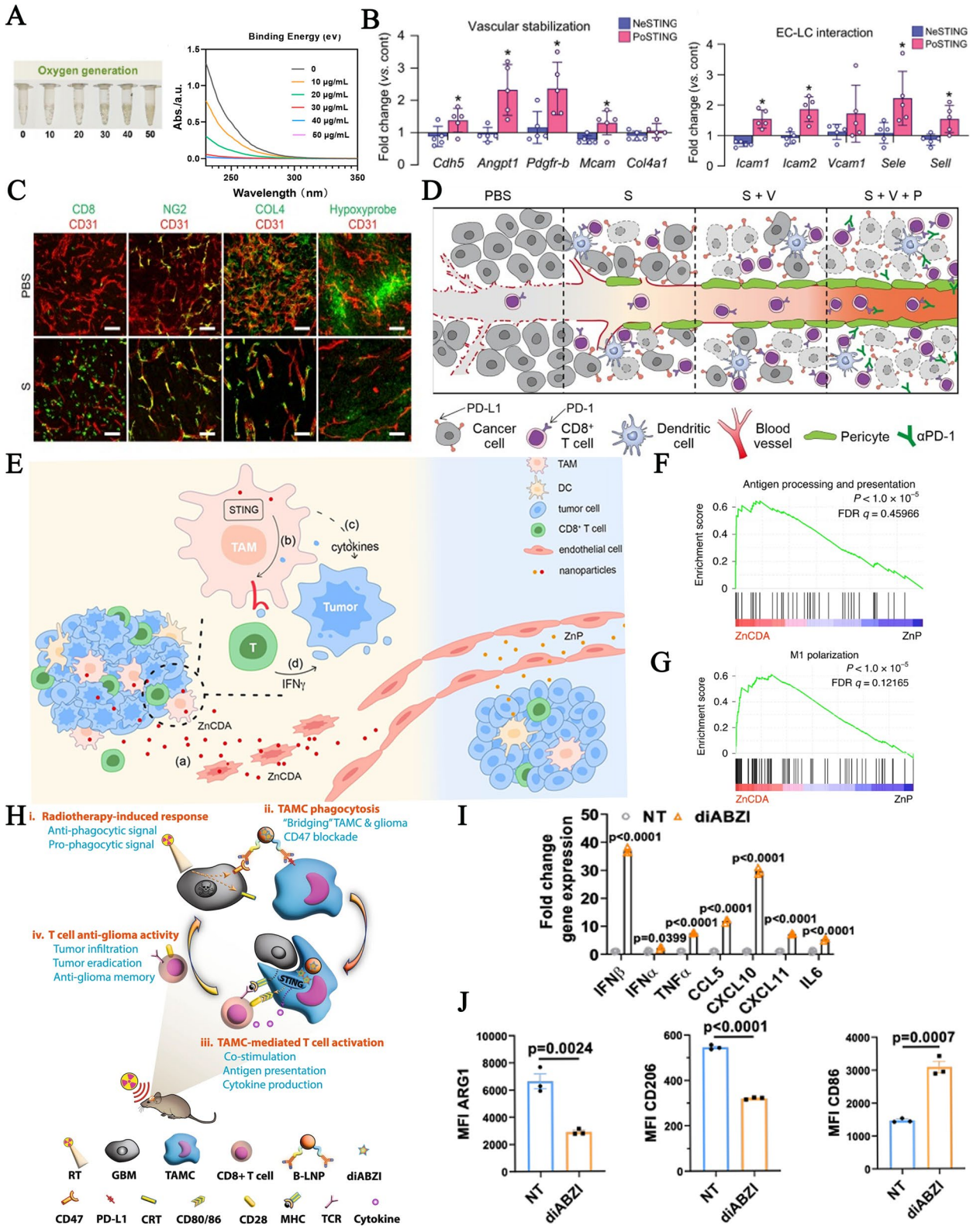

Fig. 7 (See legend on previous page.)

T cells, but with a large presence of immunosuppressive tumor-associated myeloid cells (TAMCs) [249]. A bridging lipid nanoparticle (B-LNP/diABZI) [187] enables the combination of RT with the STING agonist diABZI for targeted therapeutic intervention in TAMCs (Fig. 7H). TAMCs are one of the most important immune cell populations in the TME, derived from heterogeneous phagocytic population groupings of common myeloid progenitor (CMP) cells [250]. $CD45^{+}CD11b^{+}$TAMCs highly express PD-L1. B-LNP promotes TAMC-glioma interactions through anti-CD47/PD-L1 dual ligation, and promote phagocytosis of tumor cells (Fig. 7H). RT upregulates CD47 in glioma cells and upregulates PD-L1 in TME, thereby synergizing B-LNP. After treatment with B-LNP/diABZI, immunosuppressive TAMCs are reprogrammed into pro-inflammatory cells by activating the cGAS-STING pathway in TAMCs (Fig. 7I-J), promoting the expression of type I IFN, CCL5, and CXCL10 (Fig. 7I), thereby promoting T cell recruitment and activation. Treatment with diABZI resulted in a decrease in the expression of immunosuppressive factors ARG1 and CD206 in TAMCs, while the activation marker CD86 was elevated (Fig. 7J). T cells also overexpress several interferon-stimulated genes, such as Isg15, Usp18, Irf7, Bst2, Zbp1, and Rtp4, indicating the response of T cells to interferons. The reprogramming of TAMCs correlates with increased expression of CD69, IFN-γ, granzyme B (GzmB), and Ki67 in T cells, while the expression of PD-1 is reduced. These results indicates that T cells are in an activated and proliferative state, characterized by heightened cytotoxic activity. In preclinical mouse models (CT-2 A), B-LNP/diABZI collaborates with RT to promote intracranial tumor regression and induce anti-glioma immune memory.

Combination therapies with STING agonists, RT, and other treatments

Combination therapies involving STING agonists and RT with other treatment modalities hold significant clinical value in anti-tumor therapy. They mainly included ICIs, TLR agonists, phototherapy (PTT and PDT), RDT, surgery, and chemotherapy. The integration of multiple therapeutic approaches can generate synergistic effects to maximally activate anti-tumor immunity. For example, on one hand, the addition of ICIs counteracts PD-L1 upregulation induced by cGAS-STING pathway activation, thereby maximizing T cell activation. On the other hand, STING agonists enhance T cell infiltration into tumors, potentiating the efficacy of ICIs [81]. Concurrently, incorporating chemotherapeutic agents not only intensifies DNA damage to activate the cGAS-STING pathway but also reduces required drug doses and mitigates chemotherapy-related adverse effects.

Immune checkpoint inhibitors (ICIs)

RT combined ICIs have moderate clinical benefit, and how to go about enhancing the effect of this combination therapy remains an urgent clinical question. The addition of nano-mediated STING agonists enhances the synergistic effect of RT with ICIs, thereby increasing the abscopal effect. The nanomaterial HfMnH prepared by Cao [213] et al. could enhance the therapeutic effect of RT and ICIs through the activation of cGAS-STING in CT26 tumor bearing mice model. RT combined with ICIs could enhance local tumor control but not increase the control of metastases, and the addition of HfMnH had stronger control of both primary and metastatic foci. Deng [209] et al. also found that αPDL1@MnO2 NP + X-ray induced abscopal effect and enhanced control of metastases compared to αPDL1 + X-ray and IgG@MnO2 + X-ray in CT26 tumor model. αPDL1 blocks the binding of PD-L1 on tumor cells and PD-1 on cytotoxic T lymphocytes (CTL). αPDL1@MnO2 combined with RT overcomes the immunosuppressive TME by promoting maturation of DCs, infiltration of CD8 + T cells, phenotypic polarization of TAMs from M2 to M1, and secretion of TNF-α, IFN-γ, and IFN-β.

Most anti-PD-L1/PD-1 monoclonal antibodies sensitize RT only to a certain extent, due to the fact that intracellularly localized PD-L1 proteins are unaffected by these antibodies, and thus cytoplasmic PD-L1 proteins accelerate DNA damage repair (DDR), thereby inducing radiation therapy resistance [251]. Tpp-Met@MnO_2@Alb synthesized by Yi [215] et al. solved this thorny issue by cGAS-STING pathway activation and extraordinary PD-L1 and TGF-β1 downregulation, and two-stage oxygen improvement, thereby significantly enhancing antitumor immunity in bladder cancer (Fig. 8A). Tpp-Met@MnO_2@Alb doubly ameliorates tumor hypoxia by generating oxygen from MnO_2 and reducing oxygen consumption by Tpp-Met (Fig. 8B). The triphenylphosphine analogue metformin (Tpp-Met) leads to phosphorylation of PD-L1 and TGF-β by AMPK through inhibition of mitochondrial respiration (OXPHOS), ultimately leading to reduced expression of PD-L1 in the cell membrane and cytoplasm, as well as TGF-β (Fig. 8C-F, H-I). PD-L1 degradation decreases mRNA levels of DDR-related genes (NBS1, MRE11 and RAD50), which enhances radiation damage to tumor cells (Fig. 8G). Such changes contribute to reversing the immunosuppressive nature of the TME, thereby enhancing T cell activation. In MB49 tumor models, Tpp-Met@MnO_2@Alb demonstrated a synergistic effect with RT, resulting in the inhibition of both primary and distal metastatic tumors.

Immune checkpoints also help cancer cells easily evade phagocytosis by APCs. CD47 is a novel immune checkpoint that promotes cancer cell evasion of

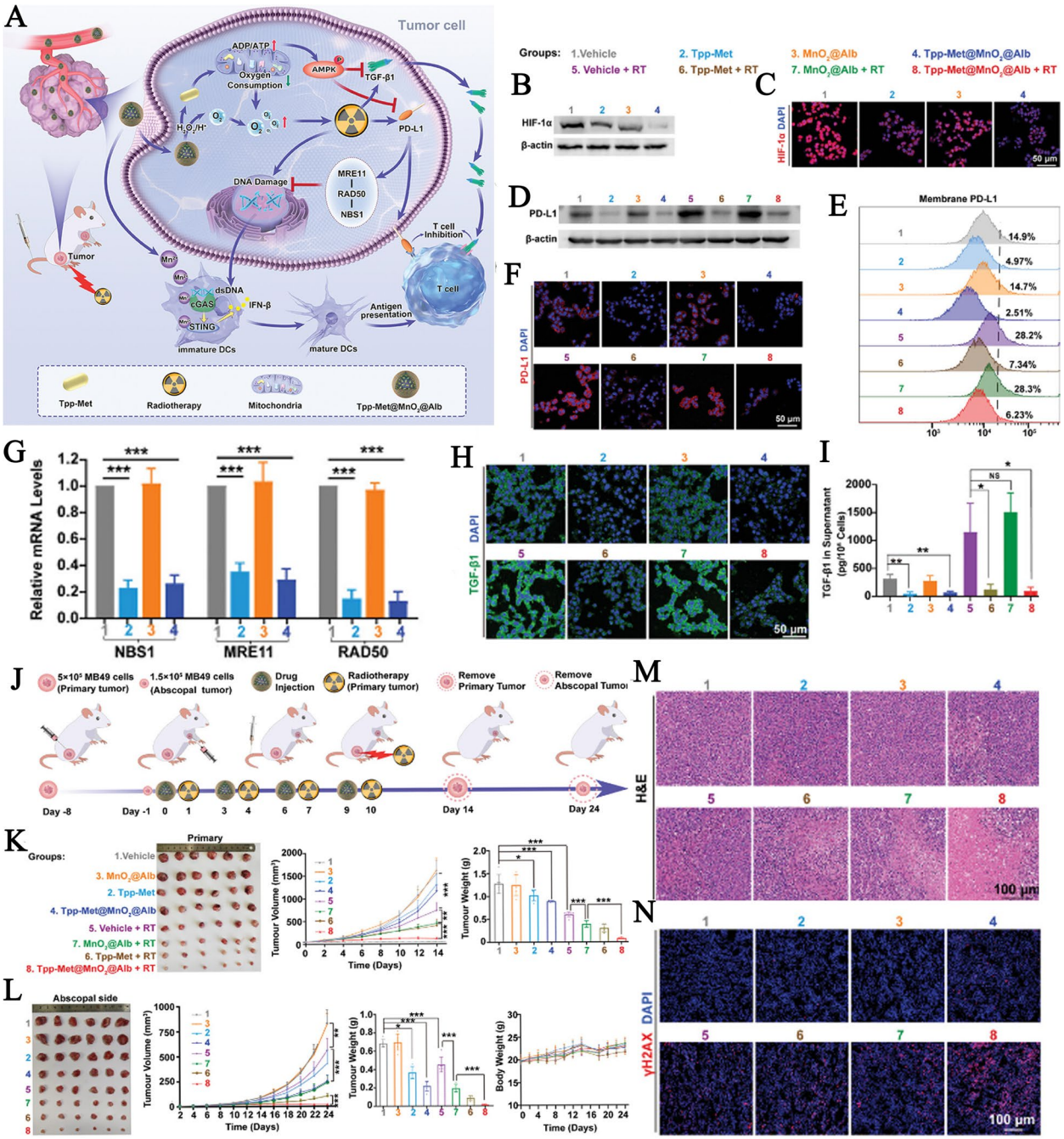

Fig. 8 Combination therapies with STING agonists, RT, and ICIs. **A** Mechanism of Tpp-Met@MnO_2@Alb enhanced radioimmunotherapy. **B** Quantitative analysis of HIF-1α protein expression in MB49 cells through western blot analysis under distinct treatment ($n = 3$). **C** Representative fluorescence images of HIF-1α in MB49 cells following various interventions. **D** Detection of PD-L1 in MB49 cells by western blot analysis following diverse interventions ($n = 3$). **E** Flow cytometric quantification of PD-L1 levels on the membrane of MB49 cells post-treatment. **F** Immunofluorescence characterization of PD-L1 in MB49 cells after various interventions. **G** Relative mRNA expression levels of NBS1, MRE11, and RAD50 in MB49 cells assessed by RT-qPCR after various treatments. **H** Representative fluorescence pictures of TGF-β1 in MB49 cells following various interventions. **I** Quantification of TGF-β1 secretory levels in the supernatants of MB49 cells following various treatments by ELISA ($n = 3$). **J** Schematic of tumor implantation and treatment plan. Inhibition of primary foci (**K**) and metastases (**L**) after various treatments. (**M–N**) Representative fluorescence images of H&E staining and γ-H2 AX of tumors following diverse interventions. Reproduced with permission from ref [215]

macrophage-mediated phagocytosis by interacting with signaling regulatory protein α (SIRPα) on the surface of macrophages [252]. Zhang [187] designed a bridge lipid NP (B-LNP) containing diABZI and double bonds of αCD47 and αPD-L1, which could enhance the phagocytosis of GBM by TAMC through enhancing ligand-receptor interactions. αCD47 in B-LNP inhibited CD47 overexpression in glioma cells to evade phagocytosis by macrophages, whereas αPD-L1 was used to block up-regulated PD-L1 in TAMC to promote T cell activation. The combination of RT with the B-LNP promoted the activation of the immune system, which enhances both the response of tumor cells to ICIs and the direct phagocytosis of tumor cells by macrophages (TAMC).

Toll-like receptors (TLR) agonists

Toll-like receptors (TLRs), a family of evolutionarily conserved pathogen recognition molecules, bridge innate and acquired immunity [253]. TLR agonists include TLR7/8 agonist R848 and TLR9 agonist CpG. Cytosine phosphoguanine oligodeoxynucleotides (CpG-ODNs) are TLR9 agonists that promote cytokine release from APCs to expand cytotoxic T lymphocytes [254]. Co-administration of CpG-ODN and the STING agonist CDN can activate both TLR-dependent and TLR-independent DNA recognition pathways, respectively. This combination increases the production of cytokines (IFN-γ, IL-6, TNF-α, IP-10), enhances the expression of costimulatory molecules (MHC class II, CD86), and promotes antigen-specific adaptive immune responses, thereby synergistically boosting immune responses [255]. He [216] et al. synthesized a multifunctional nanogel, PVCL-MnO_2-CpG, which could promote the activation of CpG-ODN-associated TLR9 signaling pathway and Mn^{2+}-mediated cGAS/STING pathway (Fig. 9A). PVCL-MnO_2-CpG exhibit excellent ability to cross the blood–brain barrier and successfully reach glioma sites through traversing the disrupted blood–brain barrier (Fig. 9B-C). Combination of PVCL-MnO_2-CpG and RT enhanced the DC maturation and infiltration of $CD3^+/CD8^+$ T cells in the LN and spleen, reprogramming the immunosuppressive TME of GBM (Fig. 9E-M).

Photothermal therapy (PTT)

Photothermal therapy (PTT) works by absorbing light by photothermal agents and converting it into heat, which leads to immune tumor death and induces a strong immune response [256]. Gu [191] et al. synthesized a polymer NP (PLGA-PEG/DMXAA), in which the loaded STING agonist DMXAA could cause tumor vascular disruption and trigger tumor-specific thrombosis (Fig. 10A-C). Tumor thrombi, characterized by elevated hemoglobin levels that are minimally affected by hemodilution, exhibit strong absorption of 808 nm laser irradiation, enabling efficient PTT and induction of ICD. Elevated hemoglobin, serving as a photothermal agent, fundamentally regulates the optical properties and oxygen content within the tumor. Therefore, the researchers employed a small-animal photoacoustic imaging system to longitudinally track photoacoustic (PA) signals in PPD-administered tumor-bearing mice, revealing peak PA signal intensity at 12 h post-injection (Fig. 10D-E). At 12 h post-PPD injection, PTT elevates localized temperatures to approximately 48.5 °C, prompting hemoglobin to release oxygen and transiently alleviate hypoxia within the TME for enhanced PTT/RT (Fig. 10A). Notably, while vascular disruption-induced hypoxia progressively intensifies over time, tumor hypoxia remains controllably mitigated at the 12 h timepoint post-PPD administration due to this oxygen-replenishment mechanism, enabling the sensitization of radiotherapy at a specific time. This strategy uniquely leverages hemoglobin's intrinsic photothermal and oxygen-carrying properties, eliminating the need for synthetic photoabsorbers and reducing biocompatibility concerns. The dual effects of vascular targeting and transient oxygenation enable spatiotemporal control over PTT and RT. Vascular damage limits sustained oxygen supply, necessitating further optimization of treatment frequency and combination therapies. Besides PTT/RT, the tumor vascular damage induced by DMXAA would lead to starvation treatment of cancer. RT and PTT and DMXAA-mediated activation of the cGAS-STING pathway promote DCs maturation, increase the $CD8^+$ T-cell ratio and the M1/M2 ratio, and decrease the T_{reg} ratio (Fig. 10 I-K). PTT/RT/starvation therapy has inhibitory effects on both primary tumors and distant metastatic tumors in 4T1 tumor bearing mice, realizing the almost complete elimination of metastasis/recurrence (Fig. 10H-K).

Notably, nanomaterials have been engineered to serve dual roles as radiosensitizers and photothermal agents. For example, Liu et al. synthesized Au@Pt nanoparticles that synergistically combined PTT with RT [257]. The growth of Pt nanobranches induced a redshift in the absorption spectrum of Au@Pt nanoparticles to the near-infrared (NIR) region, thereby enhancing PTT efficacy. High Z metals (Au and Pt) enhance RT mediated tumor cell ablation by enhancing local radiation dose deposition. Breast cancer cells treated with Au@Pt demonstrated a drastic reduction in viability (30% survival rate) under combined NIR/X-ray irradiation, directly evidencing thermo-radiotherapy efficacy. Similarly, ultrasmall zirconium carbide (ZrC) nanodots have good photothermal properties and photon attenuation to kill glioma under NIR/X-ray irradiation. Yin [258] et al. prepared ZrC

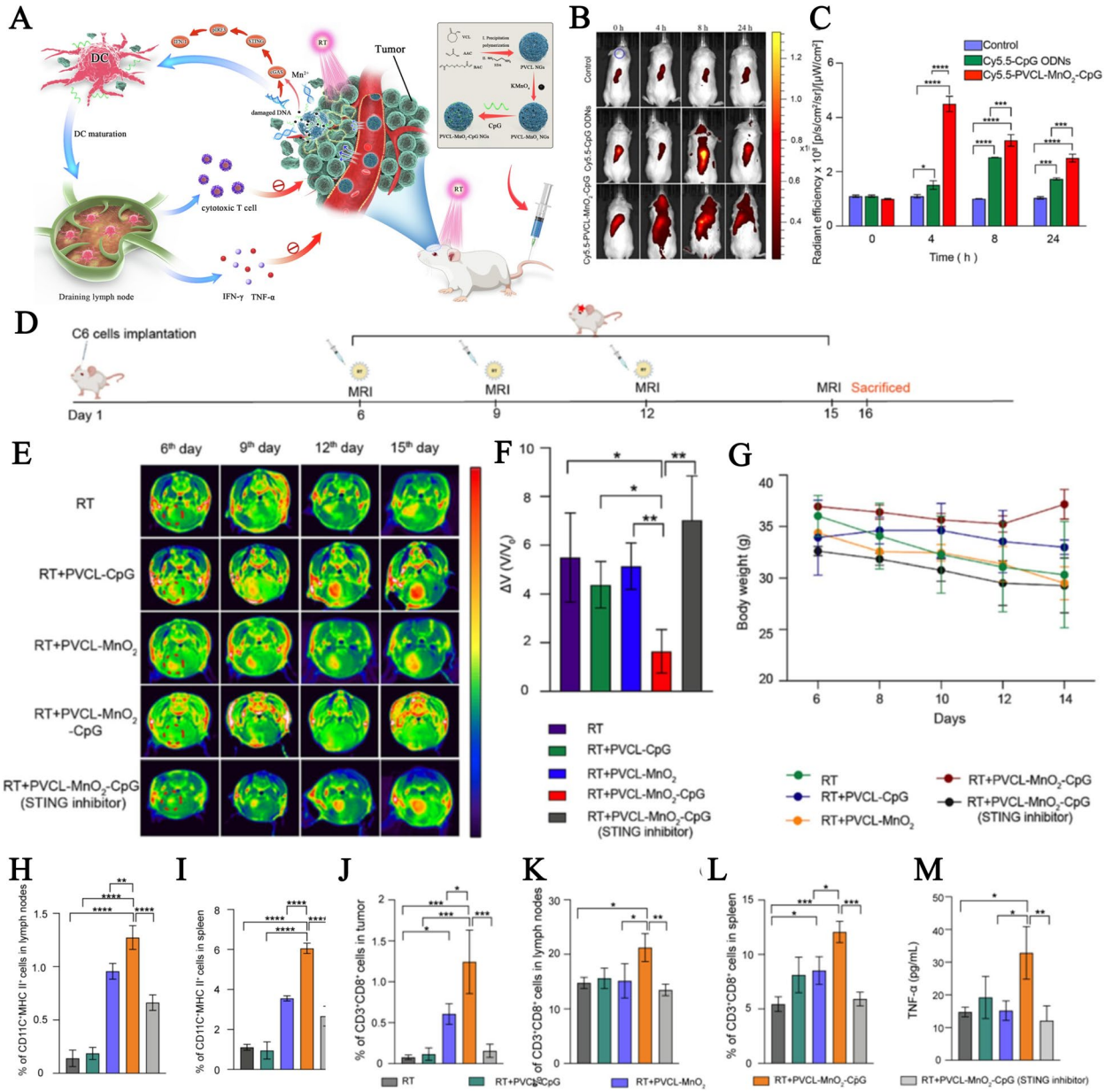

Fig. 9 Combination therapies with STING agonists, RT, and TLR agonists. **A** Schematic illustration of the mechanism underlying PVCL-MnO_2-CpG nanogels combined with RT to treat glioblastoma multiforme (GBM). The nanogels traverse the blood–brain barrier, releasing Mn^{2+} to activate the cGAS/STING pathway and CpG ODNs to trigger TLR9 signaling, thereby promoting DCs maturation and cytotoxic T cell activation. **B**, **C** In vivo evaluation of blood–brain barrier penetration by Cy5.5-labeled PVCL-MnO_2-CpG at different time points. **D** Experimental design of anti-glioblastoma therapy. **E**, **F** T1-weighted MRI images and tumor volume quantification after various treatment. **G** Monitoring of body weight changes during treatment. **H–M** Immune response analysis, including increased proportions of $CD80^+CD86^+$ DCs in lymph node (**H**) and spleen (**I**), and $CD3^+CD8^+$ cytotoxic T cells in lymph node (**J**) and spleen (**K**), along with elevated TNF-α (**L**) and IFN-γ (**M**) levels in different group. Reproduced with permission from ref [216]

PVP nanodots with an average particle size of about 4.36 nm by liquid phase exfoliation method, and modified them with surfactant polyvinylpyrrolidone (PVP), which has good absorption and photothermal conversion efficiency (53.4%) in the near-infrared region. Zr is a transition metal that acts as an effective high-Z radiosensitizer by enhancing localized radiation energy deposition in tumor tissue.

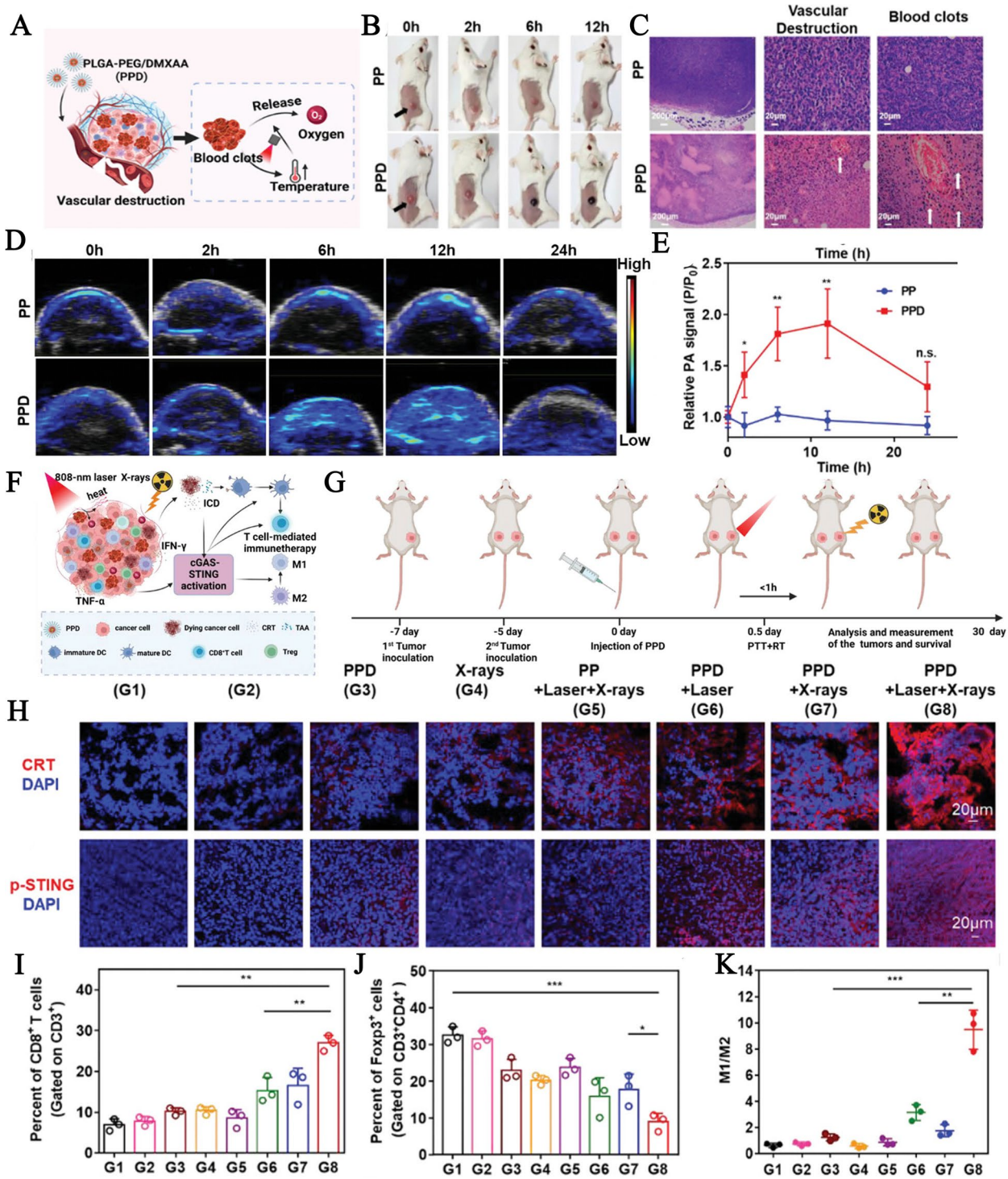

Fig. 10 Combination therapies with STING agonists, RT, and PTT. **A** Schematic of PPD-induced photothermal heating and oxygen release. **B-C** Photographs (**B**) and H&E-stained tumor sections (**C**) illustrating vascular destruction and blood clot formation post-PPD or PP treatment. **D-E** Representative photoacoustic images (**D**) and Quantification of relative photoacoustic signals (**E**) of 4T1 tumors on mice injected with PP or PPD. **F** Schematic representation of systemic anti-tumor immunity induced by PPD-mediated PTT/RT/starvation therapy. **G** Schematic representation of experimental treatment protocols for the 4T1 bilateral tumor model. The laser power was 0.8 W cm^{-2} (8 min), the dose of X-rays was 8 Gy and the dose of DMXAA was 10 mg kg^{-1}. Both PPD administration and therapies including PTT and RT are delivered as single-session treatments. **H** Immunofluorescence staining of CRT (calreticulin) and p-STING in in primary tumors. (**I-K**) Quantification of $CD8^+$ T cells (**I**), $Foxp3.^+$ T_{reg} cells (**J**), and M1/M2 macrophage polarization ratio (**K**) in distant tumors. Reproduced with permission from ref [191]

STING activation combined with RT-RDT

Radiodynamic therapy (RDT) combines the RT and photochemical therapy, and activates the photosensitizer retained in tumor tissue through external X-rays to cause oxidative damage to tumor cells by generating $^1O_2$. The high concentration of $^1O_2$ can destroy the inner membrane pores of mitochondria to induce apoptosis of tumor cells, thus achieving the goal of complete tumor elimination. Li [211] et al. synthesized a nanoscale metal–organic framework MOF (named TZM) synthesized by co-doping the high-Z metal Ta and Zr and photosensitizer TCPP, to enhance RT-RDT effects for killing osteosarcoma cell. The sensitizing RT-RDT effects of TZM can promote the up-regulation of cGAS-STING pathway and PD-L1 expression by inducing ICD of cancer cell, thus triggering a powerful anti-tumor immune response. TZM, anti-PD-L1 and X-ray can enhance antitumor immunotherapy and effectively inhibit the primary and metastasis tumor of osteosarcoma. Luo [97] et al. also reported a two-dimensional nanoplatform cGAMP/MOL, through conjugating cGAMP and photosensitizers DBB-Ir to a metal organic layer Hf_{12}-Ir MOL for STING activation combined with RT-RDT to antagonize tumor (Fig. 11A). Metal organic layers (MOLs) are two-dimensional analogues of metal organic frameworks (MOFs), which have unique chemical properties and remarkable characteristics such as ultra-thin thickness, adjustable structure, large surface area, accessible active site, large pore volume, etc. [259](Fig. 11B). The intracellular phosphate concentration is significantly higher than the extracellular, and this concentration gradient leads to cGAMP/MOL release of cGAMP (Fig. 11C-E). This nanoplatform acts as a radiosensitizer, amplifying RT's tumor-damaging effects while releasing cGAMP for sustained STING activation. This dual action not only improves tumor regression but also strengthens immune responses by triggering both innate and adaptive immunity (Fig. 11F). Combined with ICIs, the approach offers potential for robust systemic anti-tumor effects (Fig. 11G).

Nitric oxide (NO)

NO improves vascular permeability thereby ameliorating hypoxia, prevents DNA damage repair, as well as having an immunostimulatory effect as evidenced by the ability to induce T cell infiltration [260–262]. Suitable NO donor has not been investigated for the time being. Liu [212] et al. synthesized a nanoscale coordination polymer, Hf-nIm@PEG (HNP), which can sensitize RT by activating the cGAS-STING pathway via Hf^{4+}, and preventing DNA damage repair and relieving hypoxia immunosuppressive TME via NO released from 2nlm. Hf-nIm@PEG (HNP) combined with RT promotes maturation of DCs and T-cell infiltration, NK-cell proliferation, M2 to M1 polarization, and decreases the proportion of T_{reg} and MDSCs, thus achieving the maximal killing effect on CT26 tumors.

Surgery

Surgery is the most commonly used treatment modality in oncology, but the immunosuppressive microenvironment created during wound healing can promote tumor recurrence and metastasis. Immunostimulating hydrogels are a promising platform for postoperative oncology. It is 90% water and highly porous [263], easily binding to STING agonists to inhibit metastasis and recurrence of postoperative tumors. Sun [201] et al. developed a ROS-responsive hydrogel (ADU-AAV-PD1@Gel) that sustained the release of the STING agonists ADU- S100 (ADU) and soluble PD-1 (sPD-1) and was used in conjunction with RT in a GBM surgical resection model. RT increases ROS production in TME, leading to hydrogel hydrolysis, which releases ADU- S100 and AAV-PD1. RT combined with intracavity-injectable ADU-AAV-PD1@Gel induced long-term immune memory and prevented GBM recurrence. The hydrogel XCL1@CaMnP [214] synthesized by Wu et al. activates anti-tumor immunity by promoting the activation of cGAS-STING in DCs in combination with postoperative RT, leading to a complete remission rate of 60% in the CT26 tumor model, with no recurrence within 60 days of observation. In this study, the tumor was not completely resected, only 50% of the tumor was removed, followed by a combination of XCL1@CaMnP and RT.

Chemotherapy

Chemotherapy targets all of the body's cells, both tumor cells and normal cells, which means that the drugs used can cause a variety of side effects. Irinotecan (IRIN) is a very important chemotherapy drug for the treatment of colorectal cancer. The investigation by Lu [264] et al. synthesized a mesoporous silica nanoparticle coated with a lipid bilayer to deliver irinotecan (IRIN), and when this nanomedicine is combined with RT to achieve activation of the cGAS-STING pathway, this approach may increase $CD8^+$ T cell, $CD4^+$ T cell, and DCs in the MC38 CRC syngeneic tumor model. Compared to free IRIN plus RT, IRIN silicasome combined with RT provided greater anti-tumor efficacy and reduced side effects. In Duo [265] et al. found that an Au based AIEgen-inactivated cancer cell vector could target tumors and achieve a triple-modal chemo-radio-immunotherapy effects on melanoma under x-ray irradiation. AIEgen triggers DNA damage and ROS generation to effectively induce ICD. This combination therapy upregulates various cytokines including TNFα, IFN-γ, IL-2, and IL-12, as well as activates the

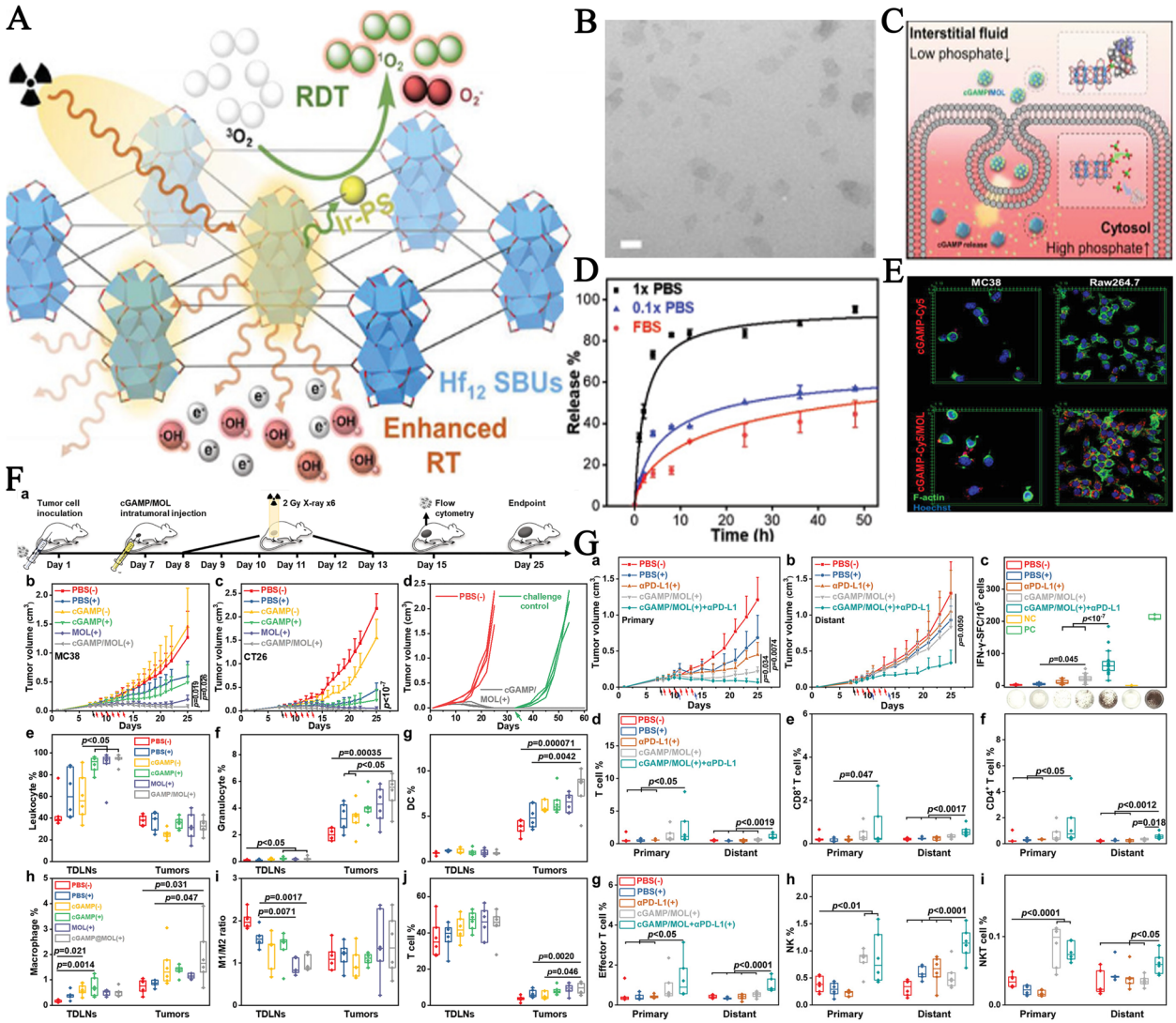

Fig. 11 Nano-STING agonists combined with RT-RDT to antagonize tumor. **A** Illustration showing the 2D architecture of Hf12-Ir MOL and its augmented RT-RDT capabilities. Upon X-ray irradiation, Hf_{12} SBUs enhance RT by absorbing X-ray energy and producing more hydroxyl radicals (·OH) through radiolysis. The SBUs transfer energy to DBB-Ir photosensitizer (Ir-PS) ligands to enable RDT by generating singlet oxygen ($^1O_2$), superoxide anions (O_2^{-}·) and other ROS. **B** TEM image showing a nanosheet morphology of the MOL (scale bar = 200 nm). **C** Mechanistic diagram illustrating cellular uptake of cGAMP/MOL and controlled release of cGAMP inside cells via the intracellular/extracellular phosphate gradients. **D** Release profiles of cGAMP/MOL under different physiological conditions by LC–MS. cGAMP/MOL was dispersed in 0.1 × PBS (1.18 mM phosphate), 1 × PBS (11.8 mM phosphate), and fetal bovine serum (FBS, ≈1 mM phosphate) at 37 °C to simulate interstitial, intracellular, and serum environments, respectively. **E** Three-dimensional CLSM reconstruction comparing cellular uptake efficiency between free Cy5-cGAMP and Cy5-cGAMP/MOL complexes in MC38 and Raw264.7 cell lines at 8 h post-treatment (Blue: Hoechst 33,342 nuclear staining; Green: F-actin cytoskeletal staining; Red: Cy5-cGAMP localization). **F** cGAMP/MOL combines RT-RDT and STING activation for tumor regression. **G** The combination of cGAMP/MOL (+) and αPD-L1 treatment demonstrates robust growth inhibition in both primary and distal tumors. Reproduced with permission from ref [97]

cGAS-STING pathway, thereby activating innate and adaptive immunity in melanoma tumor models.

Summary and prospect

Most studies have demonstrated that nano-mediated STING activation combined with RT stimulates potent anti-tumor immunity, inhibits the growth of primary and metastatic tumors and provides systemic memory anti-cancer effect. The immunostimulatory effects of this combined treatment strategy are reflected in the enhancement of responses from both tumor cells and immune cells, as well as the remodeling of the TME. The versatility of nanobiomaterials offers new opportunities for the development of combination therapies

incorporating cGAS-STING stimulators and other antitumor treatments. STING agonists can be used in combination with other cancer immunotherapies, including surgery, chemoradiotherapy, cancer vaccines, ICB, TLR7/8 agonist, antibody–drug conjugate (ADC), CAR-T and CAR-NK therapy that will hold promise for treating cancers [266, 267]. However, these studies have been validated in mouse models, and only a few nanomedicines can be utilized in human clinical trials at present. The transition from trials to clinical use still requires a lot of effort. Priority should be given to conducting studies in porcine or non-human primate models to evaluate systemic toxicity and immune responses that more closely recapitulate human physiology. Concurrently, continued efforts should be devoted to developing innovative nanomedicines, such as engineered extracellular vesicles, to advance therapeutic delivery platforms. Future research efforts could focus on establishing biomarkers (e.g., STING expression, or baseline IFN signature) to stratify patients most likely to benefit from combination therapies. The phosphorylation of TBK1 and IRF3 is critical for downstream signaling in the cGAS-STING pathway; thus, pTBK1 and pIRF3 can serve as predictive biomarkers [268]. The chromosomal instability (CIN) phenotype, determined by loss of heterozygosity (LOH) status, can be used to identify patients who are candidates for STING agonist [269]. CIN^{low} tumors exhibit a more proinflammatory environment, characterized by activated DCs and $CD4^{+}$ T helper cells, whereas CIN^{high} tumors contain anti-inflammatory macrophages, granulated MDSCs, and dysfunctional T cells [270]. The application of STING agonists may not be ideal for tumors with a CIN^{high} phenotype. Tumors exhibiting impaired STING signaling may necessitate additional therapeutic interventions to overcome pathway deficiencies.

a) Precise targeting of STING agonists

Currently, in most studies based on nano-mediated STING activation in combination with RT, the targeting site of nanoparticles loaded with STING agonists is the tumor cell or APCs. In the precision targeting of STING agonists, the selection of target cells should be informed by the tumor type and its TME. For instance, glioblastoma is characterized as an immunologically "cold" or "quiet" tumor, posing significant treatment challenges due to the insufficient presence of effector T cells and the abundance of immunosuppressive TAMCs. Reprogramming TAMCs into proinflammatory cells through targeted activation of the cGAS-STING pathway enhances the recruitment and activation of T cells [249, 271]. A deeper understanding of the markers and signaling pathways that shape specific TME is essential for the development of targeted STING agonists. When specific target-driven mutations are present in tumors, STING agonists can be employed in conjunction with targeted therapeutics aimed at these mutations. Encouraging preclinical studies have demonstrated the potential of combining antibody–drug conjugates (ADCs) with gene-based strategies and STING agonists, paving the way for innovative approaches in the development of STING agonist therapies [272]. ADCs combining STING agonists with antibodies targeting EGFR have been synthesized. HER2 mutations are prevalent in certain subtypes of breast cancer. Cai et al. elucidated that the inhibition of the cGAS-STING pathway is a critical factor contributing to immune escape in Herceptin-resistant breast cancers. Combining STING agonists with DS-8201 presents a promising novel strategy for targeting HER2-positive breast cancers that are resistant to Herceptin [273]. Tumor heterogeneity impacts the efficacy of cGAS-STING targeted therapies. Genetic mutations and epigenetic modifications contribute to variations in STING signaling, leading to differential responses among cancer types [274]. In gliomas, hypermethylation of the CpG site cg16983159 located in the STING promoter may render cells less sensitive to cGAMP, but this sensitivity can be restored using DNA methyltransferase inhibitors [275]. In melanoma, STING signaling is often compromised due to methylation of the STING promoter. DNA methylation inhibitors can restore STING functionality and enhance tumor immunogenicity [276]. These insights highlight the complexity of cGAS-STING signaling across different cancer types and underscore the need for patient stratification strategies, including genomic and epigenetic analyses, to optimize cGAS-STING targeted therapies.

b) Considerations of RT with STING agonists

The combination of RT and STING agonists may increase the risk of autoimmune diseases, systemic inflammatory storms, and radiation pneumonitis [277]. Although RT effectively targets tumors, it also has the unintended consequence of damaging immune cells. If STING agonists are used to target and activate the cGAS-STING pathway in immune cells, it is critical to ensure that the viability of these immune cells is not adversely affected by RT. The emergence of these adverse reactions requires further investigation to determine the optimal dosing of STING agonists and RT, as well as the sequencing of their administration. During the implementation of radiotherapy, the dosage of STING agonists should be minimized. And Low-dose segmentation maximizes activation of the

cGAS-STING pathway. Radiation doses above 12–18 Gy induce the production of the three prime repair exonuclease 1 (Trex1) in various cancer cells [278]. Trex1 is a DNA exonuclease that degrades DNA accumulated in the cytoplasm during radiation to reduce its immunogenicity [50, 51]. Novel radiation delivery technologies can lead to synergistic effects with STING agonists by eliciting different responses from the immune system compared to conventional radiation therapy. For instance, FLASH radiotherapy delivers high dose rates (> 40 Gy/s, while standard radiation therapy is 2 Gy/min), avoiding the toxicity associated with STING activation in normal tissues observed at conventional dose rates, while preserving efficacy against tumors [279]. Personalized ultrahypofractionated stereotactic adaptive radiotherapy (PULSAR) allows for higher radiation doses spaced further apart in time, capitalizing on tumor shrinkage and changes in the TME. Clinical trial results of PULSAR in combination with STING agonists may provide insights to guide the future direction of combination therapies.

c) The influencing factors of cGAS-STING pathway activated by RT
RT-activated cGAS-STING-IFN signaling can be influenced by other factors such as ZBP1-MLKL necrosis cascade, ferroptosis, activation of caspases during apoptosis, autophagy, and non-canonical NF-κB pathways. Activation of cGAS-STING-IFN signaling can be promoted by facilitating or inhibiting these factors.

Necroptosis is considered the major mode of ICD [280]. The ZBP1-MLKL necrosis cascade is crucial for the anti-tumor immunity of irradiated tumor cells, promoting $CD8^{+}$T cell response by enhancing the activation of DCs after radiation [281]. Mechanistically, the activated MLKL can be localized in mitochondria, which may promote the formation of mitochondrial pores and the efflux of mtDNA into the cytoplasm, thereby promoting the activation of the cGAS-STING pathway in tumor cells after RT [282]. Ablation of caspase-8 enhances STING pathway activation and the anti-tumor effect of radiation by activating MLKL [281]. Caspase-8, a major regulator of intrinsic apoptosis, blocks the ZBP1-MLKL necrosis cascade by cleaving the ZBP1-RIPK3 complex [283]. RT can also promote ferroptosis through diverse mechanisms [284]. Ferroptosis, a ROS-dependent cell death, relates to iron accumulation and lipid peroxidation [285] which promotes DC maturation, and subsequently enhances T cell activation. Hu et al. synthesized a glucose oxidase (GOx)-doped nanoplatform (HfO2@MnO_2@GOx, HMG) to trigger ferroptosis through glutathione depletion and ROS generation [286]. This ferroptosis cascade is further sensitized to RT by enhancing DNA damage in 4 T1 breast cancer cells.

Tumor recurrence often occurs after RT due to immune privilege induced by both intrinsic tumor and extrinsic factors in various types of human cancers. For instance, non-canonical NF-κB pathway can lead to impaired type I IFN production and inhibit DCs function. It negatively regulates the anti-tumor immune response through the competitive binding of RelB in p52/RelB to the IFNB gene promoter with RelA in p50/RelA, resulting in impaired type I IFN [287]. Moreover, intrinsic autophagy [288, 289] and caspase-9 signaling [47] in tumor cells generate radiation resistance by suppressing STING-mediated cytosolic DNA sensing after irradiation. Inhibition of these pathways can promote the activation of the cGAS-STING pathway, thereby sensitizing tumors to RT. Considering the connection between the cGAS- STING pathway and other pathways, therefore, we can maximally enhance the activation of the cGAS-STING pathway by modulating other pathways.

Authors' contributions

Kelong Ai, Rongrong Zhou, and Qian Zeng were responsible for conducting the literature review, organizing the manuscript structure, and drafting the primary sections of the review. Qian Zeng and Min Liu provided assistance in collecting and analyzing relevant publications, as well as contributing to the preparation of figures and tables. Ziqi Wang aided in the conceptualization of the review's focus and offered critical revisions of the manuscript. Rongrong Zhou and Kelong Ai, as co-corresponding authors, supervised the overall project, provided expert guidance, and contributed to the critical review and final approval of the manuscript. All authors read and approved the final version of the manuscript.

Funding

This work was supported by the National Natural Science Foundation of China (No. 82373871, 81,974,508). Innovation-Driven Project of Central South University (No. 202045005). Central South University Research Programme of Advanced Interdisciplinary Studies (2023QYJC017), Key Research Project of Ningxia Hui Autonomous Region of China (Major Project) (No. 2023BEG02038). The Key Program of Ningxia Hui Autonomous Region Natural Science Foundation of China (No. 2022 AAC02058). The Natural Science Foundation of Hunan (2022 JJ30992). The National Clinical Research Center for Geriatric Disorders, Xiangya Hospital, Central South University (No. 2022LNJJ10).

Data availability

No datasets were generated or analysed during the current study.

Declarations

Ethics approval and consent to participate

Not applicable.

Competing interests

The authors declare no competing interests.

Received: 31 March 2025 Accepted: 26 May 2025
Published online: 11 June 2025

References

1. Chai LF, Prince E, Pillarisetty VG, Katz SC. Challenges in assessing solid tumor responses to immunotherapy. Cancer Gene Ther. 2020;27:528–38.
2. Martin JD, Cabral H, Stylianopoulos T, Jain RK. Improving cancer immunotherapy using nanomedicines: progress, opportunities and challenges. Nat Rev Clin Oncol. 2020;17:251–66.
3. Chen DS, Mellman I. Elements of cancer immunity and the cancer-immune set point. Nature. 2017;541:321–30.
4. Viel S, Vivier E, Walzer T, Marçais A. Targeting metabolic dysfunction of CD8 T cells and natural killer cells in cancer. Nature Reviews Drug Discovery. 2025;24:190–208.
5. Wu B, Zhang B, Li B, Wu H, Jiang M. Cold and hot tumors: from molecular mechanisms to targeted therapy. Signal Transduct Target Ther. 2024;9:274.
6. Duan Q, Zhang H, Zheng J, Zhang L. Turning cold into hot: firing up the tumor microenvironment. Trends in cancer. 2020;6:605–18.
7. Butterfield LH, Najjar YG. Immunotherapy combination approaches: mechanisms, biomarkers and clinical observations. Nat Rev Immunol. 2024;24:399–416.
8. Morris ZS, Demaria S, Monjazeb AM, Formenti SC, Weichselbaum RR, Welsh J, et al. Proceedings of the National Cancer Institute Workshop on combining immunotherapy with radiotherapy: challenges and opportunities for clinical translation. Lancet Oncol. 2025;26:e152–70.
9. Kim JS, Chang AR. Abscopal effect in metastatic breast cancer treated with stereotactic body radiotherapy in the absence of immunotherapy. Front Oncol. 2023;13:1243053.
10. Piercey O, Tomaszewski JM, Smith K. Intracranial response after extracranial radiation in a patient with rapidly progressing metastatic melanoma. BMJ Case Reports CP. 2021;14: e240921.
11. MacManus MP, Hofman MS, Hicks RJ, Campbell BA, Wirth A, Seymour JF, et al. Abscopal Regressions of Lymphoma After Involved-Site Radiation Therapy Confirmed by Positron Emission Tomography. Int J Radiat Oncol Biol Phys. 2020;108:204–11.
12. D'Andrea MA, Reddy GK. Immune system activation in patients with metastatic renal cell carcinoma induced by the systemic abscopal effects of radiation therapy. Oncology Research and Treatment. 2023;46:33–44.
13. Golden EB, Chhabra A, Chachoua A, Adams S, Donach M, Fenton-Kerimian M, et al. Local radiotherapy and granulocyte-macrophage colony-stimulating factor to generate abscopal responses in patients with metastatic solid tumours: a proof-of-principle trial. Lancet Oncol. 2015;16:795–803.
14. Craig DJ, Nanavaty NS, Devanaboyina M, Stanbery L, Hamouda D, Edelman G, et al. The abscopal effect of radiation therapy. Future Oncol. 2021;17:1683–94.
15. Mole RH. Whole body irradiation; radiobiology or medicine? Br J Radiol. 1953;26:234–41.
16. Demaria S, Formenti SC. Radiotherapy effects on anti-tumor immunity: implications for cancer treatment. Front Oncol. 2013;3:128.
17. Barker HE, Paget JT, Khan AA, Harrington KJ. The tumour microenvironment after radiotherapy: mechanisms of resistance and recurrence. Nat Rev Cancer. 2015;15:409–25.
18. Guo S, Yao Y, Tang Y, Xin Z, Wu D, Ni C, et al. Radiation-induced tumor immune microenvironments and potential targets for combination therapy. Signal Transduct Target Ther. 2023;8:205.
19. Zheng H, Guo B, Qiu X, Xia Y, Qu Y, Cheng L, et al. Polymersome-mediated cytosolic delivery of cyclic dinucleotide STING agonist enhances tumor immunotherapy. Bioactive Materials. 2022;16:1–11.
20. Yang K, Han W, Jiang X, Piffko A, Bugno J, Han C, et al. Zinc cyclic di-AMP nanoparticles target and suppress tumours via endothelial STING activation and tumour-associated macrophage reinvigoration. Nat Nanotechnol. 2022;17(12):1322–31.
21. Wang C, Sun Z, Zhao C, Zhang Z, Wang H, Liu Y, et al. Maintaining manganese in tumor to activate cGAS-STING pathway evokes a robust abscopal anti-tumor effect. J Control Release. 2021;331:480–90.
22. Luo M, Liu Z, Zhang X, Han C, Samandi LZ, Dong C, et al. Synergistic STING activation by PC7A nanovaccine and ionizing radiation improves cancer immunotherapy. J Control Release. 2019;300:154–60.
23. Liu Y, Crowe WN, Wang L, Lu Y, Petty WJ, Habib AA, et al. An inhalable nanoparticulate STING agonist synergizes with radiotherapy to confer long-term control of lung metastases. Nat Commun. 2019;10:5108.
24. Koshy ST, Cheung AS, Gu L, Graveline AR, Mooney DJ. Liposomal Delivery Enhances Immune Activation by STING Agonists for Cancer Immunotherapy. Adv Biosyst. 2017;1:1600013.
25. Linderman SW, DeRidder L, Sanjurjo L, Foote MB, Alonso MJ, Kirtane AR, et al. Enhancing immunotherapy with tumour-responsive nanomaterials. Nature Reviews Clinical Oncology. 2025;22:262–282.
26. Bonvalot S, Rutkowski PL, Thariat J, Carrère S, Ducassou A, Sunyach MP, et al. Final Safety and Health-Related Quality of LIfe Results of the Phase 2/3 Act.In.Sarc Study With Preoperative NBTXR3 Plus Radiation Therapy Versus Radiation Therapy in Locally Advanced Soft-Tissue Sarcoma. Int J Radiat Oncol Biol Phys. 2022;114:422–32.
27. Li G, Zhao X, Zheng Z, Zhang H, Wu Y, Shen Y, et al. cGAS-STING pathway mediates activation of dendritic cell sensing of immunogenic tumors. Cell Mol Life Sci. 2024;81:149.
28. Moon J, Kitty I, Renata K, Qin SS, Zhao F, Kim W. DNA Damage and Its Role in Cancer Therapeutics. Int J Mol Sci. 2023;24:4741.
29. Cao Y, Wu T, Dai W, Dong H, Zhang X. TiO2 nanosheets with the Au nanocrystal-decorated edge for mitochondria-targeting enhanced sonodynamic therapy. Chem Mater. 2019;31:9105–14.
30. Wang X, Zhong X, Gong F, Chao Y, Cheng L. Newly developed strategies for improving sonodynamic therapy. Mater Horiz. 2020;7:2028–46.
31. Pan X, Wang H, Wang S, Sun X, Wang L, Wang W, et al. Sonodynamic therapy (SDT): a novel strategy for cancer nanotheranostics. Science China Life sciences. 2018;61:415–26.
32. Baumann M, Krause M, Overgaard J, Debus J, Bentzen SM, Daartz J, et al. Radiation oncology in the era of precision medicine. Nat Rev Cancer. 2016;16:234–49.
33. Le Caër S. Water radiolysis: influence of oxide surfaces on H2 production under ionizing radiation. Water. 2011;3:235–53.
34. Hatzi VI, Laskaratou DA, Mavragani IV, Nikitaki Z, Mangelis A, Panayiotidis MI, et al. Non-targeted radiation effects in vivo: a critical glance of the future in radiobiology. Cancer Lett. 2015;356:34–42.
35. Sridharan D, Asaithamby A, Bailey S, Costes S, Doetsch P, Dynan W, et al. Understanding cancer development processes after HZE-particle exposure: roles of ROS, DNA damage repair and inflammation. Radiat Res. 2015;183:1–26.
36. Guo SY, Yao YH, Tang Y, Xin ZF, Wu D, Ni C, et al. Radiation-induced tumor immune microenvironments and potential targets for combination therapy. Signal Transduct Target Ther. 2023;8:205.
37. McLaughlin M, Patin EC, Pedersen M, Wilkins A, Dillon MT, Melcher AA, et al. Inflammatory microenvironment remodelling by tumour cells after radiotherapy. Nat Rev Cancer. 2020;20:203–17.
38. Ash C, Dubec M, Donne K, Bashford T. Effect of wavelength and beam width on penetration in light-tissue interaction using computational methods. Lasers Med Sci. 2017;32:1909–18.
39. Abe T, Barber GN. Cytosolic-DNA-mediated, STING-dependent proinflammatory gene induction necessitates canonical NF-κB activation through TBK1. J Virol. 2014;88:5328–41.
40. Schneider WM, Chevillotte MD, Rice CM. Interferon-stimulated genes: a complex web of host defenses. Annu Rev Immunol. 2014;32:513–45.
41. Borden EC. Interferons α and β in cancer: therapeutic opportunities from new insights. Nat Rev Drug Discov. 2019;18:219–34.
42. Storozynsky Q, Hitt MM. The Impact of Radiation-Induced DNA Damage on cGAS-STING-Mediated Immune Responses to Cancer. Int J Mol Sci. 2020;21:8877.
43. Marill J, Anesary NM, Paris S. DNA damage enhancement by radiotherapy-activated hafnium oxide nanoparticles improves cGAS-STING pathway activation in human colorectal cancer cells. Radiother Oncol. 2019;141:262–6.
44. Hatch EM, Fischer AH, Deerinck TJ, Hetzer MW. Catastrophic nuclear envelope collapse in cancer cell micronuclei. Cell. 2013;154:47–60.
45. Decout A, Katz JD, Venkatraman S, Ablasser A. The cGAS-STING pathway as a therapeutic target in inflammatory diseases. Nat Rev Immunol. 2021;21:548–69.
46. West AP, Shadel GS, Ghosh S. Mitochondria in innate immune responses. Nat Rev Immunol. 2011;11:389–402.
47. Wu C-C, Bratton SB. Regulation of the Intrinsic Apoptosis Pathway by Reactive Oxygen Species. Antioxid Redox Signal. 2013;19:546–58.

48. Kim J, Kim HS, Chung JH. Molecular mechanisms of mitochondrial DNA release and activation of the cGAS-STING pathway. Exp Mol Med. 2023;55:510–9.
49. Hopfner KP, Hornung V. Molecular mechanisms and cellular functions of cGAS-STING signalling. Nat Rev Mol Cell Biol. 2020;21:501–21.
50. Vanpouille-Box C, Alard A, Aryankalayil MJ, Sarfraz Y, Diamond JM, Schneider RJ, et al. DNA exonuclease Trex1 regulates radiotherapy-induced tumour immunogenicity. Nat Commun. 2017;8:15618.
51. Baris AM, Fraile-Bethencourt E, Anand S. Nucleic Acid Sensing in the Tumor Vasculature. Cancers. 2021;13:4452.
52. Carozza JA, Böhnert V, Nguyen KC, Skariah G, Shaw KE, Brown JA, et al. Extracellular cGAMP is a cancer-cell-produced immunotransmitter involved in radiation-induced anticancer immunity. Nature cancer. 2020;1:184–96.
53. Mekers VE, Kho VM, Ansems M, Adema GJ. cGAS/cGAMP/STING signal propagation in the tumor microenvironment: Key role for myeloid cells in antitumor immunity. Radiother Oncol. 2022;174:158–67.
54. Chen Q, Boire A, Jin X, Valiente M, Er EE, Lopez-Soto A, et al. Carcinoma–astrocyte gap junctions promote brain metastasis by cGAMP transfer. Nature. 2016;533:493–8.
55. Schadt L, Sparano C, Schweiger NA, Silina K, Cecconi V, Lucchiari G, et al. Cancer-cell-intrinsic cGAS expression mediates tumor immunogenicity. Cell Rep. 2019;29(1236–48): e7.
56. Zhou Y, Fei M, Zhang G, Liang W-C, Lin W, Wu Y, et al. Blockade of the phagocytic receptor MerTK on tumor-associated macrophages enhances P2X7R-dependent STING activation by tumor-derived cGAMP. Immunity. 2020;52(357–73): e9.
57. Deng L, Liang H, Xu M, Yang X, Burnette B, Arina A, et al. STING-Dependent Cytosolic DNA Sensing Promotes Radiation-Induced Type I Interferon-Dependent Antitumor Immunity in Immunogenic Tumors. Immunity. 2014;41:843–52.
58. Islam S, Islam MM, Akhand MRN, Park BY, Akanda MR. Recent advancements in cGAS-STING activation, tumor immune evasion, and therapeutic implications. Med Oncol. 2024;41:291.
59. Mistry AR, O'Callaghan CA. Regulation of ligands for the activating receptor NKG2D. Immunology. 2007;121:439–47.
60. Panaretakis T, Kepp O, Brockmeier U, Tesniere A, Bjorklund A-C, Chapman DC, et al. Mechanisms of pre-apoptotic calreticulin exposure in immunogenic cell death. EMBO J. 2009;28:578–90.
61. Hallahan D, Kuchibhotla J, Wyble C. Cell adhesion molecules mediate radiation-induced leukocyte adhesion to the vascular endothelium. Cancer Res. 1996;56:5150–5.
62. Huang L, Lemos HP, Li L, Li M, Chandler PR, Baban B, et al. Engineering DNA Nanoparticles as Immunomodulatory Reagents that Activate Regulatory T Cells. J Immunol. 2012;188:4913–20.
63. Walker LS, Sansom DM. The emerging role of CTLA4 as a cell-extrinsic regulator of T cell responses. Nat Rev Immunol. 2011;11:852–63.
64. Stanley ER, Chitu V. CSF-1 receptor signaling in myeloid cells. Cold Spring Harb Perspect Biol. 2014;6:a021857.
65. Morrissey SM, Zhang F, Ding C, Montoya-Durango DE, Hu X, Yang C, et al. Tumor-derived exosomes drive immunosuppressive macrophages in a pre-metastatic niche through glycolytic dominant metabolic reprogramming. Cell Metab. 2021;33:2040-58.e10.
66. Li K, Shi H, Zhang B, Ou X, Ma Q, Chen Y, et al. Myeloid-derived suppressor cells as immunosuppressive regulators and therapeutic targets in cancer. Signal Transduct Target Ther. 2021;6:362.
67. Liang H, Deng L, Hou Y, Meng X, Huang X, Rao E, et al. Host STING-dependent MDSC mobilization drives extrinsic radiation resistance. Nat Commun. 2017;8:1736.
68. Liang H, Deng LF, Hou YZ, Meng XJ, Huang XN, Rao EY, et al. Host STING-dependent MDSC mobilization drives extrinsic radiation resistance. Nat Commun. 2017;8:1736.
69. McDonald JT, Kim K, Norris AJ, Vlashi E, Phillips TM, Lagadec C, et al. Ionizing Radiation Activates the Nrf2 Antioxidant Response. Can Res. 2010;70:8886–95.
70. Bruno A, Mortara L, Baci D, Noonan DM, Albini A. Myeloid Derived Suppressor Cells Interactions With Natural Killer Cells and Pro-angiogenic Activities: Roles in Tumor Progression. Front Immunol. 2019;10:771.
71. Cassetta L, Bruderek K, Skrzeczynska-Moncznik J, Osiecka O, Hu XY, Rundgren IM, et al. Differential expansion of circulating human MDSC subsets in patients with cancer, infection and inflammation. J Immunother Cancer. 2020;8:e001223.
72. Kho VM, Mekers VE, Span PN, Bussink J, Adema GJ. Radiotherapy and cGAS/STING signaling: Impact on MDSCs in the tumor microenvironment. Cell Immunol. 2021;362:104298.
73. Noman MZ, Desantis G, Janji B, Hasmim M, Karray S, Dessen P, et al. PD-L1 is a novel direct target of HIF-1α, and its blockade under hypoxia enhanced MDSC-mediated T cell activation. J Exp Med. 2014;211:781–90.
74. Thomas JG, Kerrigan BCP, Hossain A, Gumin J, Shinojima N, Nwajei F, et al. Ionizing radiation augments glioma tropism of mesenchymal stem cells. J Neurosurg. 2018;128:287–95.
75. Zheng Z, Jia S, Shao C, Shi Y. Irradiation induces cancer lung metastasis through activation of the cGAS-STING-CCL5 pathway in mesenchymal stromal cells. Cell Death Dis. 2020;11:326.
76. Kalluri R. The biology and function of fibroblasts in cancer. Nat Rev Cancer. 2016;16:582–98.
77. Shevtsov M, Sato H, Multhoff G, Shibata A. Novel Approaches to Improve the Efficacy of Immuno-Radiotherapy. Front Oncol. 2019;9:156.
78. Du S-S, Chen G-W, Yang P, Chen Y-X, Hu Y, Zhao Q-Q, et al. Radiation Therapy Promotes Hepatocellular Carcinoma Immune Cloaking via PD-L1 Upregulation Induced by cGAS-STING Activation. Int J Radiat Oncol Biol Phys. 2022;112:1243–55.
79. Garcia-Diaz A, Shin DS, Moreno BH, Saco J, Escuin-Ordinas H, Rodriguez GA, et al. Interferon Receptor Signaling Pathways Regulating PD-L1 and PD-L2 Expression. Cell Rep. 2017;19:1189–201.
80. Wang N-H, Lei Z, Yang H-N, Tang Z, Yang M-Q, Wang Y, et al. Radiation-induced PD-L1 expression in tumor and its microenvironment facilitates cancer-immune escape: a narrative review. Ann Transl Med. 2022;10:1406.
81. Li A, Yi M, Qin S, Song Y, Chu Q, Wu K. Activating cGAS-STING pathway for the optimal effect of cancer immunotherapy. J Hematol Oncol. 2019;12:35.
82. Cooper BT, Chmura SJ, Luke JJ, Shiao SL, Basho RK, Iams WT, et al. TAK-676 in combination with pembrolizumab after radiation therapy in patients (pts) with advanced non-small cell lung cancer (NSCLC), triple-negative breast cancer (TNBC), or squamous-cell carcinoma of the head and neck (SCCHN): Phase 1 study design. J Clin Oncol. 2022;40:TPS2698-TPS2698.
83. Shabrish S, Mittra I. Cytokine storm as a cellular response to dsDNA breaks: a new proposal. Front Immunol. 2021;12: 622738.
84. Karki R, Kanneganti T-D. The 'cytokine storm': molecular mechanisms and therapeutic prospects. Trends Immunol. 2021;42:681–705.
85. Muskardin TLW, Niewold TB. Type I interferon in rheumatic diseases. Nat Rev Rheumatol. 2018;14:214–28.
86. Constanzo J, Faget J, Ursino C, Badie C, Pouget J-P. Radiation-induced immunity and toxicities: the versatility of the cGAS-STING pathway. Front Immunol. 2021;12: 680503.
87. Carideo Cunniff E, Sato Y, Mai D, Appleman VA, Iwasaki S, Kolev V, et al. TAK-676: A Novel Stimulator of Interferon Genes (STING) Agonist Promoting Durable IFN-dependent Antitumor Immunity in Preclinical Studies. Cancer Res Commun. 2022;2:489–502.
88. Uslu U, Sun L, Castelli S, Finck AV, Assenmacher C-A, Young RM, et al. The STING agonist IMSA101 enhances chimeric antigen receptor T cell function by inducing IL-18 secretion. Nat Commun. 2024;15:3933.
89. Ying X, Chen Q, Yang Y, Wu Z, Zeng W, Miao C, et al. Nanomedicines harnessing cGAS-STING pathway: sparking immune revitalization to transform "cold" tumors into "hot" tumors. Mol Cancer. 2024;23:277.
90. Bae Y, Nishiyama N, Fukushima S, Koyama H, Yasuhiro M, Kataoka K. Preparation and Biological Characterization of Polymeric Micelle Drug Carriers with Intracellular pH-Triggered Drug Release Property: Tumor Permeability, Controlled Subcellular Drug Distribution, and Enhanced in Vivo Antitumor Efficacy. Bioconjug Chem. 2005;16:122–30.
91. Wehbe M, Wang-Bishop L, Becker KW, Shae D, Baljon JJ, He X, et al. Nanoparticle delivery improves the pharmacokinetic properties of cyclic dinucleotide STING agonists to open a therapeutic window for intravenous administration. J Control Release. 2021;330:1118–29.
92. Larkin B, Ilyukha V, Sorokin M, Buzdin A, Vannier E, Poltorak A. Cutting Edge: Activation of STING in T Cells Induces Type I IFN Responses and Cell Death. J Immunol. 2017;199:397–402.

93. Cerboni S, Jeremiah N, Gentili M, Gehrmann U, Conrad C, Stolzenberg MC, et al. Intrinsic antiproliferative activity of the innate sensor STING in T lymphocytes. J Exp Med. 2017;214:1769–85.
94. Wu J, Dobbs N, Yang K, Yan N. Interferon-independent activities of mammalian STING mediate antiviral response and tumor immune evasion. Immunity. 2020;53(115–26): e5.
95. Wu J, Dobbs N, Yang K, Yan N. Interferon-Independent Activities of Mammalian STING Mediate Antiviral Response and Tumor Immune Evasion. Immunity. 2020;53:115-26.e5.
96. Sprooten J, Agostinis P, Garg AD. Type I interferons and dendritic cells in cancer immunotherapy. Int Rev Cell Mol Biol. 2019;348:217–62.
97. Luo T, Nash GT, Jiang X, Feng X, Mao J, Liu J, et al. A 2D Nanoradiosensitizer Enhances Radiotherapy and Delivers STING Agonists to Potentiate Cancer Immunotherapy. Adv Mater. 2022;34:e2110588.
98. Gu Y, Lin S, Wu Y, Xu P, Zhu W, Wang Y, et al. Targeting STING Activation by Antigen-inspired MnO2 Nanovaccines Optimizes Tumor Radiotherapy. Advanced healthcare materials. 2023;12:2300028.
99. de Oliveira Mann CC, Orzalli MH, King DS, Kagan JC, Lee ASY, Kranzusch PJ. Modular Architecture of the STING C-Terminal Tail Allows Interferon and NF-κB Signaling Adaptation. Cell Rep. 2019;27:1165-75.e5.
100. Wan D, Jiang W, Hao J. Research Advances in How the cGAS-STING Pathway Controls the Cellular Inflammatory Response. Front Immunol. 2020;11:615.
101. Du S, Chen G, Yuan B, Hu Y, Yang P, Chen Y, et al. DNA sensing and associated type 1 interferon signaling contributes to progression of radiation-induced liver injury. Cell Mol Immunol. 2021;18:1718–28.
102. Zhao X, Du L, Ma N, Tan X, Lei X, Zhang P, et al. The role of cGAS-STING pathway in the development of radiation-induced lung injury. J Cancer Res Clin Oncol. 2025;151:48.
103. Li M, Liu P, Ke Y, Zhang X. Research progress on macrophage in radiation induced lung injury. Journal of Zhejiang University. 2020;49:623–8.
104. Nguyen HQ, To NH, Zadigue P, Kerbrat S, De La Taille A, Le Gouvello S, et al. Ionizing radiation-induced cellular senescence promotes tissue fibrosis after radiotherapy. A review Crit Rev Oncol Hematol. 2018;129:13–26.
105. Citrin DE, Shankavaram U, Horton JA, Shield W 3rd, Zhao S, Asano H, et al. Role of type II pneumocyte senescence in radiation-induced lung fibrosis. J Natl Cancer Inst. 2013;105:1474–84.
106. Wang LK, Wu TJ, Hong JH, Chen FH, Yu J, Wang CC. Radiation Induces Pulmonary Fibrosis by Promoting the Fibrogenic Differentiation of Alveolar Stem Cells. Stem Cells Int. 2020;2020:6312053.
107. Khoo LT, Chen L-Y. Role of the cGAS-STING pathway in cancer development and oncotherapeutic approaches. EMBO Rep. 2018;19:e46935.
108. Dunn GP, Bruce AT, Sheehan KCF, Shankaran V, Uppaluri R, Bui JD, et al. A critical function for type I interferons in cancer immunoediting. Nat Immunol. 2005;6:722–9.
109. Li Y, Li X, Yi J, Cao Y, Qin Z, Zhong Z, et al. Nanoparticle-Mediated STING Activation for Cancer Immunotherapy. Adv Healthc Mater. 2023;12(19):e2300260.
110. Huang Y, Kim BYS, Chan CK, Hahn SM, Weissman IL, Jiang W. Improving immune-vascular crosstalk for cancer immunotherapy. Nat Rev Immunol. 2018;18:195–203.
111. Munn LL, Jain RK. Vascular regulation of antitumor immunity. Science. 2019;365:544–5.
112. Jain RK. Normalization of tumor vasculature: an emerging concept in antiangiogenic therapy. Science. 2005;307:58–62.
113. Lanitis E, Irving M, Coukos G. Targeting the tumor vasculature to enhance T cell activity. Curr Opin Immunol. 2015;33:55–63.
114. Dayan F, Mazure NM, Brahimi-Horn MC, Pouysségur J. A dialogue between the hypoxia-inducible factor and the tumor microenvironment. Cancer Microenviron. 2008;1:53–68.
115. Pober JS, Sessa WC. Evolving functions of endothelial cells in inflammation. Nat Rev Immunol. 2007;7:803–15.
116. Muller WA. Leukocyte-endothelial-cell interactions in leukocyte transmigration and the inflammatory response. Trends Immunol. 2003;24:327–34.
117. Langer HF, Chavakis T. Leukocyte-endothelial interactions in inflammation. J Cell Mol Med. 2009;13:1211–20.
118. Huang H, Langenkamp E, Georganaki M, Loskog A, Fuchs PF, Dieterich LC, et al. VEGF suppresses T-lymphocyte infiltration in the tumor microenvironment through inhibition of NF-κB-induced endothelial activation. Faseb j. 2015;29:227–38.
119. Bouzin C, Feron O. Targeting tumor stroma and exploiting mature tumor vasculature to improve anti-cancer drug delivery. Drug Resist Updat. 2007;10:109–20.
120. Griffioen AW, Damen CA, Martinotti S, Blijham GH, Groenewegen G. Endothelial intercellular adhesion molecule-1 expression is suppressed in human malignancies: the role of angiogenic factors. Cancer Res. 1996;56:1111–7.
121. Nelson J, Bagnato A, Battistini B, Nisen P. The endothelin axis: emerging role in cancer. Nat Rev Cancer. 2003;3:110–6.
122. Rossin A, Miloro G, Hueber AO. TRAIL and FasL Functions in Cancer and Autoimmune Diseases: Towards an Increasing Complexity. Cancers (Basel). 2019;11:639.
123. Jain RK. Normalizing tumor microenvironment to treat cancer: bench to bedside to biomarkers. J Clin Oncol. 2013;31:2205–18.
124. Goel S, Duda DG, Xu L, Munn LL, Boucher Y, Fukumura D, et al. Normalization of the vasculature for treatment of cancer and other diseases. Physiol Rev. 2011;91:1071–121.
125. Zhao Y, Ting KK, Li J, Cogger VC, Chen J, Johansson-Percival A, et al. Targeting Vascular Endothelial-Cadherin in Tumor-Associated Blood Vessels Promotes T-cell-Mediated Immunotherapy. Cancer Res. 2017;77:4434–47.
126. Tian L, Goldstein A, Wang H, Ching Lo H, Sun Kim I, Welte T, et al. Mutual regulation of tumour vessel normalization and immunostimulatory reprogramming. Nature. 2017;544:250–4.
127. Anastasiou M, Newton GA, Kaur K, Carrillo-Salinas FJ, Smolgovsky SA, Bayer AL, et al. Endothelial STING controls T cell transmigration in an IFNI-dependent manner. JCI Insight. 2021;6:e149346.
128. Demaria O, De Gassart A, Coso S, Gestermann N, Di Domizio J, Flatz L, et al. STING activation of tumor endothelial cells initiates spontaneous and therapeutic antitumor immunity. Proc Natl Acad Sci USA. 2015;112:15408–13.
129. Yang H, Lee WS, Kong SJ, Kim CG, Kim JH, Chang SK, et al. STING activation reprograms tumor vasculatures and synergizes with VEGFR2 blockade. J Clin Investig. 2019;129:4350–64.
130. Stein SC, Lam E, Falck-Pedersen E. Cell-specific regulation of nucleic acid sensor cascades: a controlling interest in the antiviral response. J Virol. 2012;86:13303–12.
131. Ma F, Li B, Yu Y, Iyer SS, Sun M, Cheng G. Positive feedback regulation of type I interferon by the interferon-stimulated gene STING. EMBO Rep. 2015;16:202–12.
132. Go E-J, Yang H, Park W, Lee SJ, Han J-H, Kong SJ, et al. Systemic Delivery of a STING Agonist-Loaded Positively Charged Liposome Selectively Targets Tumor Immune Microenvironment and Suppresses Tumor Angiogenesis. Small. 2023;19:e2300544.
133. Kammertoens T, Friese C, Arina A, Idel C, Briesemeister D, Rothe M, et al. Tumour ischaemia by interferon-γ resembles physiological blood vessel regression. Nature. 2017;545:98–102.
134. Wang-Bishop L, Kimmel BR, Ngwa VM, Madden MZ, Baljon JJ, Florian DC, et al. STING-activating nanoparticles normalize the vascular-immune interface to potentiate cancer immunotherapy. Sci Immunol. 2023;8:eadd1153.
135. Yang H, Lee WS, Kong SJ, Kim CG, Kim JH, Chang SK, et al. STING activation reprograms tumor vasculatures and synergizes with VEGFR2 blockade. J Clin Invest. 2019;129:4350–64.
136. Huang LS, Hong Z, Wu W, Xiong S, Zhong M, Gao X, et al. mtDNA Activates cGAS Signaling and Suppresses the YAP-Mediated Endothelial Cell Proliferation Program to Promote Inflammatory Injury. Immunity. 2020;52:475-86.e5.
137. Shen L, Hu P, Zhang Y, Ji Z, Shan X, Ni L, et al. Serine metabolism antagonizes antiviral innate immunity by preventing ATP6V0d2-mediated YAP lysosomal degradation. Cell Metab. 2021;33:971-87.e6.
138. Vandekeere S, Dubois C, Kalucka J, Sullivan MR, García-Caballero M, Goveia J, et al. Serine synthesis via PHGDH is essential for heme production in endothelial cells. Cell Metab. 2018;28(573–87): e13.
139. Del Prete A, Salvi V, Soriani A, Laffranchi M, Sozio F, Bosisio D, et al. Dendritic cell subsets in cancer immunity and tumor antigen sensing. Cell Mol Immunol. 2023;20(5):432–47.

140. Savina A, Jancic C, Hugues S, Guermonprez P, Vargas P, Moura IC, et al. NOX2 controls phagosomal pH to regulate antigen processing during crosspresentation by dendritic cells. Cell. 2006;126:205–18.
141. Guilliams M, Dutertre CA, Scott CL, McGovern N, Sichien D, Chakarov S, et al. Unsupervised High-Dimensional Analysis Aligns Dendritic Cells across Tissues and Species. Immunity. 2016;45:669–84.
142. Barry KC, Hsu J, Broz ML, Cueto FJ, Binnewies M, Combes AJ, et al. A natural killer-dendritic cell axis defines checkpoint therapy-responsive tumor microenvironments. Nat Med. 2018;24:1178–91.
143. Michea P, Noël F, Zakine E, Czerwinska U, Sirven P, Abouzid O, et al. Adjustment of dendritic cells to the breast-cancer microenvironment is subset specific. Nat Immunol. 2018;19:885–97.
144. Merad M, Sathe P, Helft J, Miller J, Mortha A. The dendritic cell lineage: ontogeny and function of dendritic cells and their subsets in the steady state and the inflamed setting. Annu Rev Immunol. 2013;31:563–604.
145. Merad M, Manz MG, Karsunky H, Wagers A, Peters W, Charo I, et al. Langerhans cells renew in the skin throughout life under steady-state conditions. Nat Immunol. 2002;3:1135–41.
146. Reizis B. Plasmacytoid Dendritic Cells: Development, Regulation, and Function. Immunity. 2019;50:37–50.
147. Deb P, Dai J, Singh S, Kalyoussef E, Fitzgerald-Bocarsly P. Triggering of the cGAS-STING Pathway in Human Plasmacytoid Dendritic Cells Inhibits TLR9-Mediated IFN Production. J Immunol. 2020;205:223–36.
148. Cheng S, Li Z, Gao R, Xing B, Gao Y, Yang Y, et al. A pan-cancer single-cell transcriptional atlas of tumor infiltrating myeloid cells. Cell. 2021;184:792-809.e23.
149. Ribeiro ARS, Neuper T, Horejs-Hoeck J. The Role of STING-Mediated Activation of Dendritic Cells in Cancer Immunotherapy. Int J Nanomedicine. 2024;19:10685–97.
150. Shin EC, Seifert U, Kato T, Rice CM, Feinstone SM, Kloetzel PM, et al. Virus-induced type I IFN stimulates generation of immunoproteasomes at the site of infection. J Clin Invest. 2006;116:3006–14.
151. Shin EC, Seifert U, Urban S, Truong KT, Feinstone SM, Rice CM, et al. Proteasome activator and antigen-processing aminopeptidases are regulated by virus-induced type I interferon in the hepatitis C virus-infected liver. J Interferon Cytokine Res. 2007;27:985–90.
152. McRae BL, Nagai T, Semnani RT, van Seventer JM, van Seventer GA. Interferon-alpha and -beta inhibit the in vitro differentiation of immunocompetent human dendritic cells from CD14(+) precursors. Blood. 2000;96:210–7.
153. Goriely S, Goldman M. The interleukin-12 family: new players in transplantation immunity? Am J Transplant. 2007;7:278–84.
154. Hossain MK, Wall KA. Use of Dendritic Cell Receptors as Targets for Enhancing Anti-Cancer Immune Responses. Cancers. 2019;11:418.
155. Pang ES, Daraj G, Balka KR, De Nardo D, Macri C, Hochrein H, et al. Discordance in STING-Induced Activation and Cell Death Between Mouse and Human Dendritic Cell Populations. Front Immunol. 2022;13:794776.
156. Parlato S, Santini SM, Lapenta C, Di Pucchio T, Logozzi M, Spada M, et al. Expression of CCR-7, MIP-3 beta, and Th-1 chemokines in type IIFN-induced monocyte-derived dendritic cells: importance for the rapid acquisition of potent migratory and functional activities. Blood. 2001;98:3022–9.
157. Harlin H, Meng Y, Peterson AC, Zha Y, Tretiakova M, Slingluff C, et al. Chemokine expression in melanoma metastases associated with CD8+ T-cell recruitment. Cancer Res. 2009;69:3077–85.
158. Hu Z, Yu X, Ding R, Liu B, Gu C, Pan X-W, et al. Glycolysis drives STING signaling to facilitate dendritic cell antitumor function. J Clin Invest. 2023;133:e166031.
159. Hu Z, Teng XL, Zhang T, Yu X, Ding R, Yi J, et al. SENP3 senses oxidative stress to facilitate STING-dependent dendritic cell antitumor function. Mol Cell. 2021;81:940-52.e5.
160. Kumar V, Bauer C, Stewart JHt. Targeting cGAS/STING signaling-mediated myeloid immune cell dysfunction in TIME. J Biomed Sci. 2023;30:48.
161. Noy R, Pollard JW. Tumor-Associated Macrophages: From Mechanisms to Therapy. Immunity. 2014;41:49–61.
162. Kumar V, Bauer C, Stewart JH. Targeting cGAS/STING signaling-mediated myeloid immune cell dysfunction in TIME. J Biomed Sci. 2023;30:48.
163. Ou L, Zhang A, Cheng Y, Chen Y. The cGAS-STING Pathway: A Promising Immunotherapy Target. Front Immunol. 2021;12:795048.
164. Sun Y, Hu H, Liu Z, Xu J, Gao Y, Zhan X, et al. Macrophage STING signaling promotes NK cell to suppress colorectal cancer liver metastasis via 4–1BBL/4–1BB co-stimulation. J Immunother Cancer. 2023;11:e006481.
165. Miao X, Leng X, Zhang Q. The Current State of Nanoparticle-Induced Macrophage Polarization and Reprogramming Research. Intern J Mol Sci. 2017;18:336.
166. Chen Y, Hu M, Wang L, Chen W. Macrophage M1/M2 polarization. Eur J Pharmacol. 2020;877:173090.
167. Yao Y, Xu XH, Jin L. Macrophage Polarization in Physiological and Pathological Pregnancy. Front Immunol. 2019;10:792.
168. Ma RH, Ji TT, Chen DG, Dong WQ, Zhang HF, Yin XN, et al. Tumor cell-derived microparticles polarize M2 tumor-associated macrophages for tumor progression. Oncoimmunology. 2016;5:e1118599.
169. Delamarre L, Pack M, Chang H, Mellman I, Trombetta ES. Differential lysosomal proteolysis in antigen-presenting cells determines antigen fate. Science. 2005;307:1630–4.
170. Lee AJ, Ashkar AA. The Dual Nature of Type I and Type II Interferons. Front Immunol. 2018;9:2061.
171. Baumann D, Drebant J, Hägele T, Burger L, Serger C, Lauenstein C, et al. p38 MAPK signaling in M1 macrophages results in selective elimination of M2 macrophages by MEK inhibition. J Immunother Cancer. 2021;9:e002319.
172. Majeti R, Chao MP, Alizadeh AA, Pang WW, Jaiswal S, Gibbs KD Jr, et al. CD47 is an adverse prognostic factor and therapeutic antibody target on human acute myeloid leukemia stem cells. Cell. 2009;138:286–99.
173. Zhou Y, Fei M, Zhang G, Liang WC, Lin W, Wu Y, et al. Blockade of the Phagocytic Receptor MerTK on Tumor-Associated Macrophages Enhances P2X7R-Dependent STING Activation by Tumor-Derived cGAMP. Immunity. 2020;52:357-73.e9.
174. Doshi AS, Cantin S, Prickett LB, Mele DA, Amiji M. Systemic nano-delivery of low-dose STING agonist targeted to CD103+dendritic cells for cancer immunotherapy. J Control Release. 2022;345:721–33.
175. Böttcher JP, Bonavita E, Chakravarty P, Blees H, Cabeza-Cabrerizo M, Sammicheli S, et al. NK Cells Stimulate Recruitment of cDC1 into the Tumor Microenvironment Promoting Cancer Immune Control. Cell. 2018;172:1022-37.e14.
176. Poli A, Michel T, Thérésine M, Andrès E, Hentges F, Zimmer J. CD56bright natural killer (NK) cells: an important NK cell subset. Immunology. 2009;126:458–65.
177. Maskalenko NA, Zhigarev D, Campbell KS. Harnessing natural killer cells for cancer immunotherapy: dispatching the first responders. Nat Rev Drug Discov. 2022;21:559–77.
178. Bauer S, Groh V, Wu J, Steinle A, Phillips JH, Lanier LL, et al. Activation of NK cells and T cells by NKG2D, a receptor for stress-inducible MICA. Science. 1999;285:727–9.
179. Garrido F, Aptsiauri N, Doorduijn EM, Garcia Lora AM, van Hall T. The urgent need to recover MHC class I in cancers for effective immunotherapy. Curr Opin Immunol. 2016;39:44–51.
180. Müller L, Aigner P, Stoiber D. Type I Interferons and Natural Killer Cell Regulation in Cancer. Front Immunol. 2017;8:304.
181. Barnes SA, Audsley KM, Newnes HV, Fernandez S, de Jong E, Waithman J, et al. Type I interferon subtypes differentially activate the anti-leukaemic function of natural killer cells. Front Immunol. 2022;13:1050718.
182. Gotthardt D, Trifinopoulos J, Sexl V, Putz EM. JAK/STAT Cytokine Signaling at the Crossroad of NK Cell Development and Maturation. Front Immunol. 2019;10:2590.
183. Ming Q, Liu J, Lv Z, Wang T, Fan R, Zhang Y, et al. Manganese boosts natural killer cell function via cGAS-STING mediated UTX expression. MedComm. 2020;2024(5): e683.
184. Lu L, Yang C, Zhou X, Wu L, Hong X, Li W, et al. STING signaling promotes NK cell antitumor immunity and maintains a reservoir of TCF-1+ NK cells. Cell Rep. 2023;42:113108.
185. Li S, Mirlekar B, Johnson BM, Brickey WJ, Wrobel JA, Yang N, et al. STING-induced regulatory B cells compromise NK function in cancer immunity. Nature. 2022;610:373–80.

186. Tang CA, Lee AC, Chang S, Xu Q, Shao A, Lo Y, et al. STING regulates BCR signaling in normal and malignant B cells. Cell Mol Immunol. 2021;18:1016–31.
187. Zhang P, Rashidi A, Zhao J, Silvers C, Wang H, Castro B, et al. STING agonist-loaded, CD47/PD-L1-targeting nanoparticles potentiate antitumor immunity and radiotherapy for glioblastoma. Nat Commun. 2023;14:1610.
188. Yan J, Wang G, Xie L, Tian H, Li J, Li B, et al. Engineering Radiosensitizer-Based Metal-Phenolic Networks Potentiate STING Pathway Activation for Advanced Radiotherapy. Adv Mater. 2022;34: e2105783.
189. Chen B, Xiao L, Wang W, Xu L, Jiang Y, Zhang G, et al. Bi2−xMnxO3 Nanospheres Engaged Radiotherapy with Amplifying DNA Damage. ACS Appl Mater Interfaces. 2023;15:33903–15.
190. Chen W, Zhong S, Cai Q, Jiang Z, Hu Q, Tang C, et al. A triboelectric-field-mediated cuproptosis induction patch for melanoma recurrence suppression. Matter. 2025;8:102088.
191. Gu J, Liu X, Ji Z, Shen M, Zhu M, Ren Y, et al. Tumor Vascular Destruction and cGAS-STING Activation Induced by Single Drug-Loaded Nano-Micelles for Multiple Synergistic Therapies of Cancer. Small. 2023;19:e2303517.
192. Yang J, Zhang C, Chen X, Zhou D, Sun Z, Niu R, et al. Ultra-efficient radio-immunotherapy for reprogramming the hypoxic and immunosuppressive tumor microenvironment with durable innate immune memory. Biomaterials. 2023;302:122303.
193. McAndrews KM, Che SP, LeBleu VS, Kalluri R. Effective delivery of STING agonist using exosomes suppresses tumor growth and enhances antitumor immunity. J Biol Chem. 2021;296:100523.
194. Heyes J, Palmer L, Bremner K, MacLachlan I. Cationic lipid saturation influences intracellular delivery of encapsulated nucleic acids. J Control Release. 2005;107:276–87.
195. Pei D, Buyanova M. Overcoming Endosomal Entrapment in Drug Delivery. Bioconjug Chem. 2019;30:273–83.
196. Nichols JW, Bae YH. EPR: Evidence and fallacy. J Control Release. 2014;190:451–64.
197. Wang S, Shi X, Xiong T, Chen Q, Yang Y, Chen W, et al. Inhibiting Mitochondrial Damage for Efficient Treatment of Cerebral Ischemia-Reperfusion Injury Through Sequential Targeting Nanomedicine of Neuronal Mitochondria in Affected Brain Tissue. Adv Mater. 2024;36:2409529.
198. Chen Q, Yang Y, Ying X, Huang C, Chen J, Wang J, et al. Hierarchical Targeting Nanodrug with Holistic DNA Protection for Effective Treatment of Acute Kidney Injury. Advanced Science. 2025;12:2411254.
199. Sun X, Zhou X, Lei YL, Moon JJ. Unlocking the promise of systemic STING agonist for cancer immunotherapy. J Control Release. 2023;357:417–21.
200. Harding SM, Benci JL, Irianto J, Discher DE, Minn AJ, Greenberg RA. Mitotic progression following DNA damage enables pattern recognition within micronuclei. Nature. 2017;548:466–70.
201. Sun S, Gu W, Wu H, Zhao Q, Qian S, Xiao H, et al. Immunostimulant In Situ Hydrogel Improves Synergetic Radioimmunotherapy of Malignant Glioblastoma Relapse Post-Resection. Adv Funct Mater. 2022;32:2205038.
202. Wu Y-H, Chen R-J, Chiu H-W, Yang L-X, Wang Y-L, Chen Y-Y, et al. Nanoparticles augment the therapeutic window of RT and immunotherapy for treating cancers: pivotal role of autophagy. Theranostics. 2023;13:40–58.
203. Huang J, Huang Q, Liu M, Chen Q, Ai K. Emerging Bismuth Chalcogenides Based Nanodrugs for Cancer Radiotherapy. Front Pharmacol. 2022;13: 844037.
204. Sancey L, Lux F, Kotb S, Roux S, Dufort S, Bianchi A, et al. The use of theranostic gadolinium-based nanoprobes to improve radiotherapy efficacy. Bri J Radiol. 2014;87:20140134.
205. Habiba K, Aziz K, Sanders K, Santiago CM, Mahadevan LSK, Makarov V, et al. Enhancing Colorectal Cancer Radiation Therapy Efficacy using Silver Nanoprisms Decorated with Graphene as Radiosensitizers. Sci Rep. 2019;9:17120.
206. Wang H, Mu X, He H, Zhang X-D. Cancer Radiosensitizers. Trends Pharmacol Sci. 2018;39:24–48.
207. Wang D, Nie T, Huang C, Chen Z, Ma X, Fang W, et al. Metal-Cyclic Dinucleotide Nanomodulator-Stimulated STING Signaling for Strengthened Radioimmunotherapy of Large Tumor. Small. 2022;18:e2203227.
208. Gou S, Liu W, Wang S, Chen G, Chen Z, Qiu L, et al. Engineered Nanovaccine Targeting Clec9a(+) Dendritic Cells Remarkably Enhances the Cancer Immunotherapy Effects of STING Agonist. Nano Lett. 2021;21:9939–50.
209. Deng Z, Xi M, Zhang C, Wu X, Li Q, Wang C, et al. Biomineralized MnO2 Nanoplatforms Mediated Delivery of Immune Checkpoint Inhibitors with STING Pathway Activation to Potentiate Cancer Radio-Immunotherapy. Acs Nano. 2023;17(5):4495–506.
210. Huang W, Shi S, Lv H, Ju Z, Liu Q, Chen T. Tellurium-driven maple leaf-shaped manganese nanotherapeutics reshape tumor microenvironment via chemical transition in situ to achieve highly efficient radioimmunotherapy of triple negative breast cancer. Bioactive Materials. 2023;27:560–73.
211. Li T, Gao M, Wu Z, Yang J, Mo B, Yu S, et al. Tantalum-Zirconium Co-Doped Metal-Organic Frameworks Sequentially Sensitize Radio-Radiodynamic-Immunotherapy for Metastatic Osteosarcoma. Advanced science (Weinh). 2023;10:e2206779.
212. Liu N, Zhu J, Zhu W, Chen L, Li M, Shen J, et al. X-ray-Induced Release of Nitric Oxide from Hafnium-Based Nanoradiosensitizers for Enhanced Radio-Immunotherapy. Adv Mater. 2023;35:e2302220.
213. Cao Y, Ding S, Hu Y, Zeng L, Zhou J, Lin L, et al. An Immunocompetent Hafnium Oxide-Based STING Nanoagonist for Cancer Radio-immunotherapy. ACS Nano. 2024;18:4189–204.
214. Wu Y, Li Q, Yan Y, Hao Y, Wang C, Liu B, et al. Gel-mediated recruitment of conventional type 1 dendritic cells potentiates the therapeutic effects of radiotherapy. Biomaterials. 2024;305: 122470.
215. Yi L, Jiang X, Zhou Z, Xiong W, Xue F, Liu Y, et al. A Hybrid Nanoadjuvant Simultaneously Depresses PD-L1/TGF-β1 and Activates cGAS-STING Pathway to Overcome Radio-Immunotherapy Resistance. Adv Mater. 2024;36(15):e2304328.
216. He M, Xiao T, Wang Y, Yu H, Wang Z, Shi X, et al. Multifunctional PVCL nanogels enable magnetic resonance imaging and immunostimulated radiotherapy of orthotopic glioblastoma. Chem Eng J. 2023;453:139634.
217. Liu R, Zhang C, Wu X, Wang C, Zhao M, Ji C, et al. Hafnium oxide nanoparticles coated ATR inhibitor to enhance the radiotherapy and potentiate antitumor immune response. Chem Eng J. 2023;461:142085.
218. Nagata S, Tanaka M. Programmed cell death and the immune system. Nat Rev Immunol. 2017;17:333–40.
219. Wang-Bishop L, Wehbe M, Shae D, James J, Hacker BC, Garland K, et al. Potent STING activation stimulates immunogenic cell death to enhance antitumor immunity in neuroblastoma. J Immunother Cancer. 2020;8:e000282.
220. Galluzzi L, Vitale I, Warren S, Adjemian S, Agostinis P, Martinez AB, et al. Consensus guidelines for the definition, detection and interpretation of immunogenic cell death. J Immunother Cancer. 2020;8:e000337.
221. Galluzzi L, Guilbaud E, Schmidt D, Kroemer G, Marincola FM. Targeting immunogenic cell stress and death for cancer therapy. Nat Rev Drug Discov. 2024;23:445–60.
222. Huang Z, Huang S, Song S, Ding Y, Zhou H, Zhang S, et al. Two-dimensional coordination risedronate-manganese nanobelts as adjuvant for cancer radiotherapy and immunotherapy. Nat Commun. 2024;15:8692.
223. Zhang F, Zhang Z, Yang W, Peng Z, Sun J, Li G, et al. Engineering Autologous Cell-Derived Exosomes to Boost Melanoma-Targeted Radio-Immunotherapy by Cascade cGAS-STING Pathway Activation. Small. 2024;21(4):e2408769.
224. Kim J, Mooney DJ. In vivo modulation of dendritic cells by engineered materials: Towards new cancer vaccines. Nano Today. 2011;6:466–77.
225. Liu H, Moynihan KD, Zheng Y, Szeto GL, Li AV, Huang B, et al. Structure-based programming of lymph-node targeting in molecular vaccines. Nature. 2014;507:519–22.
226. Huysamen C, Willment JA, Dennehy KM, Brown GD. CLEC9A is a novel activation C-type lectin-like receptor expressed on BDCA3+ dendritic cells and a subset of monocytes. J Biol Chem. 2008;283:16693–701.
227. Luo M, Wang H, Wang Z, Cai H, Lu Z, Li Y, et al. A STING-activating nanovaccine for cancer immunotherapy. Nat Nanotechnol. 2017;12:648–54.
228. Curtsinger JM, Valenzuela JO, Agarwal P, Lins D, Mescher MF. Type I IFNs provide a third signal to CD8 T cells to stimulate clonal expansion and differentiation. J Immunol. 2005;174:4465–9.
229. Benoit-Lizon I, Jacquin E, Rivera Vargas T, Richard C, Roussey A, Dal Zuffo L, et al. CD4 T cell-intrinsic STING signaling controls the differentiation

and effector functions of T(H)1 and T(H)9 cells. J Immunother Cancer. 2022;10:e003459.
230. Li W, Lu L, Lu J, Wang X, Yang C, Jin J, et al. cGAS-STING-mediated DNA sensing maintains CD8(+) T cell stemness and promotes antitumor T cell therapy. Sci Transl Med. 2020;12:eaay9013.
231. Cerwenka A, Lanier LL. Natural killer cells, viruses and cancer. Nat Rev Immunol. 2001;1:41–9.
232. Chen J, Liu X, Zeng Z, Li J, Luo Y, Sun W, et al. Immunomodulation of NK Cells by Ionizing Radiation. Front Oncol. 2020;10:874.
233. Joyce JA. Therapeutic targeting of the tumor microenvironment. Cancer Cell. 2005;7:513–20.
234. Quail DF, Joyce JA. Microenvironmental regulation of tumor progression and metastasis. Nat Med. 2013;19:1423–37.
235. Wu T, Dai Y. Tumor microenvironment and therapeutic response. Cancer Lett. 2017;387:61–8.
236. Liu Y, Wang S, Zhang J, Sun Q, Xiao Y, Chen J, et al. Reprogramming the myocardial infarction microenvironment with melanin-based composite nanomedicines in mice. Nat Commun. 2024;15:6651.
237. Nordsmark M, Bentzen SM, Rudat V, Brizel D, Lartigau E, Stadler P, et al. Prognostic value of tumor oxygenation in 397 head and neck tumors after primary radiation therapy. An international multi-center study Radiother Oncol. 2005;77:18–24.
238. Singleton DC, Macann A, Wilson WR. Therapeutic targeting of the hypoxic tumour microenvironment. Nat Rev Clin Oncol. 2021;18:751–72.
239. Sang W, Xie L, Wang G, Li J, Zhang Z, Li B, et al. Oxygen-Enriched Metal-Phenolic X-Ray Nanoprocessor for Cancer Radio-Radiodynamic Therapy in Combination with Checkpoint Blockade Immunotherapy. Adv Sci (Weinh). 2021;8:2003338.
240. Wang S, Zhou X, Zeng Z, Sui M, Chen L, Feng C, et al. Atovaquone-HSA nano-drugs enhance the efficacy of PD-1 blockade immunotherapy by alleviating hypoxic tumor microenvironment. J Nanobiotechnology. 2021;19:302.
241. Zhong S, Zhang Z, Wang Z, Zhao Q, Chen W, Chen G, et al. Synergizing Catalysis with Post-catalysis Pseudo-Iron Release by Building Dynamic Catalytic Active Sites in Diatomic Nanozymes for Boosting Cancer Therapy. J Am Chem Soc. 2025;147(18):15814–26.
242. Go EJ, Yang H, Park W, Lee SJ, Han JH, Kong SJ, et al. Systemic Delivery of a STING Agonist-Loaded Positively Charged Liposome Selectively Targets Tumor Immune Microenvironment and Suppresses Tumor Angiogenesis. Small. 2023;19: e2300544.
243. Kleibeuker EA, Griffioen AW, Verheul HM, Slotman BJ, Thijssen VL. Combining angiogenesis inhibition and radiotherapy: a double-edged sword. Drug Resist Updat. 2012;15:173–82.
244. Geng L, Donnelly E, McMahon G, Lin PC, Sierra-Rivera E, Oshinka H, et al. Inhibition of vascular endothelial growth factor receptor signaling leads to reversal of tumor resistance to radiotherapy. Cancer Res. 2001;61:2413–9.
245. Garcia-Barros M, Paris F, Cordon-Cardo C, Lyden D, Rafii S, Haimovitz-Friedman A, et al. Tumor response to radiotherapy regulated by endothelial cell apoptosis. Science. 2003;300:1155–9.
246. Siemann DW, Chaplin DJ, Horsman MR. Realizing the Potential of Vascular Targeted Therapy: The Rationale for Combining Vascular Disrupting Agents and Anti-Angiogenic Agents to Treat Cancer. Cancer Invest. 2017;35:519–34.
247. Zheng H, Qian J, Carbone CJ, Leu NA, Baker DP, Fuchs SY. Vascular endothelial growth factor-induced elimination of the type 1 interferon receptor is required for efficient angiogenesis. Blood. 2011;118:4003–6.
248. Mandai M, Hamanishi J, Abiko K, Matsumura N, Baba T, Konishi I. Dual Faces of IFNγ in Cancer Progression: A Role of PD-L1 Induction in the Determination of Pro- and Antitumor Immunity. Clin Cancer Res. 2016;22:2329–34.
249. Klemm F, Maas RR, Bowman RL, Kornete M, Soukup K, Nassiri S, et al. Interrogation of the Microenvironmental Landscape in Brain Tumors Reveals Disease-Specific Alterations of Immune Cells. Cell. 2020;181:1643-60.e17.
250. Sica A, Porta C, Morlacchi S, Banfi S, Strauss L, Rimoldi M, et al. Origin and Functions of Tumor-Associated Myeloid Cells (TAMCs). Cancer Microenviron. 2012;5:133–49.
251. Tu X, Qin B, Zhang Y, Zhang C, Kahila M, Nowsheen S, et al. PD-L1 (B7–H1) Competes with the RNA Exosome to Regulate the DNA Damage Response and Can Be Targeted to Sensitize to Radiation or Chemotherapy. Mol Cell. 2019;74:1215-26.e4.
252. Huang CY, Ye ZH, Huang MY, Lu JJ. Regulation of CD47 expression in cancer cells. Transl Oncol. 2020;13: 100862.
253. Lien E, Ingalls RR. Toll-like receptors. Crit Care Med. 2002;30:S1-11.
254. Krieg AM. Therapeutic potential of Toll-like receptor 9 activation. Nat Rev Drug Discov. 2006;5:471–84.
255. Yildiz S, Alpdundar E, Gungor B, Kahraman T, Bayyurt B, Gursel I, et al. Enhanced immunostimulatory activity of cyclic dinucleotides on mouse cells when complexed with a cell-penetrating peptide or combined with CpG. Eur J Immunol. 2015;45:1170–9.
256. Shang T, Yu X, Han S, Yang B. Nanomedicine-based tumor photothermal therapy synergized immunotherapy. Biomater Sci. 2020;8:5241–59.
257. Liu X, Zhang X, Zhu M, Lin G, Liu J, Zhou Z, et al. PEGylated Au@ Pt nanodendrites as novel theranostic agents for computed tomography imaging and photothermal/radiation synergistic therapy. ACS Appl Mater Interfaces. 2017;9:279–85.
258. Yin M, Chen X, Guo Q, Xiao L, Gao P, Zang D, et al. Ultrasmall zirconium carbide nanodots for synergistic photothermal-radiotherapy of glioma. Nanoscale. 2022;14:14935–49.
259. Varsha MV, Nageswaran G. Review-2D Layered Metal Organic Framework Nanosheets as an Emerging Platform for Electrochemical Sensing. J Electrochem Soc. 2020;167:136502.
260. Xiang Y, Chen Q, Nan Y, Liu M, Xiao Z, Yang Y, et al. Nitric Oxide-Based Nanomedicines for Conquering TME Fortress: Say "NO" to Insufficient Tumor Treatment. Adv Funct Mater. 2024;34:2312092.
261. Yang C, Mu G, Zhang Y, Gao Y, Zhang W, Liu J, et al. Supramolecular Nitric Oxide Depot for Hypoxic Tumor Vessel Normalization and Radiosensitization. Adv Mater. 2022;34: e2202625.
262. Zhang J, Wang S, Sun Q, Zhang J, Shi X, Yao M, et al. Peroxynitrite-Free Nitric Oxide-Embedded Nanoparticles Maintain Nitric Oxide Homeostasis for Effective Revascularization of Myocardial Infarcts. ACS Nano. 2024;18:32650–71.
263. Narayanaswamy R, Torchilin VP. Hydrogels and Their Applications in Targeted Drug Delivery. Molecules. 2019;24:603.
264. Wang L, Zhang T, Zheng Y, Li Y, Tang X, Chen Q, et al. Combination of irinotecan silicasome nanoparticles with radiation therapy sensitizes immunotherapy by modulating the activation of the cGAS/STING pathway for colorectal cancer. Materials Today Bio. 2023;23:100809.
265. Duo Y, Chen Z, Li K, Yang Y, Wang H, Hu J, et al. Targeted delivery of novel Au(I)-based AIEgen via inactivated cancer cells for trimodal chemo-radio-immunotherapy and vaccination against advanced tumor. Nano Today. 2023;51:101920.
266. Li C, Zhang Y, Wan Y, Wang J, Lin J, Li Z, et al. STING-activating drug delivery systems: Design strategies and biomedical applications. Chin Chem Lett. 2021;32:1615–25.
267. Liu Y, Fei Y, Wang X, Yang B, Li M, Luo Z. Biomaterial-enabled therapeutic modulation of cGAS-STING signaling for enhancing antitumor immunity. Mol Ther. 2023;31(7):1938–59.
268. Wei K, Chen T, Fang H, Shen X, Tang Z, Zhao J. Mitochondrial DNA release via the mitochondrial permeability transition pore activates the cGAS-STING pathway, exacerbating inflammation in acute Kawasaki disease. Cell Commun Signal. 2024;22:328.
269. Watanabe T, Kobunai T, Yamamoto Y, Matsuda K, Ishihara S, Nozawa K, et al. Chromosomal instability (CIN) phenotype, CIN high or CIN low, predicts survival for colorectal cancer. J Clin Oncol. 2012;30:2256–64.
270. Gehrcken L, Deben C, Smits E, Van Audenaerde JR. STING Agonists and How to Reach Their Full Potential in Cancer Immunotherapy. Adv Sci. 2025;12:2500296.
271. Quail DF, Joyce JA. The Microenvironmental Landscape of Brain Tumors. Cancer Cell. 2017;31:326–41.
272. Wu YT, Fang Y, Wei Q, Shi H, Tan H, Deng Y, et al. Tumor-targeted delivery of a STING agonist improvescancer immunotherapy. Proc Natl Acad Sci U S A. 2022;119: e2214278119.
273. Cai R, Chen Q, Zhao D, Wang Y, Zhou L, Zhang K, et al. A High Immune-Related Index with the Suppression of cGAS-STING Pathway is a Key Determinant to Herceptin Resistance in HER2+ Breast Cancer. Int J Biol Sci. 2024;20:3497–514.
274. Konno H, Yamauchi S, Berglund A, Putney RM, Mulé JJ, Barber GN. Suppression of STING signaling through epigenetic silencing and missense

mutation impedes DNA damage mediated cytokine production. Oncogene. 2018;37:2037–51.
275. Low JT, Chandramohan V, Bowie ML, Brown MC, Waitkus MS, Briley A, et al. Epigenetic STING silencing is developmentally conserved in gliomas and can be rescued by methyltransferase inhibition. Cancer Cell. 2022;40:439–40.
276. Falahat R, Berglund A, Perez-Villarroel P, Putney RM, Hamaidi I, Kim S, et al. Epigenetic state determines the in vivo efficacy of STING agonist therapy. Nat Commun. 2023;14:1573.
277. Ni J, Guo T, Zhou Y, Jiang S, Zhang L, Zhu Z. STING signaling activation modulates macrophage polarization via CCL2 in radiation-induced lung injury. J Transl Med. 2023;21:590.
278. Vanpouille-Box C, Alard A, Aryankalayil MJ, Sarfraz Y, Diamond JM, Schneider RJ, et al. DNA exonuclease Trex1 regulates radiotherapy-induced tumour immunogenicity. Nat Commun. 2017;8:15618.
279. Shi X, Yang Y, Zhang W, Wang J, Xiao D, Ren H, et al. FLASH X-ray spares intestinal crypts from pyroptosis initiated by cGAS-STING activation upon radioimmunotherapy. Proc Natl Acad Sci U S A. 2022;119:e2208506119.
280. Galluzzi L, Buque A, Kepp O, Zitvogel L, Kroemer G. Immunogenic cell death in cancer and infectious disease. Nat Rev Immunol. 2017;17:97–111.
281. Yang Y, Wu M, Cao D, Yang C, Jin J, Wu L, et al. ZBP1-MLKL necroptotic signaling potentiates radiation-induced antitumor immunity via intratumoral STING pathway activation. Sci Adv. 2021;7:eabf6290.
282. Yang Z, Wang Y, Zhang Y, He X, Zhong C-Q, Ni H, et al. RIP3 targets pyruvate dehydrogenase complex to increase aerobic respiration in TNF-induced necroptosis. Nat Cell Biol. 2018;20:186–97.
283. Pasparakis M, Vandenabeele P. Necroptosis and its role in inflammation. Nature. 2015;517:311–20.
284. Zhang S, Zhang J, Fan X, Liu H, Zhu M, Yang M, et al. Ionizing Radiation-Induced Ferroptosis Based on Nanomaterials. Int J Nanomed. 2022;17:3497–507.
285. Dixon SJ, Lemberg KM, Lamprecht MR, Skouta R, Zaitsev EM, Gleason CE, et al. Ferroptosis: An Iron-Dependent Form of Nonapoptotic Cell Death. Cell. 2012;149:1060–72.
286. Hu H, Zheng S, He C, Zheng Y, Wei Q, Chen S, et al. Radiotherapy-sensitized cancer immunotherapy via cGAS-STING immune pathway by activatable nanocascade reaction. J Nanobiotechnology. 2024;22:234.
287. Saha I, Jaiswal H, Mishra R, Nel HJ, Schreuder J, Kaushik M, et al. RelB suppresses type I Interferon signaling in dendritic cells. Cellular Immunology. 2020;349:104043.
288. Liang Q, Seo GJ, Choi YJ, Kwak M-J, Ge J, Rodgers MA, et al. Crosstalk between the cGAS DNA Sensor and Beclin-1 Autophagy Protein Shapes Innate Antimicrobial Immune Responses. Cell Host Microbe. 2014;15:228–38.
289. Johansen T, Birgisdottir ÅB, Huber J, Kniss A, Dötsch V, Kirkin V, et al. Methods for Studying Interactions Between Atg8/LC3/GABARAP and LIR-Containing Proteins. Methods Enzymol. 2017;587:143–69.

Publisher's Note